

Modelling the respiratory system

Guldager Christiansen, Tine; Dræby, Claus

Publication date:
1996

Document Version
Publisher's PDF, also known as Version of record

Citation for published version (APA):
Guldager Christiansen, T., & Dræby, C. (1996). *Modelling the respiratory system*. Roskilde Universitet. Tekster fra IMFUFA No. 318 <http://milne.ruc.dk/ImfufaTekster/>

General rights

Copyright and moral rights for the publications made accessible in the public portal are retained by the authors and/or other copyright owners and it is a condition of accessing publications that users recognise and abide by the legal requirements associated with these rights.

- Users may download and print one copy of any publication from the public portal for the purpose of private study or research.
- You may not further distribute the material or use it for any profit-making activity or commercial gain.
- You may freely distribute the URL identifying the publication in the public portal.

Take down policy

If you believe that this document breaches copyright please contact rucforsk@kb.dk providing details, and we will remove access to the work immediately and investigate your claim.

TEKST NR 318

1996

Modelling the Respiratory System

By:

Tine Guldager Christiansen

Claus Dræby

Supervisors:

Viggo Andreasen

Michael Danielsen

TEKSTER fra

IMFUFA

ROSKILDE UNIVERSITETSCENTER

INSTITUT FOR STUDIET AF MATEMATIK OG FYSIK SAMT DERES
FUNKTIONER I UNDERVISNING, FORSKNING OG ANVENDELSER

IMFUFA, Roskilde Universitetscenter, Postboks 260, 4000 Roskilde, Denmark

Modelling the Respiratory System

Master Thesis by: Tine Guldager Christiansen, Claus Dræby

Supervisors: Viggo Andreasen, Michael Danielsen

IMFUFA-tekst nr. 318/96

172 pages

ISSN 0106-6242

Abstract:

The thesis deals with modelling of the human respiratory system. A model of the human respiratory system is developed for use in the anaesthesia simulator SIMA. The model contains lung mechanics, airway dynamics, the blood transport system, the dissociation of gasses in blood and tissue, the metabolism and the pH value of blood.

The models are basically compartment models extended with vector compartment variables and a technique that allows the distribution in inhomogeneous compartments to be found by use of the derived of the dissociation function. This supports interactions between several transported substances well.

Contents

1	Introduction	3
1.1	Identification of the problem	4
1.2	Methods	5
2	The respiratory system	9
2.1	The physiology of the respiratory system	10
2.2	Requirements of the models	19
2.3	The other models in SIMA	21
2.4	Modelling done by others	22
2.5	Our modelling	26
3	Modelling the lung	29
3.1	The pressure model	30
3.2	The gas model	36
4	The models of the blood transport system	43
4.1	The mass balance equations	44
4.2	Metabolism	51
4.3	Gas dissociation and the pH value	54
4.4	The models of gas dissociation and pH value	59
4.5	Control of respiration	65
5	Solving the model	69
5.1	Model summary	70
5.2	Existence, uniqueness, and stability of solutions	77

6	Parameters of the model	85
6.1	Parameters of the Lung Model	86
6.2	Parameters of the transport model	89
6.3	The three compartment model	93
6.4	Solubility of intravenous anaesthetics	98
6.5	Conclusion	101
7	Testing the model	103
7.1	The lung model	104
7.2	The pH model	107
7.3	The dissociation curves	108
7.4	The blood transport model	113
7.5	Conclusion	121
8	Discussion and conclusion	123
8.1	Evaluating the model	123
8.2	Model contributions	125
8.3	Conclusion	128
A	The implementation	129
A.1	The implementation	129
A.2	Numerical Methods	133
A.3	Program source listing	134
B	Glossary	159
C	Symbol list	163
	Bibliography	167

Chapter 1

Introduction

When in the summer of 1995 we faced the start of our master thesis, our only firm decision on the topic was one of modelling dynamic systems. The university curriculum requires that the modelling should be made to meet the requirements of a group of non-mathematicians. This coincided luckily with the SIMA group at the very moment needing a model of the human respiratory system.

SIMA is a project, which aims at creating an anaesthesia simulator for training and educating of nurses and anaesthesiologists. The project relies partially on experiences acquired in an earlier simulator project and started in February 1995. The planned simulator includes a computer, which will run the models of the reactions of the patient in various situations, and the necessary hardware to transfer the output of the models from the computer to standard anaesthesia monitors.

The SIMA group consists of people from different professions; medical doctors, mathematicians, engineers, and programmers. Both of the MDs Per Føge Jensen, and John Jacobsen, Herlev Hospital, have experiences from the previous simulator project, and are our experts on physiology and use of the simulator. The engineers from Anaesthesia Laboratory, Herlev Hospital are responsible for the interface between the computer and the anaesthesia monitors. The mathematicians from Roskilde University are creating the models in the simulator, which includes models of the cardio vascular system, pharmacokinetics and dynamics, temperature, electrolytes and fluid balance, the control by the central nervous system, and the respiratory system. The programmers from the company Math-Tech are responsible for implementation of the real time models in the simulator.

1.1 Identification of the problem

The SIMA requirement specification [Fre] from May 1995, says about the respiratory system

The respiratory model must describe the gas exchange, ventilation and concentration of carbondioxide, oxygen and the pH of blood.

This description leaves the level of detail needed unspecified. Should every organ be modelled as a specific part of the system, or would a model describing lungs and the rest of the body as a whole suffice? Must the model include the pulsatility of breath, or are mean values of the ventilation sufficient? Should the pulsatility of the blood flow be modelled? This, and similar questions, depend on what the output is to be used for, and on constraints on the computability of the models created.

We therefore realized that a part of our assignment, above the actual creation of a model, was the job of finding out exactly what the model was meant to be able to do. A preliminary literature survey gave us an overview of what existing model of the respiratory system offered and a continual dialog with the MDs of the SIMA group convinced us that none of the existing models met all requirements.

The model we present in this thesis is a model of the respiratory system without the control system. For use in the simulator the model must be connected to the other models of the simulator. During our participation in the project the interactions between the submodels in the simulator have been defined and revised. Thus model organization has been the subject for several seminars and meetings, we have participated in. We have developed the model with the intention that it should be part of the simulator, not an independent piece of work. This purpose has had an influence on the delimitation of our work, for instance manifesting the choice we have made of not modelling the control of the respiratory model, because the control of the respiratory system is a part of the control system of all the models of the simulator. We have put the transport of respiratory gasses with the blood into a wider frame, the transport system. Our requirements for the model of transport system are that the model can treat both the kinetics of the respiratory system and the pharmacokinetics. Furthermore we wish the model to be extendable to simulate transport of any substance, which is distributed by the blood.

The fact that our model must cooperate with the other models of the simulator, being developed alongside with our work, make demands of the maintainability and extendability of our model. In order to comply with these requirements it is our task to develop a theory based model. The model has to be close to the physiology: variables and parameters should correspond to recognizable physiological quantities. This should ease the communication with the MD experts and improve the well-definedness of the interface to the other models. The close resemblance also makes it easier to detect, when short cuts and approximations have been made, and thus supports later extensions.

1.2 Methods

In attacking the problems identified above, we found communication with the MDs to be difficult, perhaps due to the lack of a common language in which one can describe the physiology, and to a difference of professional tradition. In order to overcome this obstacle we made a list of scenarios that contained a description of special courses of events the model should be able to simulate. The model had to meet the expectations of the medical doctors by ensuring that it could respond to anything they wanted.

When modelling, we have made extensive use of the results from other fields. Obviously physiology has been the source of information of the working of the system in question, but physiology relies heavily on physics, and we had to do as well. Chemistry has also proved relevant, as several chemical reactions are involved in the transport of matter in the blood. As the purpose of it all has been to develop a mathematical model, mathematics has of course been the central field. Furthermore we have also experienced that mathematics proved very valuable in structuring the information we have drawn from the other fields. Finally some amount of computer programming skill has gone into solving our models, and the computer science discipline of system development has supplied some understanding to the complexity of the process of extracting the "real" requirements from the future users of the model. Fortunately we are well equipped in most of these fields as Tine does physics as her second subject, and Claus does computer science.

Our prior knowledge of physiology, medicine, chemistry and biology was not very extensive. We have therefore spent quite some time studying the subjects in question and have also used the expertise that we have access to.

A very useful way of understanding the physiological processes has been to

read and discuss the modelling efforts described in literature. By studying the equations of models, we have got a different line of approach to the dynamic processes. Often leading to a comprehension of the assumptions behind the models, and giving a good inspiration for our own modelling efforts. Even though the actual implementation of the models in the final simulator computer program will not be our task, we have worked on implementing the models, we found adequate. This work has been necessary in order to determine if the models behaved in a realistic way. In addition we got knowledge of the dynamics of the models by simulations, a knowledge that we could afterwards verify by an analysis of the model equations.

How to read the thesis

It is our hope that people with different interests can benefit from reading this thesis. We have aimed at describing the physiological background for our modelling efforts in a way that will enable people without any knowledge of mathematics to draw conclusions on the extent of the models. In addition this means that the thesis is supposed to be understandable without any prior knowledge to physiology.

In chapter 2 we will describe the system, we are aiming at modelling. We specify the requirement of the model and give a overview of existing models from the literature of the system in question. Our modelling is presented in chapter 3 and 4, describing the models of the transport of substances in the lung and the blood respectively. In chapter 5 we give an overview of the model equations and discuss the mathematical properties of the model. The parameters of the models and their physiological range are stated in chapter 6, and in chapter 7 output of the model is discussed.

The composition of this thesis reflect the intention of developing a theory based model, in which the particular output of the model has had a limited impact on the modelling process. The simulations have benefitted our understanding of the dynamic system modelled, but has not suggested drastic changes or new approaches to the modelling. Thus the chapter evaluating the output of the models is placed in the end of this thesis, and the parameters of the models are treated before the testing, since the parameters have to lie within certain theoretically based ranges.

In this thesis the primary focus is the creation of the models, rather than on the analysis of them. Therefore the mathematical challenge has been finding the relevant mathematical tools for setting up the equations. The field of

our work, modelling the respiratory system, includes a more general study of compartment models based on [Jac0] and [Gib].

Section	Page	Section	Page	Section	Page	Section	Page
1. Introduction	8	2. The Problem	10	3. The Solution	12	4. Conclusion	14
5. Appendix A	16	6. Appendix B	18	7. Appendix C	20	8. Appendix D	22
9. Appendix E	24	10. Appendix F	26	11. Appendix G	28	12. Appendix H	30
13. Appendix I	32	14. Appendix J	34	15. Appendix K	36	16. Appendix L	38
17. Appendix M	40	18. Appendix N	42	19. Appendix O	44	20. Appendix P	46
21. Appendix Q	48	22. Appendix R	50	23. Appendix S	52	24. Appendix T	54
25. Appendix U	56	26. Appendix V	58	27. Appendix W	60	28. Appendix X	62
29. Appendix Y	64	30. Appendix Z	66	31. Appendix AA	68	32. Appendix AB	70
33. Appendix AC	72	34. Appendix AD	74	35. Appendix AE	76	36. Appendix AF	78
37. Appendix AG	80	38. Appendix AH	82	39. Appendix AI	84	40. Appendix AJ	86
41. Appendix AK	88	42. Appendix AL	90	43. Appendix AM	92	44. Appendix AN	94
45. Appendix AO	96	46. Appendix AP	98	47. Appendix AQ	100	48. Appendix AR	102
49. Appendix AS	104	50. Appendix AT	106	51. Appendix AU	108	52. Appendix AV	110
53. Appendix AW	112	54. Appendix AX	114	55. Appendix AY	116	56. Appendix AZ	118
57. Appendix BA	120	58. Appendix BB	122	59. Appendix BC	124	60. Appendix BD	126
61. Appendix BE	128	62. Appendix BF	130	63. Appendix BG	132	64. Appendix BH	134
65. Appendix BI	136	66. Appendix BJ	138	67. Appendix BK	140	68. Appendix BL	142
69. Appendix BM	144	70. Appendix BN	146	71. Appendix BO	148	72. Appendix BP	150
73. Appendix BQ	152	74. Appendix BR	154	75. Appendix BS	156	76. Appendix BT	158
77. Appendix BU	160	78. Appendix BV	162	79. Appendix BW	164	80. Appendix BX	166
81. Appendix BY	168	82. Appendix BZ	170	83. Appendix CA	172	84. Appendix CB	174
85. Appendix CC	176	86. Appendix CD	178	87. Appendix CE	180	88. Appendix CF	182
89. Appendix CG	184	90. Appendix CH	186	91. Appendix CI	188	92. Appendix CJ	190
93. Appendix CK	192	94. Appendix CL	194	95. Appendix CM	196	96. Appendix CN	198
97. Appendix CO	200	98. Appendix CP	202	99. Appendix CQ	204	100. Appendix CR	206
101. Appendix CS	208	102. Appendix CT	210	103. Appendix CU	212	104. Appendix CV	214
105. Appendix CW	216	106. Appendix CX	218	107. Appendix CY	220	108. Appendix CZ	222
109. Appendix DA	224	110. Appendix DB	226	111. Appendix DC	228	112. Appendix DD	230
113. Appendix DE	232	114. Appendix DF	234	115. Appendix DG	236	116. Appendix DH	238
117. Appendix DI	240	118. Appendix DJ	242	119. Appendix DK	244	120. Appendix DL	246
121. Appendix DM	248	122. Appendix DN	250	123. Appendix DO	252	124. Appendix DP	254
125. Appendix DQ	256	126. Appendix DR	258	127. Appendix DS	260	128. Appendix DT	262
129. Appendix DU	264	130. Appendix DV	266	131. Appendix DW	268	132. Appendix DX	270
133. Appendix DY	272	134. Appendix DZ	274	135. Appendix EA	276	136. Appendix EB	278
137. Appendix EC	280	138. Appendix ED	282	139. Appendix EE	284	140. Appendix EF	286
141. Appendix EG	288	142. Appendix EH	290	143. Appendix EI	292	144. Appendix EJ	294
145. Appendix EK	296	146. Appendix EL	298	147. Appendix EM	300	148. Appendix EN	302
149. Appendix EO	304	150. Appendix EP	306	151. Appendix EQ	308	152. Appendix ER	310
153. Appendix ES	312	154. Appendix ET	314	155. Appendix EU	316	156. Appendix EV	318
157. Appendix EW	320	158. Appendix EX	322	159. Appendix EY	324	160. Appendix EZ	326
161. Appendix FA	328	162. Appendix FB	330	163. Appendix FC	332	164. Appendix FD	334
165. Appendix FE	336	166. Appendix FF	338	167. Appendix FG	340	168. Appendix FH	342
169. Appendix FI	344	170. Appendix FJ	346	171. Appendix FK	348	172. Appendix FL	350
173. Appendix FM	352	174. Appendix FN	354	175. Appendix FO	356	176. Appendix FP	358
177. Appendix FQ	360	178. Appendix FR	362	179. Appendix FS	364	180. Appendix FT	366
181. Appendix FU	368	182. Appendix FV	370	183. Appendix FW	372	184. Appendix FX	374
185. Appendix FY	376	186. Appendix FZ	378	187. Appendix GA	380	188. Appendix GB	382
189. Appendix GC	384	190. Appendix GD	386	191. Appendix GE	388	192. Appendix GF	390
193. Appendix GH	392	194. Appendix GI	394	195. Appendix GJ	396	196. Appendix GK	398
197. Appendix GL	400	198. Appendix GM	402	199. Appendix GN	404	200. Appendix GO	406
201. Appendix GP	408	202. Appendix GQ	410	203. Appendix GR	412	204. Appendix GS	414
205. Appendix GT	416	206. Appendix GU	418	207. Appendix GV	420	208. Appendix GW	422
209. Appendix GX	424	210. Appendix GY	426	211. Appendix GZ	428	212. Appendix HA	430
213. Appendix HB	432	214. Appendix HC	434	215. Appendix HD	436	216. Appendix HE	438
217. Appendix HF	440	218. Appendix HG	442	219. Appendix HH	444	220. Appendix HI	446
221. Appendix HJ	448	222. Appendix HK	450	223. Appendix HL	452	224. Appendix HM	454
225. Appendix HN	456	226. Appendix HO	458	227. Appendix HP	460	228. Appendix HQ	462
229. Appendix HR	464	230. Appendix HS	466	231. Appendix HT	468	232. Appendix HU	470
233. Appendix HV	472	234. Appendix HW	474	235. Appendix HX	476	236. Appendix HY	478
237. Appendix HZ	480	238. Appendix IA	482	239. Appendix IB	484	240. Appendix IC	486
241. Appendix ID	488	242. Appendix IE	490	243. Appendix IF	492	244. Appendix IG	494
245. Appendix IH	496	246. Appendix II	498	247. Appendix IJ	500	248. Appendix IK	502
249. Appendix IL	504	250. Appendix IM	506	251. Appendix IN	508	252. Appendix IO	510
253. Appendix IP	512	254. Appendix IQ	514	255. Appendix IR	516	256. Appendix IS	518
257. Appendix IT	520	258. Appendix IU	522	259. Appendix IV	524	260. Appendix IW	526
261. Appendix IX	528	262. Appendix IY	530	263. Appendix IZ	532	264. Appendix JA	534
265. Appendix JB	536	266. Appendix JC	538	267. Appendix JD	540	268. Appendix JE	542
269. Appendix JF	544	270. Appendix JG	546	271. Appendix JH	548	272. Appendix JI	550
273. Appendix JJ	552	274. Appendix JK	554	275. Appendix JL	556	276. Appendix JM	558
277. Appendix JN	560	278. Appendix JO	562	279. Appendix JP	564	280. Appendix JQ	566
281. Appendix JR	568	282. Appendix JS	570	283. Appendix JT	572	284. Appendix JU	574
285. Appendix JV	576	286. Appendix JW	578	287. Appendix JX	580	288. Appendix JY	582
289. Appendix JZ	584	290. Appendix KA	586	291. Appendix KB	588	292. Appendix KC	590
293. Appendix KD	592	294. Appendix KE	594	295. Appendix KF	596	296. Appendix KG	598
297. Appendix KH	600	298. Appendix KI	602	299. Appendix KJ	604	300. Appendix KK	606
301. Appendix KL	608	302. Appendix KM	610	303. Appendix KN	612	304. Appendix KO	614
305. Appendix KP	616	306. Appendix KQ	618	307. Appendix KR	620	308. Appendix KS	622
309. Appendix KT	624	310. Appendix KU	626	311. Appendix KV	628	312. Appendix KW	630
313. Appendix KX	632	314. Appendix KY	634	315. Appendix KZ	636	316. Appendix LA	638
317. Appendix LB	640	318. Appendix LC	642	319. Appendix LD	644	320. Appendix LE	646
321. Appendix LF	648	322. Appendix LG	650	323. Appendix LH	652	324. Appendix LI	654
325. Appendix LJ	656	326. Appendix LK	658	327. Appendix LL	660	328. Appendix LM	662
329. Appendix LN	664	330. Appendix LO	666	331. Appendix LP	668	332. Appendix LQ	670
333. Appendix LR	672	334. Appendix LS	674	335. Appendix LT	676	336. Appendix LU	678
337. Appendix LV	680	338. Appendix LW	682	339. Appendix LX	684	340. Appendix LY	686
341. Appendix LZ	688	342. Appendix MA	690	343. Appendix MB	692	344. Appendix MC	694
345. Appendix MD	696	346. Appendix ME	698	347. Appendix MF	700	348. Appendix MG	702
349. Appendix MH	704	350. Appendix MI	706	351. Appendix MJ	708	352. Appendix MK	710
353. Appendix ML	712	354. Appendix MN	714	355. Appendix MO	716	356. Appendix MP	718
357. Appendix MQ	720	358. Appendix MR	722	359. Appendix MS	724	360. Appendix MT	726
361. Appendix MU	728	362. Appendix MV	730	363. Appendix MW	732	364. Appendix MX	734
365. Appendix MY	736	366. Appendix MZ	738	367. Appendix NA	740	368. Appendix NB	742
369. Appendix NC	744	370. Appendix ND	746	371. Appendix NE	748	372. Appendix NF	750
373. Appendix NG	752	374. Appendix NH	754	375. Appendix NI	756	376. Appendix NJ	758
377. Appendix NK	760	378. Appendix NL	762	379. Appendix NM	764	380. Appendix NO	766
381. Appendix NP	768	382. Appendix NQ	770	383. Appendix NR	772	384. Appendix NS	774
385. Appendix NT	776	386. Appendix NU	778	387. Appendix NV	780	388. Appendix NW	782
389. Appendix NX	784	390. Appendix NY	786	391. Appendix NZ	788	392. Appendix OA	790
393. Appendix OB	792	394. Appendix OC	794	395. Appendix OD	796	396. Appendix OE	798
397. Appendix OF	800	398. Appendix OG	802	399. Appendix OH	804	400. Appendix OI	806
401. Appendix OJ	808	402. Appendix OK	810	403. Appendix OL	812	404. Appendix OM	814
405. Appendix ON	816	406. Appendix OO	818	407. Appendix OP	820	408. Appendix OQ	822
409. Appendix OR	824	410. Appendix OS	826	411. Appendix OT	828	412. Appendix OU	830
413. Appendix OV	832	414. Appendix OW	834	415. Appendix OX	836	416. Appendix OY	838
417. Appendix OZ	840	418. Appendix PA	842	419. Appendix PB	844	420. Appendix PC	846
421. Appendix PD	848	422. Appendix PE	850	423. Appendix PF	852	424. Appendix PG	854
425. Appendix PH	856	426. Appendix PI	858	427. Appendix PJ	860	428. Appendix PK	862
429. Appendix PL	864	430. Appendix PM	866	431. Appendix PN	868	432. Appendix PO	870
433. Appendix PP	872	434. Appendix PQ	874	435. Appendix PR	876	436. Appendix PS	878
437. Appendix PT	880	438. Appendix PU	882	439. Appendix PV	884	440. Appendix PW	886
441. Appendix PX	888	442. Appendix PY	890	443. Appendix PZ	892	444. Appendix QA	894
445. Appendix QB	896	446. Appendix QC	898	447. Appendix QD	900	448. Appendix QE	902
449. Appendix QF	904	450. Appendix QG	906	451. Appendix QH	908	452. Appendix QI	910
453. Appendix QJ	912	454. Appendix QK	914	455. Appendix QL	916	456. Appendix QM	918
457. Appendix QN	920	458. Appendix QO	922	459. Appendix QP	924	460. Appendix QQ	926
461. Appendix QR	928	462. Appendix QS	930	463. Appendix QT	932	464. Appendix QU	934
465. Appendix QV	936	466. Appendix QW	938	467. Appendix QX	940	468. Appendix QY	942
469. Appendix QZ	944	470. Appendix RA	946	471. Appendix RB	948	472. Appendix RC	950
473. Appendix RD	952	474. Appendix RE	954	475. Appendix RF	956	476. Appendix RG	958
477. Appendix RH	960	478. Appendix RI	962	479. Appendix RJ	964	480. Appendix RK	966
481. Appendix RL	968	482. Appendix RM	970	483. Appendix RN	972	484. Appendix RO	974
485. Appendix RP	976	486. Appendix RQ	978	487. Appendix RR	980	488. Appendix RS	982
489. Appendix RT	984	490. Appendix RU	986	491. Appendix RV	988	492. Appendix RW	990
493. Appendix RX	992	494. Appendix RY	994	495. Appendix RZ	996	496. Appendix SA	998
497. Appendix SB	1000	498. Appendix SC	1002	499. Appendix SD	1004	500. Appendix SE	1006
501. Appendix SF	1008	502. Appendix SG	1010	503. Appendix SH	1012	504. Appendix SI	1014
505. Appendix SJ	1016	506. Appendix SK	1018	507. Appendix SL	1020	508. Appendix SM	1022
509. Appendix SN	1024	510. Appendix SO	1026	511. Appendix SP	1028	512. Appendix SQ	1030
513. Appendix SR	1032	514. Appendix SS	1034	515. Appendix ST	1036	516. Appendix SU	1038
517. Appendix SV	1040	518. Appendix SW	1042	519. Appendix SX	1044	520. Appendix SY	1046
521. Appendix SZ	1048	522. Appendix TA	1050	523. Appendix TB	1052	524. Appendix TC	1054
525. Appendix TD	1056	526. Appendix TE	1058	527. Appendix TF	1060	528. Appendix TG	1062
529. Appendix TH	1064	530. Appendix TI	1066	531. Appendix TJ	1068	532. Appendix TK	1070
533. Appendix TL	1072	534. Appendix TM	1074	535. Appendix TN	1076	536. Appendix TO	1078
537. Appendix TP	1080	538. Appendix TQ	1082	539. Appendix TR	1084	540. Appendix TS	1086
541. Appendix TT	1088	542. Appendix TU	1090	543. Appendix TV	1092	544. Appendix TW	1094
545. Appendix TX	1096	546. Appendix TY	1098	547. Appendix TZ	1100	548. Appendix UA	1102
549. Appendix UB	1104	550. Appendix UC	1106	551. Appendix UD	1108	552. Appendix UE	1110
553. Appendix UF	1112	554. Appendix UG	1114	555. Appendix UH	1116	556. Appendix UI	1118
557. Appendix UJ	1120	558. Appendix UK	1122	559. Appendix UL	1124	560. Appendix UM	1126
561. Appendix UN	1128	562. Appendix UO	1130	563. Appendix UP	1132	564. Appendix UQ	1134
565. Appendix UR	1136	566. Appendix US	1138	567. Appendix UT	1140	568. Appendix UV	1142
569. Appendix UW	1144	570. Appendix UX	1146	571. Appendix UY	1148	572. Appendix UZ	1150
573. Appendix VA	1152	574. Appendix VB	1154	575. Appendix VC	1156	576. Appendix VD	1158
577. Appendix VE	1160	578. Appendix VF	1162	579. Appendix VG	1164	580. Appendix VH	1166
581. Appendix VI	1168	582. Appendix VJ	1170	583. Appendix VK	1172	584. Appendix VL	1174
585. Appendix VM	1176	586. Appendix VN	1178	587. Appendix VO	1180	588. Appendix VP	1182
589. Appendix VQ	1184	590. Appendix VR	1186	591. Appendix VS	1188	592. Appendix VT	1190
593. Appendix VU	1192	594. Appendix VV	1194	595. Appendix VW	1196	596. Appendix VX	1198
597. Appendix VY	1200	598. Appendix VZ	1202	599. Appendix WA	1204	600. Appendix WB	1206
601. Appendix WC	1208	602. Appendix WD	1210	603. Appendix WE	1212	604. Appendix WF	1214
605. Appendix WG	1216	606. Appendix WH	1218	607. Appendix WI	1220	608. Appendix WJ	1222
609. Appendix WK	1224	610. Appendix WL	1226				

Chapter 2

The respiratory system

The purpose of this chapter is to clarify our problem through a detailed presentation of the system to be modelled, a list of the requirements that the model must meet, a survey of modelling efforts found in the literature, and finally a discussion of whether our problem can be solved by one of the existing models.

Section 2.1 gives an overview of the respiratory physiology, followed by a more detailed description of the transport mechanism of the respiratory function, in the lung, the exchange between the lung and the blood stream, and by the blood flow. The requirements stated by the MDs of the SIMA group, are in section 2.2, followed by a brief description on how the model of the respiratory system fits into the grand view of the simulator, and which requirements are introduced by this. The literature survey in section 2.4 presents models of the respiratory system or parts of this. The final discussion of how the existing models meet our requirements can be found in section 2.5.

In writing the overview of respiratory physiology, we have found it impossible to separate the description of the physiological system from models of the physiology. We ascribe this not only to our own limitations, but also to the nature of descriptions of reality. Any description of the reality, here the respiratory system, will select some features and leave out others and are thus in a way models. This applies to physics and chemistry as well as to physiology, and hence it is not surprising that complete separation is not possible. We have, however, striven to keep the description as "pure" as possible.

2.1 The physiology of the respiratory system

The respiratory system is concerned with the transport of oxygen and carbondioxide between the atmosphere and the tissue and organs in the body. Oxygen is a necessity for human life. The standard oxygen consumption of the body is at rest 260 ml/min [Nun]. The oxygen is continuously delivered from the atmosphere to the organs and tissue via the lungs and the blood circuit. Carbondioxide is a waste product of the oxidative metabolism, and is carried by the blood in the opposite direction, from the tissue to the lungs, where it is removed by ventilation. The carbondioxide elimination rate through the lung is at rest about 160 ml/min [Nun]. Since carbondioxide dissolved in blood forms carbonic acid, which affects the pH value of the blood, the removal of carbondioxide is important for the acid/base balance of the blood.

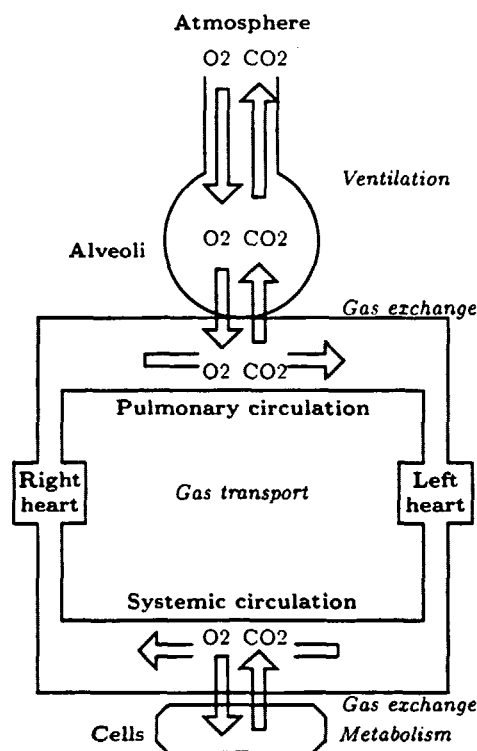


Figure 2.1: Schematic view of the respiratory system.

A tour of the respiratory cycle starts in the atmosphere outside the body. Oxygen enters the lung at inspiration as 21% by volume of the atmospheric air consist of oxygen. During the inspiration the air enters the lung through

the tree structure of the airways, and is mixed with the air already present in the lung. Down at the end of the pulmonary tree the air enters the alveoli, the sacs that form the "end" of the lung. From the alveoli the oxygen diffuses over a membrane into the blood of the small blood vessels, called the pulmonary capillaries. By this diffusion the content of oxygen in the alveoli is reduced, and hence the expiratory air contains only 16% oxygen.

Once the gas is in the blood stream, it is carried by the blood. Almost all distribution of the respiratory gasses in the body is by carriage in the blood stream. The flow of the blood is produced by the pressures created by the pumping action of the heart, so that all constituents of the blood move together. This transport of the gasses is much faster than diffusion. The branching of the blood vessels into tiny capillaries assures that the diffusion lengths are small, both in the lungs and in tissue. Almost all cells in the body are within a few cell diameters of at least one of the smallest branches [Van]. When blood flows through the capillaries of the tissue and organs the oxygen leaves the blood stream by diffusion and enters the cells, where it is used for metabolism. The metabolism produces carbondioxide, which then enters the blood by diffusion and is carried to the pulmonary capillaries. From here the carbondioxide diffuses over the lung membrane into the alveoli. From the alveoli it is transported through the airways to the atmosphere during expiration.

2.1.1 Ventilation

Under normal conditions breathing continuously renews the air in the lungs. During inspiration the air passes from the mouth and nose, through the tree-like conducting airways (figure 2.2) into the alveoli. At expiration the air flows the opposite way. In the alveoli the air and blood are brought very close so that oxygen and carbondioxide transfer can take place between them. The area of the blood-gas membrane of the 3 million alveoli of a standard man is about 90 m^2 [Gro].

The structure of the airways is a binary tree, where each new level of branching, called generation, doubles the number of pipes. Thus at the first generation (generation 0) the airways consist of a single pipe, named trachea, while at the last generation (generation 23) it consists of 8 million pipes. The first generations (0-19) are termed the conduction zone. At the later generations (20-23) small alveoli sacs appear on the pipes, and hence these generations are termed the respiratory zone.

In the following we describe the mechanism of airflow through the lung. Since

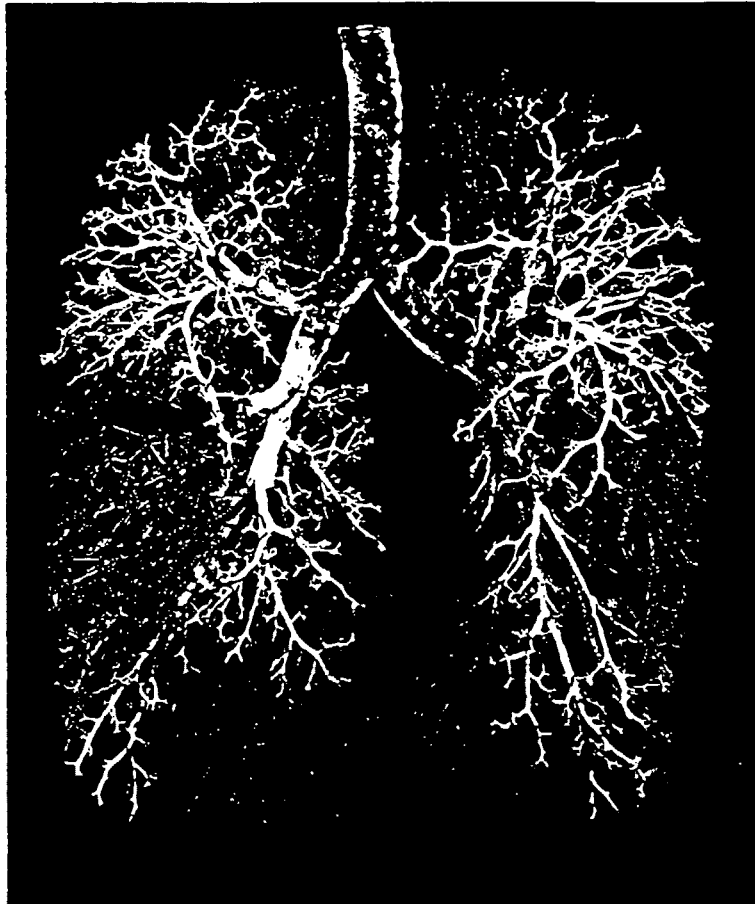


Figure 2.2: Cast of the airways of a human lung [Wes2].

the lung and airways have no muscles to drive ventilation. the lung can be compared to a bellows, with in and outflow of air driven by forces working on the outside.

Natural ventilation is similar to the normal operation of a bellows, while artificial respiration by a respirator is similar to filling the bellows by blowing into the pipe.

In the lung, natural ventilation is performed by movement of the the pulmonary walls, which cause a pressure difference and thus an airflow between the lung and the surroundings. The alveoli walls contain a fluid, the interpleural fluid, in the interstitial space between the lung and the thorax. This space makes up a single connected chamber throughout each lung, and is "fixed" on the "outside" to the thorax, and thus forces working on any wall of the interstitial space is transmitted by the fluid to all the rest of the walls by

a hydraulic principle. Natural breathing results from rhythmic contractions and relaxation of respiratory muscles. At inspiration the movements of these muscles cause the thorax to enlarge. When thorax is expanded by pulling surrounding muscles the force is transmitted to the lung via the interpleural fluid, forcing each alveolus to enlarge. The expansion causes the pressure within the alveoli to drop to less than atmospheric and the pressure difference causes an air flow into the alveoli. The ability of the lung to expand is termed the elastance and the inverse of the elastance is called the compliance.

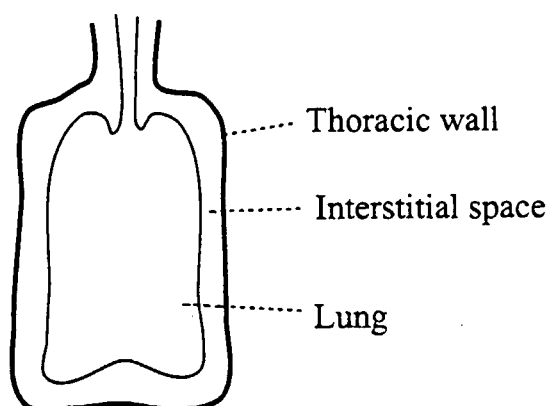


Figure 2.3: A schematic picture of the lung and the surroundings.

The pressure from the interstitial space gives the lung an elastic recoil. Normally expiration is caused only by the elastic recoil driving the air in the lungs the opposite way, but active forces contracting the thoracic cage can be applied. At end of an expiration the interstitial space has a pressure slightly below the atmospheric pressure. The force from the interpleural fluid thus prevents collapse of the alveoli.

During artificial ventilation the driving forces of the respiration muscles are replaced by an externally driven pressure source in the form of a respirator. Inspiration is obtained by raising the pressure in the ventilatory mask, and thus forcing air into the lung. When the pressure is removed elastic recoil drives expiration.

The volume of air flowing into and out of the lungs during each breath is called the tidal volume. At rest the tidal volume is about 0.5 l. Not all this air reaches the respiratory regions of the lungs, as some volume is situated in the conducting airways, and will be expired without any exchange with the blood. The volume of this air, which is about 0.15 l, is called the anatomical dead space. Gas from different regions of the lung will continuously mix due

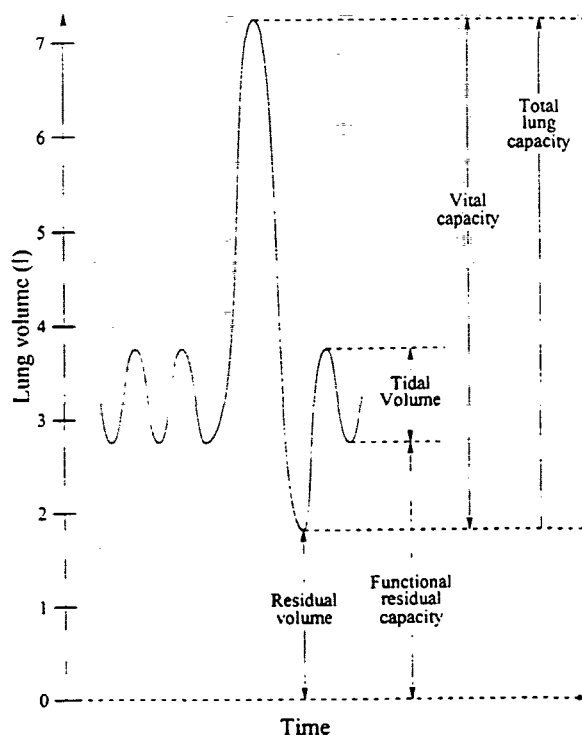


Figure 2.4: Lung volumes during the breathing cycle. The tidal volume in the normal respiration, but both expiration and inspiration can be increased, yielding the vital capacity.

to the thermal movements of the gasses. However, the anatomical dead space can be measured by analyzing the expired air and use the carbondioxide as a tracer gas. After expiration of the gas from the anatomical dead space is seen a sudden rise in carbondioxide concentration to the alveolar plateau level, which is about 3-4% [Nun].

Ventilation disorders are normally split into obstructive and restrictive. The obstructive ventilation disorders are cases in which the flow of air through the airways is obstructed. Restrictive disorders are cases in which regions of the lungs are damaged, resulting in lower compliance and possible decreased permeability of the lung membrane, cf. next section.

2.1.2 Gas exchange between lungs and blood

When the inspired air reaches the alveoli there is only a tiny permeable membrane of $0.2\mu\text{m}$ dividing the air from the blood of the typically 1800

capillary vessels that surround each alveolus, and thus O_2 and CO_2 are rapidly exchanged [Gro].

In the alveoli the atmospheric gasses exist in a mixture, but each gas behaves independently of the others, and thus it is the partial pressure of a gas that determines the movements of the gas. The partial pressure is defined as the pressure that the gas molecules exert against a wall by their thermal movements.

The oxygen and carbondioxide move between the alveoli and the blood by simple diffusion, caused by a difference in partial pressures on the two sides of the membrane, so that the net transport of a gas is from the region with high partial pressure into a region where it is low.

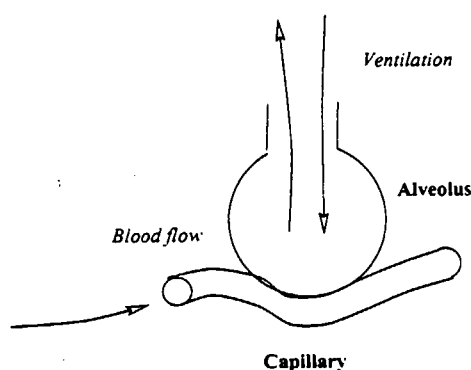


Figure 2.5: An alveolus and a capillary. Each alveolus is typically surrounded by 1800 capillaries.

To understand the diffusion mechanism between the air and the blood one can image a jam jar, half filled with water. The random thermal motions of the gas molecules will let the gas diffuse to areas where the pressure is low, even into the liquid. Thus some of the gas will dissolve into the liquid. Since the diffusion happens by random movements, a higher number of molecules in an area will result in more molecules diffusing out of the area. Thus, eventually the random movements of molecule from the gas phase to the liquid phase will equal the random movements in the other direction and an equilibrium state is obtained. The same amount of molecules passes from the air to the water as in the opposite direction and the net transport is zero. Thus in the equilibrium state the pressure of the gas is uniform throughout the jar.

The relationship between the concentration of a gas dissolved in liquid and the partial pressure expresses a distribution of gas between the two phases. If no chemical reaction takes place the concentration in the solvent is by a

good approximation proportional to the pressure, and the proportionality factor expresses the solubility of the gas in the liquid. A highly soluble gas will adjust at a equilibrium, with a large amount of molecules per volume the liquid, while a gas with a low solubility will have more gas molecules in the gas phase, see figure 2.6. The solution of a gas in a liquid may include other effects than random thermal movements, as some of the molecules may react with molecules in the liquid. Yet, regardless of how the gas dissociates in the liquid, the gas will adjust towards equal partial pressure in liquid phase and gas phase.

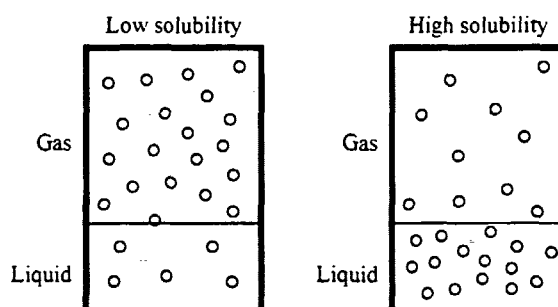


Figure 2.6: Different distributions due to different solubilities.

To distinguish between the gas in the gas phase and the gas dissolved in the liquid, we have in this report used the term pressure for the gas in the gas phase and the equivalent term tension for the pressure of the gas dissolved in the liquid.

Oxygen is poorly soluble in water. Hence it is by chemical binding to the blood components, that a sufficient oxygen concentration in the blood flow is reached. Without these oxygen carrying components a very high partial pressure of oxygen in the alveoli or a much faster blood flow would have been required, in order to transport the 260 ml of oxygen each minute, that the body utilize. At normal atmospheric pressure and with a normal content of blood components more than 98% of the oxygen in the blood is bound to blood components.

The main carrier of oxygen in the blood is hemoglobin, a protein found in the erythrocytes (red blood cells). The oxygen is reversibly bound with hemoglobin. Hemoglobin combined with oxygen is called oxyhemoglobin, and hemoglobin not combined with oxygen is called deoxyhemoglobin or reduced hemoglobin.

Carbondioxide is much more soluble in blood, but also in the case of carbondioxide the transport is improved by chemical reactions. The dissolved

carbondioxide reacts reversibly with water and with hemoglobin and some carbondioxide are therefore transported as bicarbonate or carbamino compounds.

When carbondioxide reacts with water an acid is formed, and hence there is correspondence between the carbondioxide level and the acid base balance in the blood. The acid-base balance is expressed by the pH value, which is the negative logarithm of the concentration of hydrogen ions. Variations in the pH value is buffered by the way hydrogen ions participate in the chemical reactions in the blood. The hydrogen ions combine with both bicarbonate ions and hemoglobin, and therefore the pH value influences the dissociation of both oxygen and carbondioxide in the blood.

Even in this complicated case of dissociation at which the two gasses affect the dissociation of each other through the chemical reactions, the gasses will adjust towards equal pressure in the blood and the surrounding tissue or alveoli as long as the membrane separating the two phases is permeable. This happens because the equilibrium of the chemical reactions are shifted, when soluted gas is moves across the membrane, and a new chemical equilibrium adjust as the diffusion happens.

There are several respiratory disorders that can result in imperfect gas exchange between the atmospheric air and the blood. A disorder often associated with damaged lung tissue is a defect membrane that inhibits the diffusion, called a restrictive lung disorder. Alternatively the perfusion of a part of the lung may be restricted, so that the air of some alveoli remain unexchanged. Another case is that of an obstructive lung disorder that limits ventilation to part of the lungs, and causes the blood perfusing this part of the lung to leave the lung more or less unexchanged. The latter two cases are often referred to as imperfect ventilation-perfusion ratio.

Not even for a healthy lung the ratio between perfusion and ventilation are ideal throughout the lung, but for defect lungs the differences might be extreme and thus significant for the transport of respiratory gasses.

2.1.3 The blood circuit

When gasses have been exchanged through the pulmonary membrane, the blood leaves the pulmonary capillaries. Like the air in the lungs the blood in the pulmonary capillaries is continuously renewed, as the blood is circulating. The blood flow is driven by the heart in two serially connected circuits, the pulmonary and the systemic circuit, see figure 2.7. From the right ventricle the blood is pumped into the pulmonary circuit, through the

pulmonary capillaries, where the oxygenation and carbondioxide elimination takes place, back into the left heart chambers. From there the oxygenated blood is pumped into the systemic circuit, through the capillaries of various parts of the body and back to the right heart chambers.

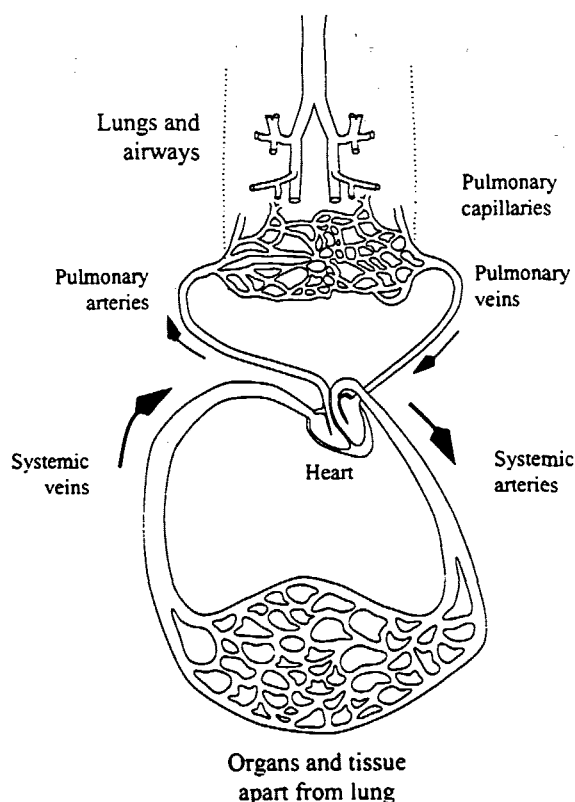


Figure 2.7: The blood circuit and the lungs.

During the circulation of the blood in the systemic circuit, the organs and tissue are supplied with oxygen to be used for metabolism, and carbondioxide, the waste product of the metabolism, is transported to the lung. Thus when blood enters the right heart chamber the oxygen content in blood is therefore lower than in arterial blood, and a higher content of carbondioxide is found in venous blood than in arterial blood. The exchange of oxygen and carbondioxide in the tissue happens by diffusion over the membranes surrounding the blood vessels, and is thus controlled by the tension gradients over the membranes.

The standard cardiac output is 5.2 l/min. Almost all of the blood flow in the pulmonary circuit is pumped through the pulmonary capillaries, only about 2% is shunted past the lung. In the systemic circuit each organ receives a

fraction of the total blood flow.

In cases of respiratory disorders or hard work, the oxygen supply might become insufficient. In such cases metabolism occurs in absence of oxygen. However, carbondioxide is also waste product of this anaerobic metabolism, and is still removed from the tissue by the blood. If the elimination of carbondioxide through the lung is reduced, the consequence will soon be an increased amount of carbondioxide and hence a decreased pH value in the blood.

There are several possible disorders in the blood transport system. Either the blood circulation can cause trouble, or the chemical balance of the blood may be displaced resulting in a impaired carriage of substances. Chemical disturbances may occur for several reasons; the chemical balance is influenced by the level of the metabolic waste products, and will therefore be affected by a changed metabolism. Or disturbing substances might enter via the ventilation, an example is carbon monoxide poisoning, which disables the hemoglobin molecules. Finally the transport system might be disordered by a change in the blood components, e.g. the blood content of hemoglobin may be low (anaemic blood).

2.2 Requirements of the models

We have found the formulation of our modelling task for this thesis rather vague. This is partly due to the lack of a common vocabulary; but even after we had acquired the necessary physiology, the extend of the model has been wide open, perhaps because the MDs had no firm idea of what it would be possible to model. Therefore it has been a non-trivial job to decide which requirements the MDs really wanted the model to meet, and to formulate these requirements in terms of inputs, outputs, variables, and parameters.

During the modelling we have had a unmistakable need to see measured data from different scenarios, in order to concretize the kind of courses the MDs are used to, and wanted the model to reproduce. Yet only in a few cases has it actually been possible for the MDs to acquire such data. It is rare that text books of physiology contains more quantitative descriptions of the dynamic course of diseases and anaesthetics. Logs of data measured during actual anaesthetics situations has also been unavailable.

In order to decide precisely what a model of the respiratory system must be able to do, we have found it necessary to describe the requested outputs of the system, and the conditions under which the model is expected to

simulate realistic physiological data. This sections give a list of specific model requirements we have compiled by a dialogue with the rest of the SIMA group. The list is the result of a process that has been carried out simultaneously with the modelling.

2.2.1 Requirements of the lung model

The purpose of a lung model is to constitute the connection between the atmosphere and alveoli in such a way that simulations of defect lungs are possible. The quantities concerning the ventilation, which are observed during surgery, are the composition of gasses in the expired air. In case of artificial respiration, the mask pressure and the tidal volume are measured as well. These quantities are usually plotted dynamically in a pressure-volume loop. Disorders of the lung can be observed by disturbances in these outputs.

The lung model must therefore produce pressure-volume diagrams and keep track of the partial pressures of gasses in the expiratory air and in the alveoli. These output must behave realistic in the simulations of respiratory disorders. Even though the alveolar partial pressures are not measurable quantities during an operation, the values will affect the gas status of the blood, and cause changes in the tensions of gas in the arterial blood. Hence it is an indirect requirement that the alveolar partial pressure are modelled.

The relevant defects to simulate are lungs with changed compliance, increased resistance to airflow, and lungs with a reduced permeability of the membrane dividing the pulmonary capillaries and the alveoli.

These cases must be simulated under different circumstances, as the patient can either be ventilated artificially or breathe naturally. Under different clinical circumstances the composition of air inspired by the patient are changed. This is for instant done when a patient is anaesthetized by inhaling the anaesthetic agents. Thus in the model the composition of inspired air must be a changeable input parameter.

2.2.2 Requirements of the model of the blood transport system

A model of the blood transport system must keep track of different quantities referring to the status of CO_2 and O_2 content in blood at various places of the body. The most important quantities are those, which is observed during surgery. This is the tension of oxygen and carbondioxide, the saturation

of hemoglobin with oxygen and the pH value of the blood plasma. These quantities are normally measured in both arterial and venous blood.

When the MDs observe changes or abnormalities in the monitored data, these are normally ascribed to disturbances in either the ventilation, the metabolism, the blood circuit or to an abnormal blood content of the components that interact with the respiratory gasses. The model is required to include the first three cases.

Changes in the blood concentration of O_2 and CO_2 are not trivial, because of the chemical interactions between the respiratory gasses, the hemoglobin and the hydrogen ions. Model requirements explicitly state that the model outputs a pH, based on the concentration of carbondioxide. If the gas dissociation model contains data of the important gas carrying blood components this will further enable simulations of a patient with abnormal content of these, e.g. hemoglobin.

As a countermeasure to disturbances the MDs can in the clinical situation, change the composition of inspired air, and/or ventilate the patient artificially. Our model must reproduce the changes in the measured blood data that are the effect of such countermeasures.

2.3 The other models in SIMA

The model of the respiratory system must coexist with the other models of the simulator, and this presents some requirements to the model. A schematic overview of the simulator can be seen in figure 2.8.

The cardiovascular system: A model that describes how the blood flows through the arteries and veins. Among the outputs of the model is the cardiac output, and how the blood is distributed to the organs and the other tissue.

Temperature: A model of the temperature at different places in the body. The temperature is linked to the metabolism, because heat is a byproduct of the metabolic processes.

Electrolytes and fluid balance: Modelling of this has not started yet, but the task will be to model the balance of certain ions and liquids in the body. The acid/base status of the blood might be seen as a special case of this problem.

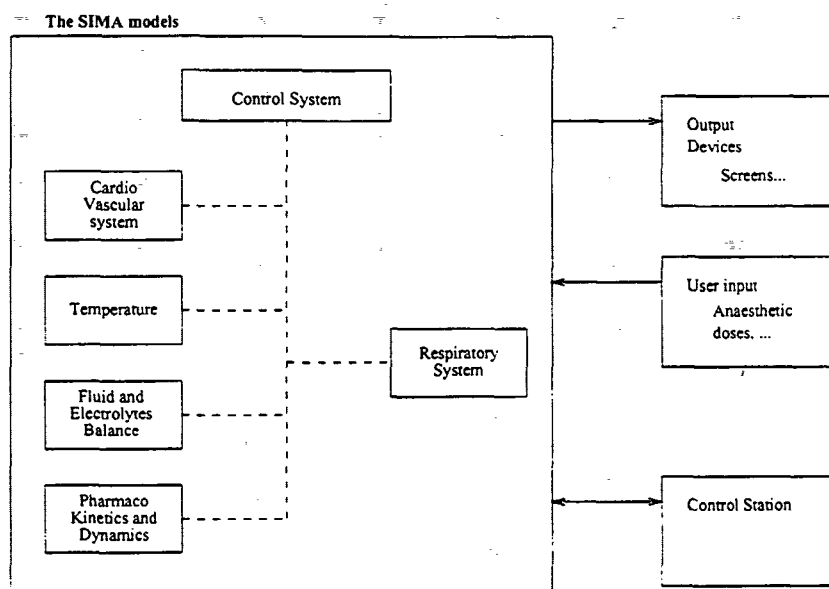


Figure 2.8: Overview of the SIMA simulator.

Pharmacokinetics and dynamics: Models of the distribution (kinetics) and effects (dynamics) of drugs, like anaesthetic agents, in the body. The main mean of distribution is by carriage in the blood stream, similar to how oxygen and carbondioxide is transported inside the body.

Control System: The control system models the central nervous system, and the way parameters of the other models are regulated. This is often a task that cannot be solved inside a single model. An example is the regulation of cardiac output, that is affected both by the current blood pressure at various receptors, and by the oxygen and carbondioxide contents of the blood. Thus the regulation of the cardiac output is affected both by the cardiovascular system and the respiratory system.

2.4 Modelling done by others

In our study of the literature, we have encountered several models of aspects of the respiratory system. Some of the models describe the total system, but not necessarily with a level of detail that can honor the requirements we have of our model. Therefore we have also examined more detailed models of parts of the respiratory system. Our review will focus on how the models treat some crucial aspects of the physiology: The gas flow in and out of the

lung, and the mixing of gas inside the lung; the gas exchange between lung and blood; the blood transport system and the modelling of gas dissociation in the blood and the tissue; and the modelling of the relation between gas dissociation and pH value in the blood.

Both in models of the blood transport system and of the lung, we have encountered a special kind of differential equation model, the compartmental model [Chi0, Olo, Rid0, Jac0]. A compartment model uses a compartment to represent an area holding an amount of matter that is instantaneous mixed inside the compartment. The differential equation describing the development of matter in compartment, is then stated by the principle of mass preservation. The change of matter in the compartment is the flows into the compartment minus the flows out of the compartment. Compartment models are widely used in the modelling of biology and medicine [Jac0], and can describe both physical flows like the gas flow over the lung membrane and the more abstract flow when a substance changes into another by chemical reaction.

2.4.1 Models of the respiratory system

The most recent models of the respiratory system are found in [Olo] and [Chi0]. Older models are found in [Fin, Hop, Lon, Sau]. A common trait is that the control system has a prominent place in these models. Even though the control system is not a concern of ours, we find these models relevant, because they are the most general models of the respiratory system, we have found. All the models uses compartments to represent areas of the body, and write mass balance equations for each compartment.

The first model, by Erik Olofsen [Olo], focuses on the special situations in which ventilation is absent (apnoea). The primary results are the blood oxygen saturation, and the CO₂ pressure curves in the blood as a function of time. The curves show that the oxygen supply to the tissue is acceptable for up to 8 minutes without ventilation, if the lung is initially filled with pure oxygen.

The second model, by Chiari et al. [Chi0], is presented as a general model of the respiratory system, that is claimed to compare well to experimental data when simulations with an increased CO₂ and decreased O₂ level in inspired air are made.

Both models use a single compartment for the lung, describing both the gas filled alveoli and the blood filled capillaries. Thus instant equilibrium between the gas and the blood phase is assumed. Olofsen represents the body

by a single compartment, while Chiari et al. has a brain compartment and a compartment representing the rest of the body. The brain compartment is used for regulation of the system, reflecting that the central chemoreceptor for carbondioxide is situated in the brain.

The transport of oxygen and carbondioxide between the compartments is decided by dissociation of the gasses in the blood. The level of theoretical foundation for the exact nature of the dissociation differs significantly in the two models, see section 2.4.5. Olofsen uses a detailed dissociation model by Siggaard-Andersen. Chiari et al. uses a piecewise linear curve for the dissociation of O_2 and a model of their own for the dissociation of CO_2 .

It is not clear how Olofsen incorporates the acid/base balance of the blood in the dissociation curves. Chiari et al. neglects it for oxygen, but their model of carbondioxide dissociation does include the effect.

2.4.2 Models of the lung

The simplest models we have found of the lung are the models that are used in the compartment models of the respiratory system, described in the previous subsection. The lung is modelled as a single compartment with a constant volume, representing the mean lung volume. The compartment represents both the alveoli and the blood in the capillaries, with instantaneous equilibrium between the gas and the blood phase, and the flow in and out of the compartment describes both flow of gas carried by blood and air flow. The air flows in and out the lung are modelled as separate non-pulsative flows. Such lung models can be found in [Chi0] and [Olo].

All models we have found which increase the level of detail above a single compartment do so by partitioning the lung into several sections, and describing a pulsative gas flow in and out of these sections. Such models, modelling the actual "bellows" of the lung, are called *models of the mechanics of the lung*. Examples of such models are [Rid0, Chap. 5] and [Gol, Jac]. Furthermore we have examined an unpublished model developed by MD Gert Galster, who kindly sent us the model in the form of a computer program source code listing [Gal].

Common for all the models of the mechanics of the lung is that they express the models in terms of an equivalent electrical network. They differ however in how they partition the lung, and in whether they use constant or variable parameters for compliances and airflow resistances.

While the single compartment models of the lung consider a uniform gas mix in the compartment, and thus easily calculate the partial pressures of gasses

in the air mix, the models of the lung mechanics are normally not concerned with the mix of gas. The sole exception we have found is the model in [Rid0], where the network model of the total pressures in various lung sections are used to drive the flows in a compartment model that keeps track of the gas mix in the lung sections.

2.4.3 Models of the gas exchange between lung and blood

Models of the gas exchange fall in two categories. One type of model describes the gas exchange based on the ratio between ventilation and perfusion [Eva, Hop, Poo, Ril, Wes0]. The ventilation-perfusion ratio is much used in literature of physiology, and a main concern of all these models is the situation where the ratio is not uniform throughout the lung.

Other models have a more direct approach. Here the focus is on the composition of gas on each side of the lung membrane, and the flux through the membrane, [Gra, Pii].

2.4.4 Models of the blood transport

Apart from the models of the blood transport system modelled in the respiratory models, we have encountered models of the transport system that aim at describing pharmacokinetics, [And, Ler, Hul, Bis].

These transport models are compartment models like the respiratory models, but generally with more compartments. But basically the structure of the models is the same as the respiratory models, except that the carriage of matter by the blood is governed by other dissociation curves.

A completely different approach to modelling the kinetics of matter in the blood transport system is found in the one, two, or three compartment models used to describe pharmacokinetics, [Gib, Hul, Jac0]. These models claim no direct connection to the physiology but are fitted to produce good approximations of the time course of the concentration of an anaesthetic agent in the blood.

2.4.5 Dissociation models

The basic dissociation model that we have found several times is known in physics as Henry's law and states that if no chemical reaction takes place

between solute and solvent the solubility is constant at low concentrations of the solute [Atk]. Even in situations in which chemical reaction takes place, Henry's law is normally regarded as valid, for the part of the solute that has not reacted chemically.

The level of detail in models of oxygen and carbondioxide dissociation varies greatly. Oxygen dissociation varies from a three piece linear curve [Lon], over a ten piece linear curve [Rid0], and a quotient between two fourth degree polynomials [Kel] to a rather complicated expression by Siggaard-Andersen [Sig0, Sig3] and [Sig5]. Siggaard-Andersen models the dissociation of carbondioxide as well.

The model by [Chi0] is based on considerations of how the dissociation of carbondioxide interacts with the acid/base balance of the blood.

In the models we have studied, the dissociation models by Siggaard-Andersen are unique in their level of detail, and in the number of effects they include. They are the only models we have encountered, in which the mutual effect of oxygen and carbondioxide on the dissociation of each other is included.

2.4.6 Models of pH

We have only found one model of the blood acid/base balance and the pH value [Chi1]. The model is a set of chemical equations, describing the reactions between components of the blood. Other treatments of the acid/base balance of the blood are found in [Sig1, Sig2] and [Sin]. However these were not really models, but the theoretical considerations that could be used for modelling.

2.5 Our modelling

Based on the previously stated requirements, and our survey of the literature, we have reached the following conclusions on the nature of our own model.

None of models we have studied can meet all our requirements, and therefore we need to create a new model. The model must include a description of the lung and of the blood transport system. In the light of the fact that the model will have to cooperate with the rest of the SIMA models, we find it natural to make the model extendable in the number of substances that are transported both through the lung and in the blood stream. In this way the

same basic model can handle intravenous and inhaled anaesthetics, as well as the respiratory gasses.

Since the lung model is required to allow simulations with different compliances and air flow resistances, and produce pressure-volume diagrams, a single constant-flow ventilated compartment is not sufficient. The approach of describing air flows between separate sections of the lung seems more appropriate. This must be combined with a model of the mix of gasses in the lung sections, as we need the partial pressures for deciding the transport over the lung membrane, as well as the composition of the expired air for output. This is similar to the approach of Rideout [Rid0], but fundamental assumptions of the model are not clear. Therefore we will use the idea of a pressure model and a gas composition model, and develop a model of the gas mix from the overall flows.

Our lung membrane model will not be based on the ventilation-perfusion ratio, even though it is a commonly used parameter in the literature. Since models of the lung and the blood are required, it seems more natural to connect these, and model the membrane flux explicitly. If ventilation-perfusion ratio is needed later, it can be calculated from the gas flow in the lung and the blood flow. Furthermore the explicit approach gives the possibility of modelling impairment of transport due to membrane limitations, as well as inhomogeneous ventilation-perfusion ratios.

In accordance with the literature we have chosen to use a compartment model to describe the dynamics of the blood transport system. The movement of matter in and out of such compartments involves both diffusion and bulk flow, and thus we will need to determine both tensions and concentrations. Therefore we need models of the dissociation of the respiratory gasses. Even though we have no explicitly stated requirements of the level of detail such dissociation functions must have, the pH value is explicitly required as output based on the content of gasses in the blood. We therefore find it reasonable to demand that our dissociation functions includes the effects of the pH value, since the literature agree that pH affects the dissociation of both carbondioxide and oxygen significantly. Without a proper link between the amount of dissociated oxygen and carbondioxide and the acid/base balance we find it unlikely that we would be able to construct an acceptable model of the pH value.

Finally we will need a model of the metabolism, that can maintain an appropriate metabolic rate under normal circumstances, produce anaerobic metabolism in situations with insufficient supply of oxygen, and be increased as a response to external input, e.g. from the temperature model.

An overview of the interconnections between the parts of our model can be seen in figure 2.9.

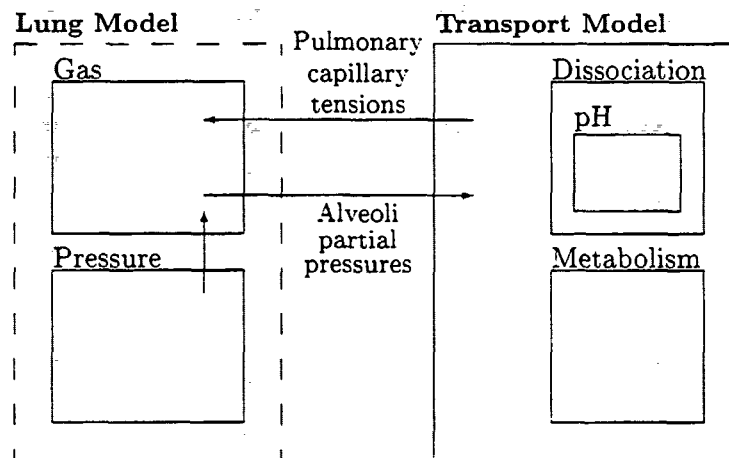


Figure 2.9: Overview of the models of the respiratory system.

Chapter 3

Modelling the lung

This chapter presents our models of the airway dynamics. Let us therefore summarize the considerations on this part of the system and the purpose of the models of the lung, which was discussed in chapter 2.

The task of the lung model is to connect the atmosphere (or the respirator mask) and the alveoli by a model of the airflow. The model must divide the lung into various parts and calculate the flow of oxygen, carbondioxide and possibly anaesthetic gasses among these parts. The output of the lung model is the pressure at the mouth and the tidal volume, which is the data usually measured with a spirometer, the partial pressures of the expired air, usually measured with a gas analyzer, and the partial pressures in the alveoli. The partial pressures of the alveoli are not directly measurable, but must be known for the modelling of the exchange of gasses through the lung membrane. The membrane transport will be part of both the lung model and the blood transport model, as it is by this transport the models interact.

When modelling airway dynamics, we split the model into two parts; the pressure model and the gas model. The former model describes the total pressure in parts of the lung, while the latter model keeps track of the gas composition in the different parts of the lungs. Hence the output of the pressure models are used to create the pV -diagrams and are further used as input to the gas model, which produces the required partial pressures in various parts of the lung.

A basic assumption of both parts of the lung model is that the gasses of the model are considered to be ideal, obeying the ideal gas law

$$pV = nRT, \quad (3.1)$$

where p is pressure, V is volume, n is amount of molecules, R is the gas constant, and T is temperature in kelvin. The ideal gas law does not hold for real gasses, and these are better described by the approximative van der Waals equation [Atk, chap.1]. However the deviations of the relevant gasses from being ideal are very small at room temperature and atmospheric pressure.

In both models we assume that the net transport of gasses through the pulmonary membrane is zero, so that the exchange of gas with the blood does not cause any differences in the total pressure. This might not be true for a situation at which the metabolism is anaerobic, but we do not expect the influence of this difference to be significant, as the carbondioxide diffusion into the lung is small compared to the alveolar volume.

3.1 The pressure model

Before we describe how to divide the lung in an appropriate way, we will discuss some assumptions on how the pressures, volume and flows in the system interact with the anatomy of the lung.

Under some circumstance an airflow through a tube will tend to be turbulent. For instance turbulence occur at branch points in the tube or if the radius of the tube changes. Both of these situation are found in the system we are modelling. At high flow rates, compared to the diameter of the tube and the physical properties of the gas, the flow becomes turbulent as well. Therefore it is likely that a mixed flow pattern occurs in the lungs. especially in situations with the inhalation of an anaesthetic gas, which has a high density and low viscosity relative to air [Nun, p. 49]. However we assume the airflow of the system to be laminar, as we find it impracticable to model a partly turbulent flow through the pulmonary tree. Furthermore none of the models from the literature we have seen treat turbulence.

We now consider the dynamics of a laminar flow. The relation between a pressure difference (ΔP) and an laminar bulk flow (F) of a fluid through a tube are describe by Poiseuilles formula [Atk, p.741]. At low pressure differences the relationship can be considered to be linear, and thus the relation is described by

$$F = \frac{\Delta P \pi r^4}{8\eta l} \quad (3.2)$$

where the proportionality factor $R = \pi r^4 / 8\eta l$ expresses a resistance to the airflow. R is determined by the viscosity of the gas η , and the length l and the

radius r of the tube. The radius of the airways change during the breathing cycle due to the elasticity of the pipes, and so does the airway resistance. However we have not found data of the variations of the airway resistance, and we will therefore model the resistance as constant during a breath.

During natural inspiration the air flow into the lung is caused by the pressure difference that arises from an enlargement of the lungs. When the lung volume is decreased at expiration, the air is pressed out of the lungs. This effect is described by the ideal gas law, which states that the product of pressure and volume pV is constant if the same amount of molecules n is present and the temperature is constant. The latter assumption is not necessarily valid, but since including variation in the temperature would increase the complexity considerably, we have chosen to assume constant temperature. This is in agreement with the models we have seen in the literature.

In figure 3.1 the relationship between the lung volume and the pressure difference between alveoli and the interpleural fluid is shown. The pressure difference is often called the transmural pressure Δp_t . The compliance of the lung C_l is found as the slope of the curve, which is almost constant for lung volumes during the normal ventilatory cycle. Thus C_l measures the ability of the lung to enlarge when pressure of the interpleural fluid decreases. We can therefore write the relationship between the transmural pressure and the volume of the lung as

$$V = C_l \Delta p_t + V_0 \quad (3.3)$$

where V_0 is the volume of the unstretched lung, found at end of an unforced expiration, when the pressure in the lungs equals the pressure of the interpleural fluid.

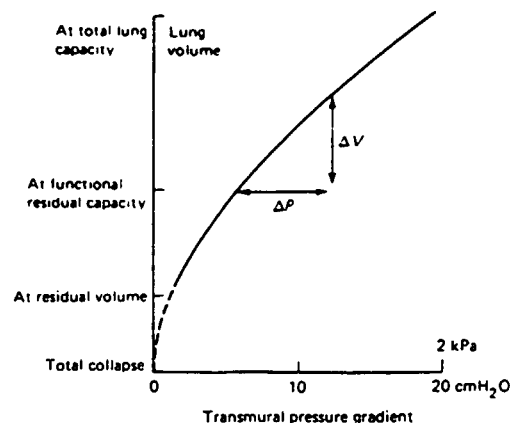


Figure 3.1: Plot of the lung volume as function of the pressure difference between the interpleural pressure and the lung pressure [Nun].

The relationships in equation 3.2 and 3.3 suggest that an equivalent electrical network is a very appropriate frame for modelling the pressure in the lungs. Air flows are equivalent to currents, pressures to potentials, flow resistances are resistances R , compliances are capacitances (C), which make volumes equivalent to charges. Inertances, resistance to accelerations of the flow are neglected, as the phenomenon of turbulence in airflow.

The instantaneous relationships between the current (I) and voltage (U) in the electrical network are given by ohm's law $U_R = RI$, equivalent to equation 3.2. The analogue law for a linear capacitance $CU_C = Q$ is added an extra term V_0 , because the origo of the transmural pressure in order to prevent a collapse of the lung differs from the atmospheric pressure, and the law becomes thus equivalent to equation 3.3.

In the electrical model the capacitors are compartments storing matters, and the currents are flows. Like the air flow in the lung, the flows in the networks are changing direction when the pressure differences change sign.

The electrical network modelling the pressure and air flows in the lung are used in several models we have seen in the literature. In this chapter we will refer to two examples of such models of the mechanical lung, because they represent two different principles of dividing the lung. The model of [Rid0] focuses on the mix of the inspired gas with the air in the deadspace before the exchange of gasses with blood in the alveoli and models serially connected parts of the lung representing the conducting airways, while the second model [Gal], we present, is focusing on a nonuniform ventilation of alveoli throughout the lung and therefore models a lung divided into several parts containing alveoli.

The model of Rideout [Rid0], see figure 3.2, consists of four serially connected sections of the airways: the larynx, the trachea, bronchi, and alveoli. Between each section is a resistance.

The driving force is implemented as an oscillating generator, on the last three chambers, as only these are expanded with the thorax, and Rideout only aims at simulating natural ventilation. This network allows for a model of restricted airflow by changing one or several resistances in the network.

From MD Gert Galster, Bispebjerg Hospital, we have received an unpublished model of the lung, in form of a computer program [Gal]. From this we have extracted the following model, see figure 3.3. The model splits the lung into several (10-50) parallel sections, and describes each with an analogue electrical network of a resistance in series with a capacitor.

With this network Galster simulates a breathing cycle that consists of an

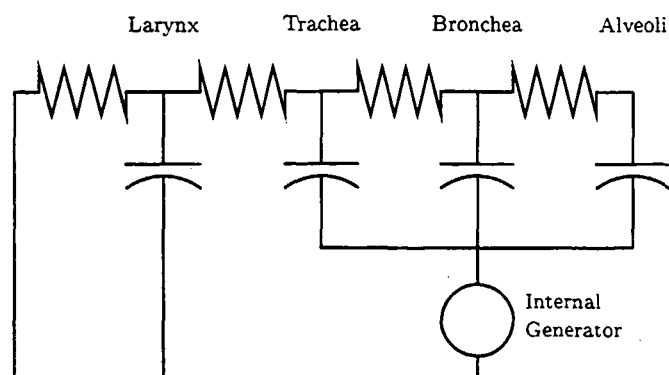


Figure 3.2: The model of the lung made by Rideout.

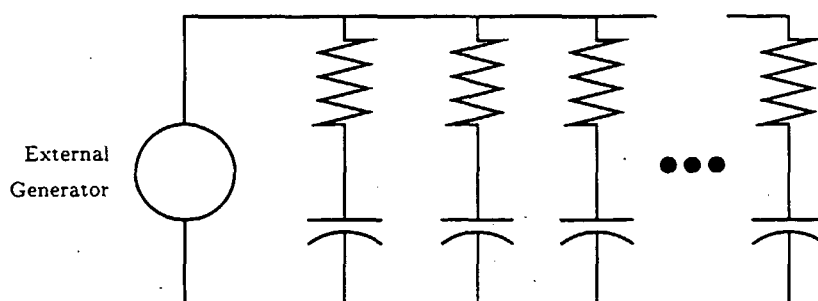


Figure 3.3: The model of the lung made by Galster.

inspiration period, an optional pause and an expiration period. The simulation can use one of two modes, one by which the inspiration is driven by an external source, and one by which the natural inspiration works with a constant inspired and expired volume at each breath. With this model non uniform ventilation of the alveoli can be modelled.

As we want to change the mechanical properties of the upper airways as well as the alveoli in different scenarios, we have developed a model, which combines aspects of both models. As in Galster's model we place several alveoli branches in parallel, each consisting of a resistance in series with a capacitor. With this electrical network we can simulate that the alveoli differs in their compliances, or that airflow is restricted in part of the lung. All these branches connect to a generator U_t (t for thorax), generating the transmural pressure induced by the respiratory muscles. The external pressure is the driving force at artificial respiration, and is represented by a generator U_m , (m for mouth) see figure 3.4. In parallel to the alveoli we have a capacitor

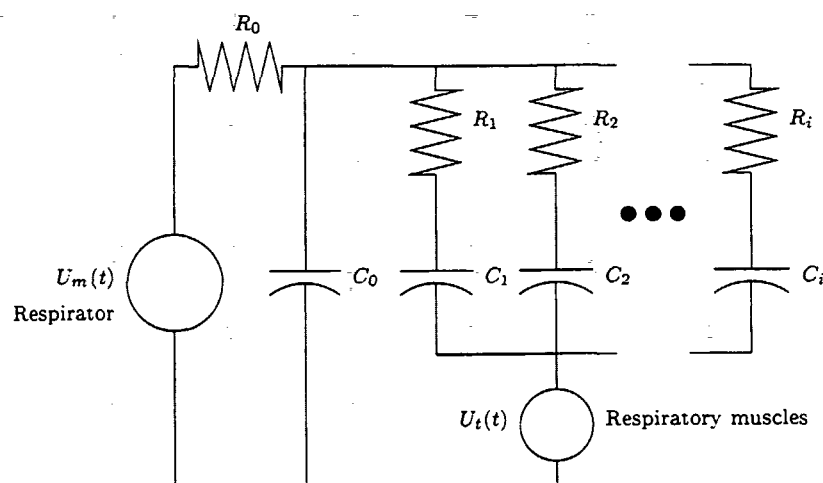


Figure 3.4: The pressure model.

C_0 representing the volume of air, which does not reach the areas in the lungs where gas exchange with the blood occurs. This volume models the anatomical dead space. The anatomical dead space is in the literature of the physiology considered to be constant, or is at least not believed to vary during a breath. We therefore model the anatomical deadspace as the unstressed volume of the capacitor C_0 , which has a low capacitance.

R_0 models the resistance of the upper airways. This is the largest resistance in the model as the resistance of the airways peaks at the fourth generation of branching, according to [Wes2]. The upper airways are in our terms the generations of branching without exchange of gasses with blood, generations 0–19. The alveoli represents generations 19–23. In figure 3.5 the pulmonary tree is depicted. The decision of only representing the upper airway with one capacitor in contrast to Rideouts model is based on advise we have received from Galster, that several serially connected parts are overkill, in order to include the mix of the inspired air with the deadspace.

The internal generator U_t is a sine wave, which can be eliminated (zero). This typically represents situations when the natural respiratory drive is inactivated. The external pressure must be an imitation of the pressure made by the respirator which is often found to be a serrated curve.

The model equations derived from the circuit in figure 3.4 express the change the pressure p in the various parts of the lung. The index of parameters and variables of the upper airways are 0, while the n alveoli parts have index i ,

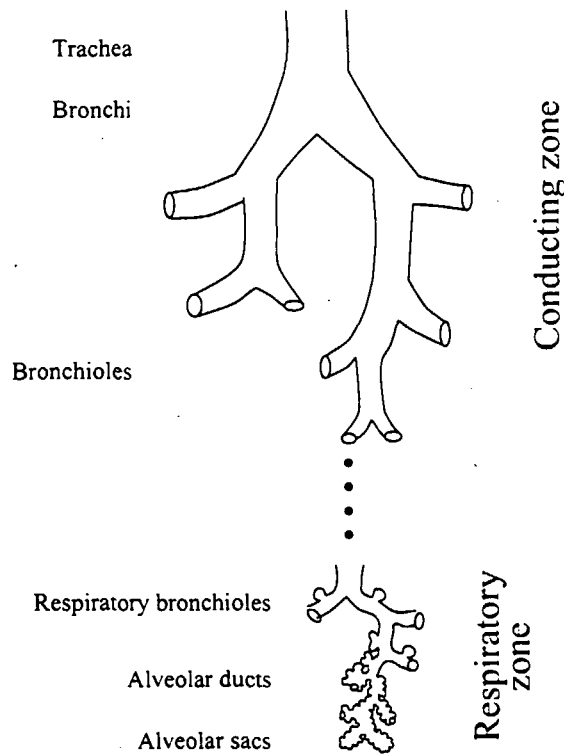


Figure 3.5: The branching of the pulmonary tree

from 1 to the number of alveoli sections n_a

$$\dot{p}_0 = \frac{1}{R_0 C_0} (U_m - p_0 - R_0 \sum_{i=1}^n C_i \dot{p}_i) \quad (3.4)$$

$$\dot{p}_i = \frac{1}{R_i C_i} (p_0 - p_i - U_i), \quad i = 1, 2, \dots, n_a \quad (3.5)$$

Equation 3.4 expresses the change in the pressure of the upper airways \dot{p}_0 calculated from the pressure in this part of the lung p_0 , the external pressure U_m and the change of pressure in the alveoli sections \dot{p}_i . The n_a equations in 3.5 express the change of pressure in the alveoli sections uses the internal and external pressures U_m and U_i and the pressure in the alveoli itself p_i . The RC terms of the equations have dimension of time and yields a characteristic time that expresses how fast the part of the lung empties or fills with air.

In order to plot the required pressure-volume (pV) diagrams we need to calculate the volumes of the different part of the lung, and we use relationship given in equation 3.3. Thus the alveolar volumes V_i and can be found from

the various alveolar pressures p_i :

$$V_i = C_i p_i + V_{0i}$$

where V_{0i} is the unstressed volume of the i 'th alveoli. The same relationship holds for the volume V_0 :

$$V_0 = C_0 p_0 + V_{00}$$

The sum of these volumes yields the total volume of the lungs, and enables the plot of the pV -loops, as the pressure at the mouth is known as the U_m , which is input to the model.

3.2 The gas model

On top of the pressure model, we need a model to calculate the partial pressures of the different lung sections, especially the alveolar partial pressures and the partial pressures of the expired air. We intend to model the partial pressures without keeping track of all gasses in the lung as for instance nitrogen has no particular interest, neither to the other parts of the model, nor as output during simulations. This approach implies that we neglect the change in the total pressure which might occur in the alveoli as result of a nonzero net diffusion through the lung membrane.

The lung sections represented by the capacitors in the pressure model, detailed in the last section, are the entities of the gas model as well. The subject in question here is the composition of the gas in each section. The gas composition is describe by a compartment model, in which each compartment models a section of the lung, precisely corresponding to the compliances of the pressure model. Thus the layout of the compartment model is decided by the layout of the network in the pressure model; the central compartment, represented by C_0 , connects to a number of alveoli compartments and to the mouth or respirator mask. Each alveoli compartment connects only to the central compartment and to the blood in the capillaries, see figure 3.6.

In the gas model of the lung, the flows between the compartments depend on the total pressures and partial pressures of gases in the compartments. The transport of gas between the lung sections includes two effects: air flow and diffusion. When a pressure difference exists throughout the lungs, the former effect is normally the most significant. The diffusion might be important when the bulk flow in case of no breathing (apnoe) is absent. According to thermodynamics, these effects will superimpose so that the bulk flow and the diffusion are not influencing each other, and we will consider the two effects apart.

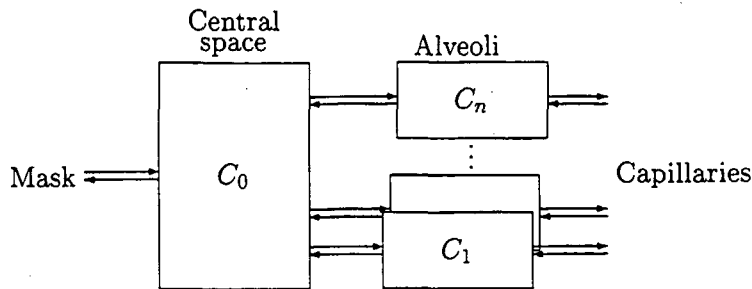


Figure 3.6: The gas model.

3.2.1 Laminar flow

We wish to model how the changes in the composition of air in the different parts of the lungs depend on the the total pressures, which is output from the pressure model, and on the composition of gas in these parts. For keeping track of several gas types, we will use vector variables, in which each coordinate refers to a specific gas. The first coordinate represents carbondioxide and the second oxygen. Two needed vector variables are the vector \mathbf{x} , which expresses the amount of each relevant gas and the fraction vector, \mathbf{f} , which expresses the fraction of the total amount of matter in mole (n) that each gas forms. Thus the relation between the two vectors are given by $\mathbf{x} = \mathbf{f}n$, and the change of matter can be expressed:

$$\frac{d\mathbf{x}}{dt} = \frac{d\mathbf{f}}{dt}n + \mathbf{f}\frac{dn}{dt} \quad (3.6)$$

For a model of all gasses in the lung the components in \mathbf{f} always adds to one, but as we do not explicitly keep track of substances like N_2 in our model the sums of fractions may be less. The equations we seek for a specific compartment must express the relationship between the total pressures and the gas compositions in the actual and the surrounding compartments. In order to find such expression, we will first examine how the composition of gasses in a compartment is affected when this compartment is connected to another compartment j with a different composition of gasses, illustrated in figure 3.7.

A flow leaving a compartment will not change the mix of gas in the compartment, as the flow has the same mix, and therefore $\frac{d\mathbf{f}}{dt} = 0$ in this case. For a flow into the compartment with a different mix, matters are a little more complicated. An inflow will result in an increase in the total number of molecules, $\frac{dn}{dt}$. The composition of the inflowing molecules are the same as

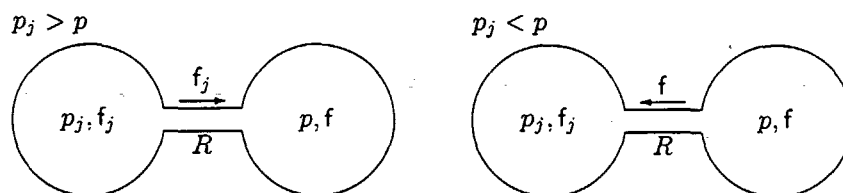


Figure 3.7: The change of a gas fraction in a compartment

the composition of gas in the compartment the flow comes from. Thus the change in amount of the gasses will be

$$\frac{dx}{dt} = f_j \frac{dn}{dt} \quad (3.7)$$

where f_j is the fraction vector of the gas in the inflowing air. The subscript j indicates that the vector refers to the gas fractions in the compartment from where the gas flows.

The laminar airflow between the compartments, discussed in section 3.1, are determined by the pressure difference ($p_j - p$) and the airflow resistance R ,

$$p_j - p = R \frac{dn}{dt} \quad (3.8)$$

Inserting $\frac{dx}{dt}$ and $\frac{dn}{dt}$ from equations 3.7 and 3.8 in equation 3.6, and isolating the term $\frac{df}{dt}$ yields:

$$\frac{df}{dt} = \frac{(f_j - f)(p_j - p)}{nR} \quad (3.9)$$

To obtain a differential equation of only one unknown variable, f , we express the amount of molecules n in equation 3.9 by the total pressure of the compartment, which is known as input from the pressure model. Gasses in our model are still assumed to obey the ideal gas law. Thus assuming that the change in volume and pressures does not introduce a change in the temperature, we can express the amount of molecules

$$n = \frac{pV}{RT} \quad (3.10)$$

where p is pressure, V is volume, n is amount of molecules, R is the gas constant, and T is temperature. The varying size of a compartment will

introduce a change in the pressures inside the compartment. We are assuming that the compliance of the lung is constant. When the gas is in an elastic compartment with compliance C and an unstressed volume V_0 , the relation between pressure and volume is $V = Cp + V_0$, and combination with equation 3.10 yields the following expression for the amount of gas in a compartment.

$$n = \frac{Cp^2 + V_0p}{RT} \quad (3.11)$$

Combining equations 3.11 and 3.9, we obtain an equation describing the change of mix when gas is flowing into a compartment:

$$\frac{df}{dt} = \frac{(p_j - p)(f_j - f)RT}{R(Cp^2 + V_0p)} \quad (3.12)$$

where $p \neq 0$ follows from the physical situation.

Combining the special cases above, the contribution to the change in the fraction vector of a compartment when air flows between this and another compartment can be expressed:

$$\frac{df}{dt} = \begin{cases} 0 & \text{when } p \geq p_j \text{ (outflow)} \\ \frac{(p_j - p)(f_j - f)RT}{R(Cp^2 + V_0p)} & \text{when } p < p_j \text{ (inflow)} \end{cases} \quad (3.13)$$

To ease the writing we introduce the function I_- , which is 0 for negative arguments, and the identity function otherwise:

$$I_-(x) = \begin{cases} 0 & \text{for } x < 0 \\ x & \text{otherwise} \end{cases}$$

With this definition 3.13 can be written

$$\frac{df}{dt} = \frac{I_-(p_j - p)(f_j - f)RT}{R(Cp^2 + V_0p)}$$

3.2.2 Diffusion

The diffusion of gasses between two compartments will cause changes in the composition of gasses in both compartments, unless these have the same distribution of gasses. We will in this section estimate how much the diffusion contributes to the change in the gas content of the compartments. Looking at diffusion we can assume that the molecules of a gas behaves independently of the other gasses in the system, since diffusion is a process caused by the

random thermal motions of the molecules. The diffusive flux J expresses the net number of molecules of a gas passing through a unit area in unit time. The flux is given by Ficks first law of diffusion, which states that J is proportional to the concentration gradient of the gas in the direction of current interest [Mor].

$$J = -D \frac{\partial c}{\partial t}$$

where D is the diffusion coefficient. This coefficient depends on the viscosity η and the density ρ of the gas,

$$D = \frac{\eta}{\rho}$$

We now want to find the diffusion of a gas between two compartments. We assume any difference in concentrations between the two compartments is equally distributed over the distance l between the compartments. Thus the concentration gradient becomes

$$\frac{\partial c}{\partial t} = \frac{c_2 - c_1}{l}$$

where c_1 and c_2 are concentrations of the gas in the two compartments, and l is the length of the tube between the compartments. Hence with a tube of a cross sectional area A , the flow I of a gas is determined by

$$I = \frac{dx}{dt} = A \frac{\eta}{\rho} \frac{(c_2 - c_1)}{l} \quad (3.14)$$

The diffusion coefficients are specific for the respective gasses. Hence with this diffusion equation used for every gas present, the net diffusion of gasses between two compartments is not necessarily zero. Different diffusion coefficients of ideal gasses will imply a net flow and hence induce a difference in the total pressure of the two compartments. The pressure difference will give rise to a laminar flow. However the diffusion coefficient of all atmospheric gasses are approximately $10^{-5} \text{m}^2/\text{s}$ [Alo]. In case of anaesthetic gas mix the diffusion coefficient might differ from this order of magnitude, but in situations when an anaesthetic gas mixture is inhaled, periods without respiration are not found and a laminar flow will be dominant.

We therefore find it acceptable to assume the gasses have the same diffusion coefficient, which ensure that the net diffusion is close to zero. If the alveoli are filled with 100% oxygen, respiration may be absent for 5–6 minutes, without the patient becoming undersupplied with oxygen (hypoxic) [Nun]. The

question is whether a part of the oxygen in the anatomical deadspace is utilized, or only the supply in the alveoli is used, and how the effect of diffusion between the lung sections should be modeled in our lung configuration. We model the conducting zone in the pulmonary tree by a central compartment, which is connected to the alveoli. The central compartment is covering the generation 0–19 of the upper airways, and the alveoli compartment covers the 20–23 generations. An average distance¹ between these compartments are assumed to be 0.1m, and the total diameter less than 0.01m². Inserting these numbers in equation 3.14 it is obvious that the effect of diffusion between the compartments in our model is negligible, even in a long period without breathing. This is a consequence of the rough partition of the lung we have made. However the ratio of area and length between the 19 and 20 generation is approximately 500, hence the diffusion of a gas is about $0.005\Delta c$ per second, and approximately a fourth of the amount of oxygen in the 19'th generation will during 300 seconds diffuse into the alveoli from the upper compartment. Hence only a model with a more detailed description of the lung would benefit from a model of diffusion. In our model it is included in the instantaneous mix of gas inside each compartment, and only the diffusion through the alveolar membrane is explicitly modelled.

3.2.3 Compartment equations

With the equations in section 3.2.1 and the above considerations we are now ready to solve the problem of finding equations for the lung compartments.

The total change to the fraction vector of each compartment consists of the sum of the contributions from the laminar flow between all connections to other compartments.

The central compartment has connections to the respiratory mask reservoir, and to each of the alveoli compartments. Hence by the contribution from the flows to and from these compartments (cf. equation 3.13) the mass balance for the central compartment yields

$$\frac{df_0}{dt} = \frac{RT}{C_0 p_0^2 + V_{00} p_0} \left(\frac{I_+(U_m - p_0)(f_e - f_0)}{R_0} + \sum_{i=1}^n \frac{I_+(p_i - p_0)(f_i - f_0)}{R_i} \right) \quad (8.15)$$

where U_m and f_e is the pressure and the fraction vector of the atmosphere or the respiratory mask in case of artificial ventilation. Each alveoli compartment connects to the central compartment and exchange gas with the blood

¹All parameters used in this section are estimated on the basis of table 6.1.

through diffusion over the membrane to the capillaries. We model the membrane diffusion as $\frac{dx}{dt} = \kappa(p_{cp} - pf)$, thus the exchange of gasses depends on the pressure difference through the membrane and the elements of a diagonal matrix κ , which expresses the permeability of the membrane with respect to the particular gas.² From equation 3.6 we know that $\frac{dx}{dt} = \frac{df}{dt}n + f\frac{dn}{dt}$. This combined with the assumption that the total flow over the membrane is null, gives $\frac{df}{dt} = -\frac{f}{n}\frac{dn}{dt}$. The assumption that the net flow is absent is not always correct, but to calculate $\frac{df}{dt}$ without it would require that the membrane transport of all gasses was calculated to find the value of $\frac{dn}{dt}$. This could be done, but the transport model would have to keep track of nitrogen as well, and we find this to be an unnecessary complication of the model, since the error introduced is usually small. Under the assumption of no net transport of gas over the membrane, we obtain, by adding the contributions of equation 3.13 and the membrane diffusion the following equation for the gas fraction vector of alveolar compartment i :

$$\begin{aligned} \frac{df_i}{dt} = & \frac{RT}{C_i p_i^2 + V_{0i} p_i} \frac{I_+(p_0 - U_t - p_i)(f_0 - f_i)}{R_i} \\ & + \frac{RT}{C_i p_i^2 + V_{0i} p_i} \kappa(p_{cp} - p_i f_i) \end{aligned} \quad (3.16)$$

where U_t is the pressure caused by the respiratory muscles. The equations 3.15 and 3.16 constitute the gas model. Together with the pressure model, given by equation 3.4 and 3.5, these equations constitute our model of the lung. In chapter 5 we will discuss the mathematical properties of the models, and afterwards use the models for simulations of selected scenarios, but first we will present the model of the blood transport system.

²Elements outside the diagonal represents the influence of one gas on the permeability of another, an effect we assume absent. Yet there may be circumstances under which a more detailed modelling of the permeability could be relevant.

Chapter 4

The models of the blood transport system

This chapter presents our models of the blood transport system. Some decisions about the models have already been made in chapter 2 on the basis of the requirements of the models and of our literature review.

In summary the blood transport must keep track of the tension¹ and the concentration of carbondioxide, oxygen and various other substances transported by the blood flow, in the arteries and veins. We intend to model the transport of all substances in one compartment model so that the influence of especially the respiratory gasses on one another is dynamically modelled.

The state variables of the model is therefore a set of vectors. There must be one vector to describe the content of matter in each compartment, the vector components thus represent a substance each. The compartment model therefore consists of a set of differential equations, one for each compartment, describing changes in the vector components. These equations all take the same form, as the change is what flows into the compartment minus what flows out of the compartment:

$$\frac{dx}{dt} = \sum I - \sum O$$

Inside a compartment there is assumed to be an instantaneous mix. Thus with a compartment modelling a specific part of the body, one has assumed an equilibrium distribution of all substances in this part regardless of changes in other parts of the body. Until now we have not decided the actual number and

¹The term tension is used for partial pressure in blood and tissue to distinguish between the partial pressure in a gas phase and the partial pressure of a dissolved gas

the configuration of the compartments. Obviously there must be an arterial and venous blood compartment, in order to calculate the required tension of oxygen and carbondioxide in the blood. These two compartments must be connected to some compartments so that the flows between compartments represent the pulmonary circuit and the systemic circuit.

Since we intend to simulate the distribution of drugs in the body by use of our compartment model, we have chosen a model with a high level of detail, originally from [Ler]. This is almost the same model as the one in 'Model 10', [And], an earlier work on pharmacokinetics of the SIMA simulator. The compartment configuration is shown in figure 4.1. In this model the compartments which represent organs in the systemic circuit consist of both a tissue part and a blood part. In addition the model includes peripheral blood pools, that because of their different sizes cause a difference in circulation times through the systemic circuit. In the pulmonary circuit, we have extended the single capillary compartment of [Ler] with multiple pulmonary capillary compartments, one for each alveoli compartment of the lung model. The blood model connects to the lung model by each capillary compartment exchanging gas with one alveoli compartment, and vice versa. By such a configuration inhomogeneous ventilation-perfusion ratios throughout the lung can be simulated in a straight forward way. The blood flow through the two central blood pools is determined by cardiac output, Q , and the distribution of the blood to the various organs in the circuit, described by z_i , determines the fraction of Q , that each compartment receives. Both cardiac output, Q , and the fractions, z_i , are supposed to be output from the cardio-vascular model, but until the two models are coupled we will use constant mean values found in the literature e.g. [Ler].

4.1 The mass balance equations

As seen in figure 4.1, our model contains $13 + n_a$ compartments: 5 blood pools, 8 organ compartments, and n_a capillary compartments. The different types of compartments have different in- and outflows. The venous and arterial blood pools have only blood flows. The pulmonary capillaries have both blood flows and gas flows to and from the alveoli. And finally the organs have blood flows and flows determined by the metabolism, representing the consumption and production of matter.

The following sections describes each type of compartment, and it will be seen how the differential equation describing the actual compartment has either the pressure or the concentration as the state variable, depending on the

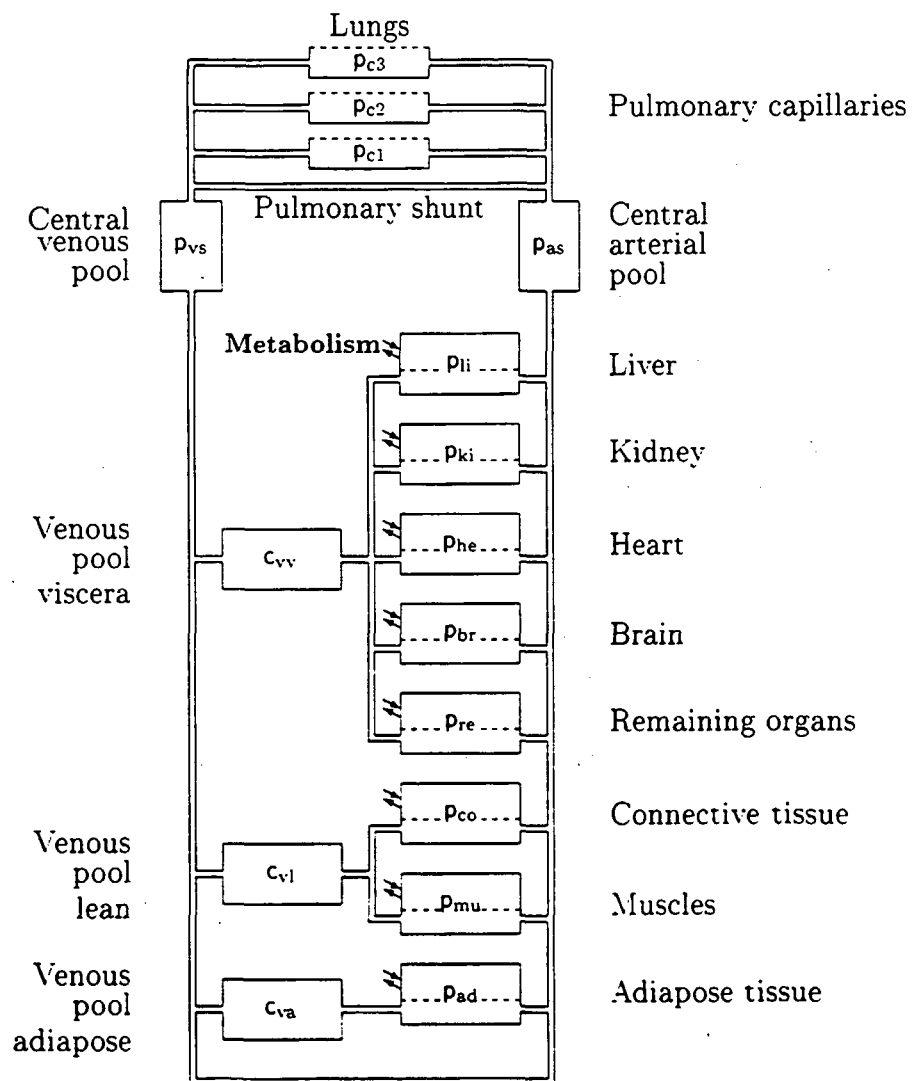


Figure 4.1: The blood transport model

nature of the compartment. The differential equation of a compartment is n dimensional, with state variable p or c vectors consisting of a CO_2 component, a O_2 component and $n - 2$ components for the present anaesthetic agents.

4.1.1 Organ compartments

An organ compartment as we find them in [Ler], [Olo] and [Rid0] consists of both a tissue and a blood part, see figure 4.2. We intend to use this dual compartment as well, in order to model regions or parts of the body with an equilibrium distribution of blood carried substances. The volumes of tissue and blood V_T and V_B in each compartment is assumed to be constant. The blood flow inside an organ branches into capillaries, in which diffusion of gases between blood and tissue takes place. This dual compartment models an assumption of instant equilibrium over the membrane between blood and tissue inside the organ. Thus the tension of each gas is assumed to be uniform throughout both tissue and blood inside the organ. This, however, does not imply that the concentration is equal in tissue and blood, as the solubility may differ, and a distribution of gas into the two solvents is found in an analogous way to the distribution of gas in a jam jar half filled with water, as discussed in section 2.1.2.

The dissociation of gasses is described by dissociation curves, which constitute a vector function containing a specific function for each gas and each solvent. The dissociation function yields a concentration c as function of the tension p of the actual substance, and might also depend on other variables of the model. e.g. the tensions of other gasses, pH value and temperature T . The dissociation function depends on the solvents, and thus we call the blood dissociation function c_b , and the tissue dissociation function c_t . The tissue dissociation function c_t may differ from compartment to compartment, while the blood dissociation function for gasses is common to all the compartments in the model.

The ability of the respiratory gasses to combine with the blood components makes the nature of the dissociation of these gasses rather complex. As we have chosen to use a model from the literature, which includes much of this complexity, the functions in the model are rather long expressions and depend on several variable quantities. In the case of carbondioxide the function is given only implicitly. We will present the dissociation models in a separate section, see section 4.3. In order to find the differential equations of the compartments, it is sufficient to know that the dissociation models exist, and that the dissociation functions are continuous and monotonously increasing.

However it is worth to notice, that because of the nature of the dissociation models, we have developed our own method for transforming the mass balance equations from describing the change of matters, x , in the compartment to an equation describing the change of tensions, p , in the compartment. By this method we avoid finding the inverse of the dissociation function, which is the method used in the model of the blood transport of respiratory gasses in the literature. In many of the models we have seen, approximated curves are used to describe the gas dissociation. This eases the task of finding the tension of a respiratory gas matching a certain concentration, but is an inadequate model of gas dissociation for our purposes.

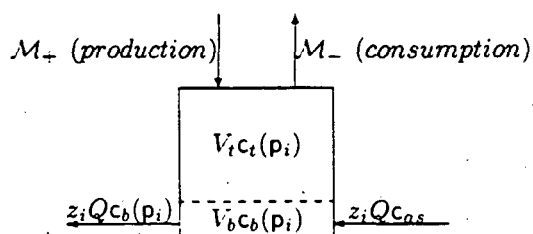


Figure 4.2: An organ compartment, with expressions for the content in the blood and the tissue phase, and the flows in and out.

We describe the organ compartments as instantaneously mixed and thus in equilibrium. This means that the tensions in the blood and the tissue are always the same. The assumption of local equilibrium, however, does not imply equilibrium between the different compartments of the model, since the transport limitation of the blood flows will allow dynamic differences. Physiologically this behaviour might be extracted from measurements of the blood content of an injected drug during the phase of distribution. In chapter 6 we will discuss the connection between our models and some typical empirical models of such measurements.

Each organ compartment receives a fraction of the total systemic blood flow z_i , all of it flowing from the arterial compartment. Since the blood volume inside the organ is considered constant, both the blood flow into and out of the compartment is $z_i Q$, where Q is cardiac output.

For an amount of matter in the compartment called x , represented by a vector with a component for each type of matter (CO_2 , O_2 and anaesthetic agents); the differential equation of the organ compartment, describing the change in x , is given by the matter flowing into the compartment minus the matter

flowing out of the compartment:

$$\frac{dx}{dt} = z_i Q(c_{as} - c_b(p)) + \mathcal{M}_+(p) - \mathcal{M}_-(p) \quad (4.1)$$

where p_i is the tension in the compartment. The in- and outflows of gas with the blood flow in equation 4.1 are calculated from the concentration of gas in the blood and the total blood flow through the compartment $z_i Q$. Concentrations in blood are found as function of the tension by use of the blood dissociation functions, $c_b(p)$. The subscribed *as* indicates that it is the gas concentration vector of the systemic arterial compartment, $c_{as} = c_b(p_{as})$. The two metabolic functions, \mathcal{M}_+ and \mathcal{M}_- , describe the tissue consumption and production, and are detailed in the section on metabolism, see section 4.2.

The gasses have uniform tension throughout the compartment, and thus the distribution of matter between the different phases can be found via the dissociation functions. The equation for the total amount of matter in the compartment is

$$x = V_t c_t(p) + V_b c_b(p)$$

where V_t and V_b are the tissue and blood volumes, and c_t and c_b are the tissue and blood dissociation functions. By substituting this into the differential equation, 4.1, we obtain:

$$\frac{d}{dt}(V_t c_t(p) + V_b c_b(p)) = z_i Q(c_{as} - c_b(p)) + \mathcal{M}_+(p) - \mathcal{M}_-(p)$$

By the chain rule $\frac{dc}{dt} = \frac{dc}{dp} \frac{dp}{dt}$, we thus can express the change in terms of $\frac{dc}{dp}$ and $\frac{dp}{dt}$:

$$V_t \frac{dc_t}{dp} \frac{dp}{dt} + V_b \frac{dc_b}{dp} \frac{dp}{dt} = z_i Q(c_{as} - c_b(p)) + \mathcal{M}_+(p) - \mathcal{M}_-(p)$$

Isolating $\frac{dp}{dt}$ we finally obtain:

$$\frac{dp}{dt} = \left(V_t \frac{dc_t}{dp} + V_b \frac{dc_b}{dp} \right)^{-1} (z_i Q(c_{as} - c_b(p)) + \mathcal{M}_+(p) - \mathcal{M}_-(p)) \quad (4.2)$$

In contrast to the models we have found in the literature, our compartment equation does not contain the inverse of the dissociation functions. This is due to the fact that we use the tension p as a state variable, and solve the question of distribution of matter between the two phases by the Jacobian

matrices $\frac{dc_i}{dp}$ and $\frac{dc_b}{dp}$. If this is to make sense we must assume the existence of $(V_t \frac{dc_i}{dp} + V_b \frac{dc_b}{dp})^{-1}$, and this will be investigated later, see section 5.2.2. Under this assumption we have arrived at a compartment equation that describes the content of gasses in the compartment by the state variable p and the dissociation functions.

4.1.2 Pulmonary capillary compartment

The pulmonary capillary compartments are the places for the exchange between the transport model and the gas model of the lung. In the lung model the oxygen, carbondioxide and anaesthetic agents are in gas phase and not dissolved in liquid. Thus the pulmonary capillaries have both blood flows carrying dissolved gasses and net diffusion of each gas through the membrane separating the capillaries and the alveoli, see figure 4.3. The gas flowing out

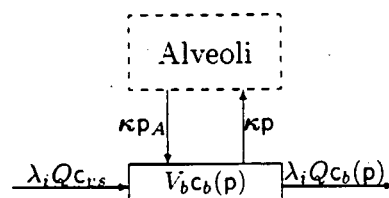


Figure 4.3: Pulmonary capillary compartment with expressions for contents and flows.

of the capillaries are determined by the tensions (partial pressures) in the blood and the permeability of the membrane with respect to the gasses κ . The gas flows into the capillaries are determined by the partial pressures in the alveoli, and is thus depending on the output of the gas model, and the permeabilities.

Normally the gas flow through the membrane is sufficiently fast to ensure that equilibrium is reached, and thus the partial pressures in the alveoli and the capillaries are equal [Nun], and [Wid]. This however is not the case if there are defects in the lungs, or in the case of injected anaesthetic agents, some of which do not penetrate the membrane. In order to enable simulations of these cases, the alveoli and pulmonary capillaries have been modelled by separate compartments. In that way instant equilibrium over the membrane is not assumed. In section 3.2 we saw the alveoli modelled as a number of compartments in parallel. The same number of capillary compartments are

chosen and connected to one alveoli compartment each. Hence we can model different abilities of gas exchange, ventilation, or blood perfusion in different parts of the lung.

According to the above considerations about in and out flows to the pulmonary capillaries, we obtain the following mass balance equation determining the amount of substance:

$$\frac{dx}{dt} = Q(1 - \lambda)(c_{vs} - c_b(p)) + \kappa(p_A - p) \quad (4.3)$$

with the factor λ being the pulmonary shunt factor (the part of the blood shunted past the lung). The permeability κ is a diagonal matrix describing the diffusion rate of the gasses through the membrane. c_{vs} is the concentration in the blood of central venous compartment, $c_{vs} = c_b(p_{vs})$.

Again we need the tensions p , since the diffusion through the membrane is determined by these. By a calculation equivalent to the one leading to the equation for the organ compartment, 4.2, we transform the mass balance equation, 4.3, to use p as the state variable:

$$\frac{dp}{dt} = (V_b \frac{dc_b}{dp})^{-1} ((Q(1 - \lambda)(c_{vs} - c_b(p)) + \kappa(p_A - p)) \quad (4.4)$$

4.1.3 Blood pools

A part of the blood is stored in the blood pools. There are two central pools, one on the venous side and one on the arterial side. Three peripheral blood pools simulate the different circulation times that exist in the body [Ler].

All flows in and out of the blood pools are blood flows, except in the case when injections are concerned. This makes concentrations an excellent system variable. Thus the following equation governs the change of the concentration in a blood pool compartment:

$$\frac{dc}{dt} = \frac{Q(c_j - c)}{V_b} \quad (4.5)$$

where Qc_j is the amounts of matters pr time flowing into the compartment, as Q is the blood flow through the compartment, and c_j is the concentration of the inflowing blood. The out flow is thus calculated as Qc , with c being the concentration of the compartment in focus, and V being the volume of the compartment.

When the blood is arriving from several compartments, the total concentration of inflowing blood c_i is found as the weighted average of the concentrations. Hence the concentration of blood when two flows merge is:

$$c_i = \frac{Q_1 c_1 + Q_2 c_2}{Q_1 + Q_2}$$

where c_i is the resulting concentration, Q_1 and c_1 the flow and concentration of one branch, and Q_2 and c_2 the flow and concentration of the other. The flow after the merge is $Q_1 + Q_2$.

Since the tensions of the arterial and venous pools are explicitly required as output from the model, we have chosen to use the tension as a state variable in these compartments, even though there are no flows that can only be decided by knowledge of this value. The reason is that we found it easier to apply the same transformation of state variable than to have to introduce the inverse of the blood dissociation function c_b . Thus by an equivalent transformation to the one used to reach equation 4.2 we find the following equation for the tension change in the central pools:

$$\frac{dp}{dt} = (V_b \frac{dc}{dp})^{-1} Q(c_x - c_b(p)) \quad (4.6)$$

where c_x is the concentration of the inflowing blood.

The transport model so far

We have now stated four different equations for the different kinds of compartments. Each type of differential equation contains terms, which has not been specified yet. This is the metabolism \mathcal{M}_+ and \mathcal{M}_- , and the dissociation functions $c_b(p)$ and $c_t(p)$. In the next sections we will present these submodels of the blood transport model. The dissociation curves depend on the pH value, so a model of the pH is presented as well.

4.2 Metabolism

Everywhere in the body metabolism takes place. In a model of the respiratory system the metabolism is an important part, together with the ventilation it constitutes the sinks and sources of the system. In our model we will neglect the metabolism in the blood and only let the organ tissue consume oxygen and produce carbondioxide. The metabolic function in the organs

is modelled by the terms \mathcal{M}_+ and \mathcal{M}_- in the differential equation for the organ compartments. These are vector functions modelling the metabolic production and consumption respectively. We have chosen to model the metabolism in these two different vector functions, because this way we can maintain the general principles of compartment models having only positive flows. The sign of each term in the differential equations determine whether it is an inflow or an outflow of the compartment.

Like the state vectors of the system, each coordinate in the vector function concerns the metabolism of a particular substance. The first coordinate is CO_2 , the second O_2 . In this section let us assume that only one substance more is carried around. This substance is an anaesthetic agent, which will be indicated by a subscript *aa*.

Carbondioxide is only removed by ventilation, so there is no consumption of CO_2 anywhere. Thus the \mathcal{M}_- consists of a zero as a first element. As long as oxygen is present in a compartment there will be a consumption. A simple view of the complicated chemical processes involved is that the metabolic consumption must tend to 0, as the concentration of O_2 tends to 0, and at high levels of oxygen some other factors will limit the metabolic rate. The O_2 metabolism is therefore modelled by a function in the Michaelis-Menten kinetic form [Bis]:

$$\frac{dx}{dt} = M \frac{c}{\beta + c} \quad (4.7)$$

where M is a constant representing the maximum metabolic rate, and β is a parameter representing the oxygen concentration when the metabolic rate is the half of the maximum value. It is easy to verify that the equation tends to the maximum metabolic rate M for c tending to infinity, and to 0 for c tending to 0.

The removal of anaesthetic agents is assumed only to take place in the liver [And]. Thus we can express \mathcal{M}_- in liver as

$$\mathcal{M}_{-li} = \begin{pmatrix} 0 \\ M_{\text{O}_2} \frac{c_{\text{O}_2}}{\beta_{\text{O}_2} + c_{\text{O}_2}} \\ M_{aa} \frac{c_{aa}}{\beta_{aa} + c_{aa}} \end{pmatrix} \quad (4.8)$$

The \mathcal{M}_- in organ compartments without anaesthetic metabolism models only a consumption of oxygen:

$$\mathcal{M}_- = \begin{pmatrix} 0 \\ M_{\text{O}_2} \frac{c_{\text{O}_2}}{\beta_{\text{O}_2} + c_{\text{O}_2}} \\ 0 \end{pmatrix} \quad (4.9)$$

The M_{O_2} differs from compartment to compartment. The sum of the maximum consumption rates of all organ compartments must under steady state conditions equal the rate which enters the body by ventilation.

The production of CO_2 only to a lesser extent depends on the present substances in the blood, as the tissue is metabolizing whether oxygen is present or not. Thus the metabolism may be either aerobic (with oxygen) or anaerobic (without oxygen), but in both cases the waste product is carbon dioxide. The total energy production compared to the amount of produced carbon dioxide is not the same at the different types of metabolism, and thus the CO_2 production is different, provided that the body produces a constant amount of energy. We have not modelled this difference.

The metabolic rates rely on the work that the body performs. In rest and under normal conditions, the production of CO_2 equals the rate, which is eliminated through the lungs, and M_+ is therefore modelled as the constant vector function, specific for each organ compartment:

$$\mathcal{M}_+ = \begin{pmatrix} M_{CO_2} \\ 0 \\ 0 \end{pmatrix} \quad (4.10)$$

Normal condition means that there is no reason for the body to perform more work. As a consequence of too low temperature, the muscles will begin to vibrate and therefore increase the CO_2 production, and as long as oxygen is present also the O_2 consumption. Thus when the coupling of the simulator models is done, the metabolic consumption and production \mathcal{M}_- and \mathcal{M}_+ , need to be modelled as functions of the temperature. It is reasonable only to model a temperature effect on the metabolism, if the temperature is too low. Else the normal metabolic rate is expected to be maintained. There can also be other conditions under which a metabolic rate will increase. In case of the allergic reaction, malign hyperthermia, the metabolic rate increases in response to a hypersensitivity to an anaesthetics. Malign hyperthermia will be modelled as a specific scenario, in which the \mathcal{M}_- is changed to a higher rate. This is an example of the dual nature of the temperature and the metabolism, as a clinical indication of malign hyperthermia is an increasing body temperature from the increased metabolism. During the malign hyperthermia the ion balance of the cells and the intracellular fluid is disturbed. Thus the scenario requires that a model of the electrolyte and fluid balance balance is coupled to the metabolic model and the model of the pH value.

4.3 Gas dissociation and the pH value

When writing the mass balance equations of the compartments in the blood transport models, we have assumed the existence of functions, which converts the partial pressures p (also called tension) to concentrations c . Furthermore when we change variables in the mass balance equation, we assume the existence of the derivative of the dissociation functions $\frac{\partial c}{\partial p}$.

The dissociation functions are specific with respect to the substances as well as to the solvents. Thus for any substance that we want to keep track of, we have to include a model of the dissociation of the substance into the different solvents in the model. Therefore to each solvent of the model, which is blood and different kinds of tissue, a dissociation vector function must be specified, in which the components are the dissociation functions of the solutes.

The dissociation of substances into tissue is considered in section 4.4.5. In this section we will describe the carriage of substances by the blood, and the interactions of the gasses in the blood on each other and the on pH value. Section 4.4 presents the models of the gas dissociation functions and the pH value. The requirements from the MDs (see section 2.2) do not include any specification of the gas dissociation, but the pH value of the blood has been required as output of the blood transport model.

The pH value is the negative logarithm of the concentration of hydrogen ions $[H^+]$. This is an important quantity measured during anaesthesia, as it interacts with the gas status of the blood. A measurement of the pH gives information about the acid-base balance, as the hydrogen ions are produced by acids, which dissociate. One acid in the blood is carbonic acid, formed by CO_2 soluted in water, and thus there are close relations between the CO_2 level and the pH value. Furthermore hydrogen, carbondioxide, and oxygen all form reversible combinations with hemoglobin, and thus changes of the blood content of one of the substances will displace the equilibrium of the reactions with hemoglobin, and change the concentration of all involved reactants.

A model of the gas dissociation in the blood must for any two tensions of carbondioxide and oxygen give the concentrations of the gasses and the pH value in the blood. The chemical interactions between these quantities imply that a change in one of the quantities causes at least three others to change as well. The only independent quantities of the five are the two tensions of gasses or the oxygen tension and the pH value.

We have no intention of modelling these interactions ourselves as our understanding of the biochemistry would not allow us to do so. In section 4.4.2 and 4.4.3 we present the models of dissociation of respiratory gasses from the

literature, which we found were the most adequate modelling of the system. The models give the concentrations of oxygen and carbondioxide as a function of tensions and the pH value. The models are developed for analyzing blood data, and they are consequently based on measurements of the pH value, the tensions of gasses, and other quantities that are not included in our work. Thus using these functions as submodels in the our blood transport model requires a model of the pH value. The pH value depends on the carbondioxide concentration and therefore the expression for the carbondioxide concentration is only implicitly given with the models of [Sig0] combined with a model of the pH value.

The criteria for the pH model is that it depends on the carbondioxide level, and produces an monotonously decreasing curve with a pH value of the venous and arterial CO_2 concentration or tension points, which is close to the physiological values.

The normal values for pH is 7.41 in arterial blood and 7.37 in venous blood [Nun]. Situations where the $[\text{H}^+]$ is raised are called acidosis, and if the concentration is below the normal level (corresponding to a high pH) one speaks about alkalosis. These changes in $[\text{H}^+]$ can either be due to a respiratory defect, where the elimination of CO_2 in the lung is too slow or too fast, or it can be a metabolic acidosis/alkalosis, referring to situations when the derivation in pH is not primarily due to respiratory problems. Models including the metabolic acidosis/alkalosis relates to the electrolyte and fluid balance, and our concern is therefore restricted to model the respiratory disturbances and the respiratory compensations to metabolic disturbances of the pH system, which will be described in the following as the respiratory buffer system.

The physiological range of pH in blood for a normal man is 7.0-7.8 [Wid]. The blood contains several buffer systems which will ensure that the $[\text{H}^+]$ varies only slightly when a concentration of some acid in the blood is changed. The buffer systems will immediately neutralize the excess H^+ by combining with it, until the body eliminates the hydrogen ions via the kidneys. We will only model the respiratory buffer system, and not include the metabolic excretion of hydrogen ions, as the excretion is a slow process, which we assume not to influence the state during an anesthesia.

The most important blood buffers are bicarbonate (produced by carbonic acid) and proteins, which make the buffer systems of the blood closely connected to the O_2 and CO_2 carriage in the blood plasma and the erythrocytes. The reactions related to the respiratory pH buffer system are described in the next subsections 4.3.1 and 4.3.2.

4.3.1 Carbondioxide carriage

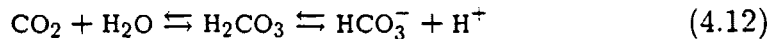
CO₂ is produced in the tissue, when metabolism takes place. As a result of a tension gradient CO₂ diffuses from the tissue into the blood system. The diffusion process will tend toward an equilibrium, and thus the same tension is found in tissue and blood. Now the question is which concentration the equilibrium tension will imply. If no chemical reactions were taking place between carbondioxide and blood components when the carbondioxide dissolves into the blood, the relation between concentration c and tension p could be expected to obey Henrys law

$$p = \alpha c \quad (4.11)$$

which describes an ideal solutions, [Atk, p. 163]. The proportionality factor α is called the solubility.

When some of the carbondioxide reacts with the solvents, more carbondioxide can diffuse into the solvents until Henrys law 4.11 again is obeyed. Therefore the total concentration of carbondioxide, some of it in a reacted form is increased. In case of blood transport of CO₂ it is the total amount transported which is of interest as the reactions are reversible, and when the net diffusion of the dissolved part goes the opposite direction, the reactions will do so as well.

Dissolved CO₂ reacts in the following way



The first reaction from dissolved CO₂ to carbonic acid (H₂CO₃) is a rather slow reaction. but it is speeded up by the enzyme carbonic anhydrase. A large part of the carbonic acid is ionized into bicarbonate and hydrogen ions. The equilibrium of these reactions is given by the K_a -value,

$$K_a = 10^{-6.1} = \frac{[\text{H}^+][\text{HCO}_3^-]}{[\text{CO}_2] + [\text{H}_2\text{CO}_3]} \quad (4.13)$$

Since the amount of dissolved CO₂ is much larger than the amount of carbonic acid [H₂CO₃], the concentration of the latter can be ignored, and equation 4.13 is thus written

$$K_a = 10^{-6.1} = \frac{[\text{H}^+][\text{HCO}_3^-]}{[\text{CO}_2]} \quad (4.14)$$

The condition 4.14 is important for the carbondioxide dissociation as well as the pH value, as it describes equilibrium of [H⁺] and [CO₂]. Using Henrys

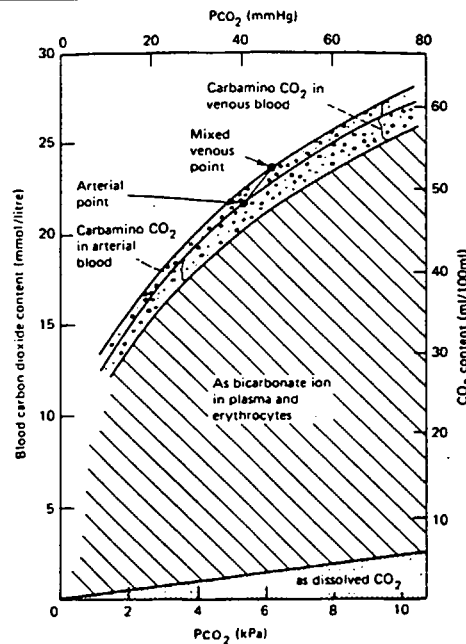


Figure 4.4: Curves of $c_{\text{CO}_2}(p_{\text{CO}_2})$ from [Nun].

law 4.11 the equilibrium condition in 4.14 can be written

$$K_a = 10^{-6.1} = \frac{[\text{H}^+][\text{HCO}_3^-]}{\alpha p_{\text{CO}_2}} \quad (4.15)$$

as the dissolved CO_2 tension is proportional to the CO_2 tension, with a factor of proportionality α , which differs in plasma and erythrocytes.

Under normal physiological conditions approximately 10% of the total CO_2 in venous blood is dissolved. 60% has reacted and is found as bicarbonate and hydrogen ions. Most of these ions are found in the erythrocytes because the catalyzing enzyme for the reaction is present here. The last 30% of CO_2 has reacted with the hemoglobin to form carbamino compounds [Van], which also donate hydrogen ions. The carbondioxide can bind oxyhemoglobin as well as deoxyhemoglobin (hemoglobin bound or not bound by oxygen), but the latter is 3.5 times as effective as oxyhemoglobin [Nun, p. 211]. This difference causes the Haldane effect, which means that a fall in oxygen gives more deoxyhemoglobin and by that a rise in carbon dioxide carried as carbamino. Therefore the ability of the blood to carry CO_2 is increased in at the venous side.

When the $[\text{H}^+]$ level is raised for some reason, the reactions are driven to the left side of the expression in 4.12 to obtain the equilibrium written in equation 4.13. Therefore the level of dissolved CO_2 in blood is raised and more CO_2

will be eliminated in the lungs. Even though there are no elimination of $[H^+]$ in this process, it results in a reduced amount of carbamino and carbonic acid, which would have been donating $[H^+]$ ions if present.

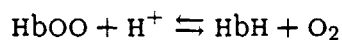
The regulatory system of the ventilation is also effected by the pH level. By a raised ventilation as a response to a decreased pH, and an increased CO_2 level in the blood either as a purpose or a consequence of the high level of $[H^+]$, the respiratory system acts as a physiological buffer system, by a faster elimination of CO_2 in lungs.

4.3.2 Oxygen carriage

Oxygen dissolves poorly in blood and nearly all oxygen is carried by hemoglobin Hb, which is found in the erythrocytes. The total concentration of oxygen c_{O_2} carried by blood is found as

$$c_{O_2} = \alpha p_{O_2} + [HbOO] \quad (4.16)$$

where the first term expresses the concentration of dissolved oxygen, by use of Henry's law 4.11 and the last term expresses the concentration of oxygen bound to hemoglobin. Each hemoglobin molecule can carry four molecules of O_2 . However, the oxygen carriage is not the only function of the hemoglobin. Deoxyhemoglobin Hb reacts with hydrogen ions, and therefore the oxygen is competing the hydrogen ions in binding hemoglobin. The competition is described by the equilibrium reaction [Van, p. 454]:



This reaction causes the pH to influence the O_2 affinity. With an increased concentration of hydrogen ions, the equilibrium conditions drive the reaction to the right, and the ability of the oxygen to bind the hemoglobin decreases. This is called the Bohr shift, and is a very useful effect for the oxygen deliverance in the tissue, where a decrease in pH of only 0.2 units (which physiologically is an acceptable change) can increase the O_2 release by 25 % at low oxygen tension [Wid, p. 65]. In case of an acidosis, the CO_2 increase may be caused by an increased metabolism and the improved deliverance of oxygen provides for a sufficient supply.

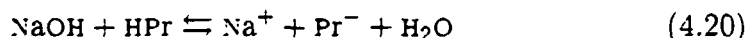
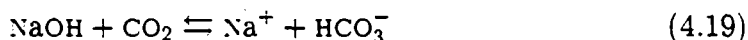
4.4 The models of gas dissociation and pH value

In the previous section we have stated the basic reactions in the blood involving carbondioxide, oxygen and/or hydrogen, and described the interactions of these three substances in the blood. In this section we will present the models of the pH value and the gas dissociation, which are all based on the reactions in the blood and the equilibrium conditions of these.

4.4.1 The pH model

In this section we present a model for the pH in blood, implemented as one of the submodels of the respiratory model. We have based our pH model directly on a model developed by Chiari et al. [Chi1]. The selection criteria are mainly that this is the only thorough model of the acid/base balance we have found, which relates the H^+ concentration and the carbondioxide concentration c_{CO_2} . The concentration of carbondioxide c_{CO_2} expresses all the CO_2 transported by blood, both as dissolved CO_2 and as bicarbonate ions (HCO_3^-).

The pH model of Chiari et al. [Chi1] is based on four chemical reaction, all involving hydrogen. The chemical reactions are reversible processes of a nature so that the concentrations will adjust to a well defined equilibrium. Thus a change in one reaction will disturb reactions that involves one or several of the same quantities, and this is exactly what happens in a system described by the four reactions of the model. The reactions of Chiaris model are the following



Where Pr represents the proteinates.

The first two reactions seem obvious to use, because the important blood buffers related to the transport of respiratory gasses are described by these. We are not able to judge whether the two last reactions are relevant or whether the four equations are sufficient for a pH model, but as the reactions lead to a model depending on the total concentration of carbondioxide carried

by the blood, we will determine the relevance of this model by the values of the output.

Based on the above reactions, Chiari et al. obtain the following equations. Expressing equilibrium for the dissociation of CO_2 and deoxyhemoglobin (Eq. 4.17 and 4.18):

$$K_{a,\text{CO}} = \frac{[\text{HCO}_3^-][\text{H}^+]}{[\text{CO}_2]}$$

$$K_{a,\text{Pr}} = \frac{[\text{Pr}^-][\text{H}^+]}{[\text{HPr}]}$$

Conservation of charge gives:

$$[\text{H}^+] + [\text{Na}^+] = [\text{HCO}_3^-] + [\text{Pr}^-]$$

Finally mass balance of the chemical substances yields

$$c_{\text{CO}_2} = [\text{CO}_2] + [\text{HCO}_3^-]$$

$$[\text{NaOH}]_0 = [\text{Na}^+]$$

$$[\text{HPr}]_0 = [\text{Pr}^-] + [\text{HPr}]$$

These 6 equations have 6 variables, with 4 initial concentrations and two equilibrium constants as parameters.

We have solved the six equations with respect to $[\text{H}^+]$, and obtained the following third degree polynomial equation, with combinations of the initial conditions and equilibrium constants as coefficients.

$$0 = [\text{H}^+]^3 + a_2[\text{H}^+]^2 + a_1[\text{H}^+] + a_0$$

$$a_2 = K_{a,\text{Pr}} + [\text{NaOH}]_0 + K_{a,\text{CO}}$$

$$a_1 = K_{a,\text{CO}}([\text{NaOH}]_0 - c_{\text{CO}_2}) + K_{a,\text{Pr}}(K_{a,\text{CO}} + [\text{NaOH}]_0 - [\text{HPr}]_0)$$

$$a_0 = K_{a,\text{CO}}K_{a,\text{Pr}}([\text{NaOH}]_0 - [\text{HPr}]_0 - c_{\text{CO}_2})$$

In general the equation has three solutions, which might be complex, however we can prove the existence of a unique positive real solution in a appropriate range of the carbondioxide concentration, see section 5.2.2.

4.4.2 The carbon dissociation function

In this section a model of the carbondioxide dissociation curve is given. The dissociation models for oxygen and carbondioxide in blood are both from MD

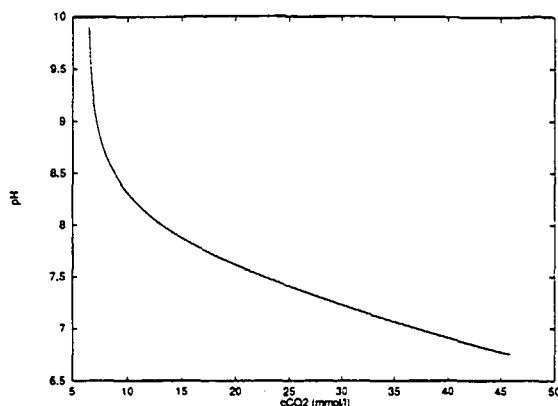


Figure 4.5: Output from the pH model

Siggaard Andersen [Sig0]. The dissociation functions are rather complex, and the fact that the derived functions are used in the differential equation of the transport model, makes this part of the model quite complex. We have chosen these dissociation functions, because it is possible to understand these functions physiologically, and because they contain physiological parameters, which enable simulation of a disordered carriage of respiratory gasses due to change in the blood components.

According to [Sig0], the total concentration of CO_2 in blood c_{CO_2} can be calculated as a weighted sum of the concentration of CO_2 in the plasma and the erythrocytes.

$$c_{\text{CO}_2}(p, \text{pH}) = c_{\text{CO}_2}^{\text{Ery}}(p, \text{pH}) \frac{C_{\text{Hb}}}{C_{\text{Ery}}} + c_{\text{CO}_2}^{\text{Pla}}(p, \text{pH}) \left(1 - \frac{C_{\text{Hb}}}{C_{\text{Hb}}}\right) \quad (4.21)$$

The total concentration of CO_2 in the erythrocytes $c_{\text{CO}_2}^{\text{Ery}}$ is a sum of the bicarbonate concentration and dissolved CO_2 in erythrocytes

$$c_{\text{CO}_2}^{\text{Ery}} = [\text{HCO}_3^-] + \alpha_{\text{CO}_2}^{\text{Ery}} p_{\text{CO}_2} \quad (4.22)$$

Using the equality $\frac{K_a}{[\text{H}^+]} = 10^{(\text{pH}-\text{pK})}$, the bicarbonate concentration, $[\text{HCO}_3^-]$, is found from equation 4.15:

$$[\text{HCO}_3^-] = \frac{K_a}{[\text{H}^+]} \alpha_{\text{CO}_2}^{\text{Ery}} p_{\text{CO}_2} \quad (4.23)$$

which implies that

$$[\text{HCO}_3^-] = \alpha_{\text{CO}_2}^{\text{Ery}} p_{\text{CO}_2} 10^{(\text{pH}-\text{pK})} \quad (4.24)$$

So the total concentration is

$$c_{\text{CO}_2}^{\text{Ery}}(p, \text{pH}) = \alpha_{\text{CO}_2}^{\text{Ery}} p_{\text{CO}_2} (1 + 10^{(\text{pH}^{\text{Ery}}(p, \text{pH}) - \text{pK}^{\text{Ery}}(p, \text{pH}))}) \quad (4.25)$$

By equivalent calculations, the concentration in the plasma $c_{\text{CO}_2}^{\text{Pla}}$ is given by:

$$c_{\text{CO}_2}^{\text{Pla}}(p, \text{pH}) = \alpha_{\text{CO}_2}^{\text{Pla}} p_{\text{CO}_2} (1 + 10^{\text{pH} - \text{pK}^{\text{Pla}}(p, \text{pH})}) \quad (4.26)$$

The pK and pH values of the erythrocytes and plasma are also given by [Sig0]:

$$\text{pK}^{\text{Ery}}(p, \text{pH}) = 6.125 - \log_{10}(1 + 10^{\text{pH}^{\text{Ery}}(p, \text{pH}) - 7.84 - 0.06 \cdot s_{\text{O}_2}(p, \text{pH})}) \quad (4.27)$$

$$\text{pH}^{\text{Ery}}(p, \text{pH}) = 7.19 + 0.77(\text{pH} - 7.4) + 0.035(1 - s_{\text{O}_2}(p, \text{pH})) \quad (4.28)$$

$$\text{pK}^{\text{Pla}}(p, \text{pH}) = 6.125 - \log_{10}(1 + 10^{\text{pH} - 8.7}) + \alpha_{\text{CO}_2}^{\text{Pla}} p_{\text{CO}_2} \quad (4.29)$$

The term s_{O_2} is the oxygen saturation of the hemoglobin, and will be detailed in next section. The pH of the plasma is output from the pH model, which was detailed in the previous section. By these equations the CO_2 concentration as function of the tension $c = \varphi_b(p)$ is only implicitly given. The reason is that pH value varies with the CO_2 concentration: $\text{pH}(c_{\text{CO}_2})$.

4.4.3 Model of oxygen dissociation in blood

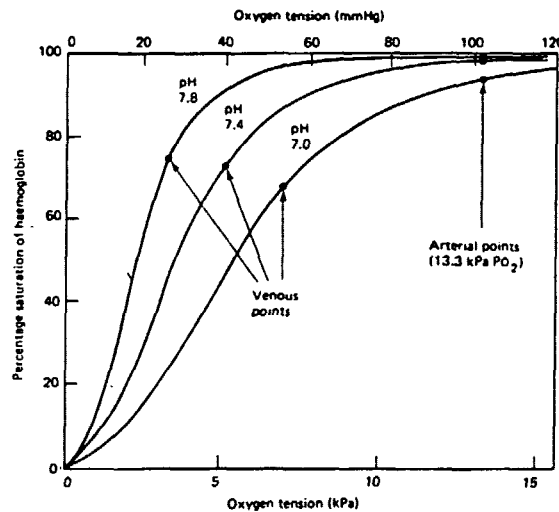


Figure 4.6: Oxygen saturation curve from [Nun, p. 265].

The total concentration of oxygen c_{O_2} is calculated as the sum of dissolved oxygen and oxyhemoglobin:

$$c_{O_2}(p) = \alpha_{O_2} p_{O_2} + c_{Hb} s_{O_2}(p) \quad (4.30)$$

where α is the solubility constant, p_{O_2} the O_2 tension, and c_{Hb} the hemoglobin concentration of the blood. $s_{O_2}(p)$ yields the fractional saturation of the hemoglobin with oxygen, which is defined as the oxyhemoglobin concentration divided by the total hemoglobin concentration: $[HbOO]/([Hb] + [HbOO])$. The model of the saturation states the relation between the saturation s_{O_2} the O_2 tension, (p_{O_2}), the CO_2 tension, (p_{CO_2}) and the pH value. In figure 4.6 the saturation curves are shown at different pH values, illustrating the Bohr effect. When the pH value or the carbondioxide tension are raised, the saturation curve is shifted to the right, because of a decrease in affinity of hemoglobin for oxygen. If the pH or p_{CO_2} is lowered the shift is to the left.

If the ability of the hemoglobin molecule to bind O_2 was the same for each hemoglobin binding site, we would expect the saturation to be a logistic function of the oxygen tension. But in a plot of $\log(p_{O_2})$ vs. $\log(s_{O_2}/(1 - s_{O_2}))$ measurements of the oxygen saturation does not describe a linear curve, but shows a symmetrical S shape, corresponding to different abilities of the hemoglobin in binding of the first through the fourth O_2 molecule [Nun]. The curves measured under different circumstance can be characterized by the point of symmetry ($x_0, 1.875$), the slope of the symmetry point n_0 , and distance $2h$ between the tangent slopes for $\log p_{O_2} \rightarrow \pm\infty$ [Sig3].

These parameters are in the model of [Sig0] used to fit measured curves. The model of the oxygen saturation of the hemoglobin is given by the following equations, where the saturation is expressed as a function of the gas tension vector p :

$$\begin{aligned} s_{O_2}(p) &= \frac{1}{1 + e^{-y(p)}} \\ y(p) &= 1.875 + x(p) - x_0(p) + h(p) \tanh(0.5343(x(p) - x_0(p))) \\ h(p) &= (3.5 + a(p)) \\ x(p) &= \log(p_{O_2}/kPa) \\ x_0(p) &= 1.946 + a(p) + 0.055(T/^{\circ}C - 37) \\ a(p) &= -0.72(pH(c_{CO_2}(p)) - 7.4) + 0.09 \log(p_{CO_2}/5.33kPa) \\ &\quad + (0.07 - 0.03x_{Hbf})(c_{dpg}/mole/l - 5) \\ &\quad - 0.368x_{HbCO} - 0.174x_{Hi} - 0.28x_{Hbf} \end{aligned}$$

The model parameters are: the substance fraction of fetal hemoglobin x_{Hbf} , the substance fraction of hemoglobin x_{Hi} , the substance fraction of carboxy-

hemoglobin x_{HbCO} , the concentration of 2,3-diphosphoglycerate in the erythrocytes c_{dpg} , and the temperature T . According to [Sig3] the equations represent a very good fit to the Servinghaus standard oxygen dissociation curve, however the parameters may easily be fitted to other oxygen dissociation curves as well.

The equations do not give an explicit expression for the saturation, as the expression depends on pH, and pH depends on carbondioxide concentration $c_{CO_2}(p)$, that in turn depends on the saturation.

4.4.4 Dissociation of anaesthetica

The dissociation functions of the anaesthetic agents we have seen or concluded from models found in the literature are all simpler than the ones of CO_2 and O_2 . This is due to the fact that the anaesthetic agents behave in a simpler way, but can also be a consequence of the lack of information about the kinetics and dynamics of the agents.

The kinetics and dynamics of many of the anaesthetic agents are described by measurements of concentration of the agent in the blood of a number of patients after injection. Parameters of models with a few compartments and linear dissociation functions are fitted to these decay curves. Later we will use information in terms of such parameters to obtain the dissociations functions of the different organ compartments and the blood, see section 6.4.

If we assume that the agents obey Henry's law and dissolve linearly, the dissociation function is given by:

$$c = \alpha p \quad (4.31)$$

where c is concentration and p is tension. The assumption of linearity is often reasonable even when chemical reaction occur, since the drug concentration is usually much lower than the concentration of the substance the drug will bind to [Hul].

4.4.5 Dissociation in tissue

The models we have found of dissociation in tissue are less complicated than the blood dissociation functions. In [Chi0] the blood dissociation function is used for CO_2 in tissue, and a simple linear solution is used for O_2 .

Our blood dissociation function [Sig0] differentiates the dissociation of plasma and erythrocytes, and thus we use the plasma part for tissue dissociation, after direct advice from MD Siggard-Andersen. For oxygen we use a linear solubility with the coefficient α_{O_2} found in equation 4.30. This reflects that no hemoglobin is present in the tissue, so the solution is simpler, but may disregard the effect of other oxygen binding proteins. In the muscles an oxygen binding protein called myoglobin is present, but we have not found any quantitative information about the binding of myoglobin with oxygen. The changes in the oxygen stores in the muscles happens slowly as the muscles is low perfused, and the effects of such change on the rest of the body are very small. In case of anaesthetic agents the dissociation curve is assumed to be linear. The solubility coefficients of anaesthetic agents determines the stores of substance in the tissue. The stores in low perfused areas are of greater importance for anaesthetic agents than for respiratory gasses, as large variations in the concentration of drugs occurs, while the respiratory gasses is restricted from variations by the central nervous system. This control will be discussed in next section.

4.5 Control of respiration

The substances carried by the blood transport system are vital for the body. Lack of O_2 in even short periods causes brain damage, but damaging effects are normally avoided, because the system is controlled in order to match the pulmonary and the metabolic gas exchange rates. In this section we will discuss the control of the respiratory system, which is performed by the central nervous system. The description is made in order to make it certain that the models we have developed can interact reasonably with the future model of the control by central nervous system.

Before we discuss the control system, we will draw some attention to the dynamics of the transport model as we have modelled it. The system already contains some mechanism to improve utilization of the oxygen and elimination of carbondioxide as a reponse to disturbances. In case of increased metabolic rate, the diffusion of oxygen and carbondioxide between blood and tissue increases because of an increased tension gradient. An additional improvement of the oxygen deliverance is caused by the Bohr shift. Increased metabolic production of CO_2 will effect the pH value in blood. At decreased pH, the oxygen dissociation curve is shifted to the right. This impairs the oxygenation of blood in the lung, but the negative effect is small compared to the improved release of oxygen in tissue [Nun]. In the same way, the Hal-

dane effect shifts the carbondioxide curve with respect to the oxygen level in blood, and yields a difference in quantity of carbondioxide carried in oxygenated and reduced blood (at constant carbondioxide tension). This results in an improve of the gas transport as well.

The principal features of behavior of the respiratory control system are to reduce the sensitivity of the system to external disturbances. Thus the signal from the central nervous system counteracts changes in the body. The behavior of the respiratory control system is conveniently described by a look at the response to exercise of a healthy person. Though one must be aware of the fact that the principal controlling mechanism is not similar under different conditions [Nun](s. 72).

Under moderate exercise the person will be able to compensate for the increased metabolic rate by a raised ventilation and blood flow. A sufficient oxygen supply is thus maintained and a new steady state can be found. At heavy exercise the supply becomes too small and anaerobic production will occur. How long time the work can continue depends on the level of arterial blood lactate. Lactic acid is the principal product of anaerobic metabolism, but ionizes to lactate and hydrogen ions. If the lactate remains constant, a state which is steady can exist during the exercise. After work has finished, there will be a period of recovery when the oxygen debt has to be repaid in order to oxide the products of the anaerobic metabolism. The mechanism for obtaining this pattern is found in the control system.

The controlled variables

The central nervous system affects the respiratory system by changing the ventilation, the blood flow, and the cardiac output. However, other systems affect the heart through the central nervous system, and hence the effect on the cardiac output is a combination of stimuli from the respiratory system, the baroreceptors, and other systems.

The controlling variables

The most important input for the control of ventilation is from the peripheral and central chemoreceptors. The peripheral receptors are called the carotid and aortic bodies. They are sensitive to changes in the arterial blood, and are stimulated by an increase hydrogen ion concentration, an increase in tension of CO_2 or a decrease in tension of O_2 tension. The central chemoreceptors are

located in the medulla, a center in the brain. They are stimulated by change in the hydrogen ion concentration.

As mentioned the heart is controlled both by variables from the transport model and from the cardio-vascular model. The controlling variables from the transport model are arterial tensions of O_2 and CO_2 .

An external control system

The anaesthetic agents affect the body and thus the transport system. The effects of the drugs must will be included in the simulator by the models of the pharmacodynamics. When a person is left to the operating theatre, he is anaesthetized. Drugs are given for different purposes, some drugs will make sure that the patient is unconsciousness, others will relax the muscles, and thus the automatical functions of the body are reduced or even absent. The automatical functions are primary the ventilation and the heart beat. These functions as well as the control of them, must therefore be performed by external sources, and the medical staff take over the control with the system in order to maintain a sufficient transport of the respiratory gasses and avoid or reduce disturbances of this transport.

Conclusion

We have now presented our models of the respiratory system, piece by piece. The equations in chapter 3 and chapter 4 constitutes our model, which reflect the physiological system described in chapter 2 in a way we find will meet the requirement of the SIMA group. In the next chapters we will present and examine the model as a whole, to support this claim.

Chapter 5

Solving the model

In this chapter we will establish an overview of the model equations, which will be summarized without any regards to the basic assumption or the interpretation of the equations. The purposes of this equation review is to emphasize which equations constitute our model, and further describe the types of the model equations by writing these in a compact form. This will ease a discussion of the mathematical properties of the model, found in section 5.2, in which the existence, uniqueness and stability of solutions to the differential equations are discussed.

The equations of the total model have the following form of an ordinary differential equation:

$$\dot{x} = f(x, t; \mu), \quad (5.1)$$

where x is the state vector, t the time, and μ the parameters. The state vector x consists of the state variables for the lung model and the blood transport model. To ease the discussion of the model, we split the model equations into the equations concerning the lung model and the equations concerning the blood transport model and the model equations now read:

$$\begin{pmatrix} \dot{x}_L \\ \dot{x}_B \end{pmatrix} = f(x_L, x_B, t; \mu), \quad (5.2)$$

where x_L are the variables of the lung model, and x_B are the variables of the blood transport model. The variables x_L and x_B are themselves vectors, consisting of all the variables for pressures and gas fractions in the lung and tensions or concentrations in the transport system. The size of the x vector, and thus the total number of equations in the model, with n_s substances,

and n_a alveoli compartments is then

$$n = (13 + n_a)n_s + (n_a + 1)(n_s + 1),$$

as each of the $(13 + n_a)$ transport compartments requires n_s variables, and each lung compartment requires one pressure variable and n_s fraction variables. In the case with one anaesthetic agent $n_s = 3$ and just a single alveoli branch $n_a = 1$, the number of equations is 50.

In the situation when a particular compartment is in focus, the components of the vector variables refer to the content of each of the n_s substances of the model. Such vectors are called compartment vectors and for these, we have uniformly used the principle that the first coordinate is carbondioxide, and the second is oxygen. For instance is the tension compartment vector if $n_s = 3$ containing the following elements:

$$p = \begin{pmatrix} p_{CO_2} \\ p_{O_2} \\ p_{aa} \end{pmatrix} \quad (5.3)$$

where aa denotes the last substance, which the model keeps track of.

If the vector variables of the model are used globally (or at least for more than one compartment), they will have one component for each compartment in the model, in all $n_a + 13$ components, which are vectors themselves, representing a compartment vector each. The tension vector contains for instance the following elements:

$$p = \begin{pmatrix} p_{liver} \\ p_{heart} \\ p_{venous\ pool} \\ \vdots \end{pmatrix} \quad (5.4)$$

where the dots represent the last of the $n_a + 13$ compartment vectors. Each element in 5.4 is given as in 5.3. We do not in our notation distinguish between these two kind of vector variables, as it appears from the context, which one is used.

5.1 Model summary

In the following we will summarize the equations of the model, the equations of the lung model in 5.1.1 and the equations of the blood transport model in section 5.1.2. The blood transport model contains submodels for the metabolism, the dissociation of gasses, and the pH value. These will be included in the summary in sections 5.1.2, 5.1.2, and 5.1.2.

5.1.1 The lung model

The lung model, which determines the vector x_L , consists of two models of differential equations, the pressure model and the gas model. The state variable of the pressure model is input to the gas model. The lung model has two equations per compartment, a one dimensional from the pressure model, and a n_s dimensional from the gas model.

The pressure model from section 3.1:

$$\dot{p}_0 = \frac{1}{R_0 C_0} (U_m - p_0 - R_0 \sum_{i=1}^n C_i \dot{p}_i) \quad (M1)$$

$$\dot{p}_i = \frac{1}{R_i C_i} (p_0 - p_i - U_i), \quad i = 1, 2, \dots, n_a \quad (M2)$$

The gas model from section 3.2:

$$\dot{f}_0 = \frac{RT}{p_0(p_0 C_0 + V_{00})} \left(\frac{I_-(U_m - p_0)(f_e - f_0)}{R_0} + \sum_{i=1}^{n_a} \frac{I_-(p_i - p_0)(f_i - f_0)}{R_i} \right) \quad (M3)$$

$$\begin{aligned} \dot{f}_i &= \frac{RT}{p_0(p_0 C_0 + V_{00})} \frac{I_-(p_0 - U_i - p_i)(f_0 - f_i)}{R_i} \\ &+ \frac{RT_i}{p_i(C_i \alpha p_i + V_{0i})} \kappa(p_{cp} - p_i f_i), \quad i = 1, 2, \dots, n_a \end{aligned} \quad (M4)$$

where subscript 0 denotes the central lung compartment, and i denotes the i -th alveoli branch.

The state variables in equations M1 to M4 are the vector x_i in equation 5.2. As the pressure model is independent of the gas model, the lung model can be written in the linear form:

$$\dot{p} = A_1 p + B_1 u_1(t) \quad (5.5)$$

$$\dot{f} = A_2(p(t))f + B_2 u_2(t, p(t)) \quad (5.6)$$

where A_1 and B_1 are constant matrices, and u_1 and u_2 are external input depending on U_i , U_m and f_e . The matrices A_2 and B_2 depend on the solutions $p(t)$ of the pressure model.

5.1.2 The transport model

The transport model consists of the differential equations for the compartments. In addition the differential equations rely on the dissociation curves and the metabolism. There are two kinds of differential equations; one in which the substance tensions p are used as state variable and another with the substance concentrations c as state variable. We could use the tension everywhere, but it would introduce unnecessary complications in the equations for the peripheral blood pools, in which the concentration is used. In compartments with more than one solvent, tensions are the only possible state variables, as there might be different solubilities of the substances in the blood and the tissue. Thus there are two concentration vectors for such compartments, c_t for the tissue concentrations of substances and c_b for the blood concentrations.

The pulmonary compartment from section 4.1.2:

$$\frac{dp_{cp}}{dt} = (V_b \frac{dc_b}{dp_{cp}})^{-1} (Q(1 - \lambda)(c_b(p_{vs}) - c_b(p_{cp})) + \kappa(p_A - p_{cp})) \quad (M5)$$

The central pools from section 4.1.3:

$$\frac{dp_{as}}{dt} = (V_b \frac{dc_b}{dp_{as}})^{-1} Q((1 - \lambda)c_b(p_{cp}) + \lambda c_b(p_{vs}) - c_b(p_{as})) \quad (M6)$$

$$\frac{dp_{vs}}{dt} = (V_b \frac{dc_b}{dp_{vs}})^{-1} Q(z_{vpv}c_{vpv} + z_{vpl}c_{vpl} + z_{ad}c_{vpa} + z_s c_b(p_{as}) - c_b(p_{vs})) \quad (M7)$$

where

$$z_{vpv} = z_{li} + z_{ki} + z_{he} + z_{br} + z_{re}$$

$$z_{vpl} = z_{mu} + z_{co}$$

$$z_s = 1 - (z_{vpv} + z_{vpl} + z_{ad})$$

The organ compartments from section 4.1.1, $i \in \{li, ki, he, br, re, co, mu, ad\}$:

$$\frac{dp_i}{dt} = \left(V_t \frac{dc_t}{dp_i} + V_b \frac{dc_b}{dp_i} \right)^{-1} (z_i Q(c_b(p_{as}) - c_b(p_i)) + \mathcal{M}_+(c_t(p_i)) - \mathcal{M}_-(c_t(p_i))) \quad (M8)$$

The peripheral venous pools from section 4.1.3:

$$\frac{dc_{vpv}}{dt} = \frac{Q(\sum_{i \in \{li, ki, he, br, re\}} z_i c_b(p_i) - c_{vpv})}{V_b} \quad (M9)$$

$$\frac{dc_{vpl}}{dt} = \frac{Q(\sum_{i \in \{co, mu\}} z_i c_b(p_i) - c_{vpl})}{V_b} \quad (M10)$$

$$\frac{dc_{vpa}}{dt} = \frac{Q(z_{ad} c_b(p_{ad}) - c_{vpa})}{V_b} \quad (M11)$$

The parameters V_b and V_t are volumes of blood and tissue in each compartment, and are consequently different parameters in each equation, while Q is the cardiac output and thus global.

Each of the differential equations have a dimension corresponding to the number of substances transported, i.e. the variables of the equations are vectors.

The metabolism

The metabolic functions \mathcal{M}_- and \mathcal{M}_+ for production and consumption respectively are submodel of the transport model, as described in section 4.2. The metabolic functions are used in the differential equations of the organ compartments with the tissue concentration of the compartment as arguments, c.f. M8.

$$\mathcal{M}_-(c) = \begin{pmatrix} 0 \\ M_{O_2} \frac{c_{O_2}}{\beta_{O_2} + c_{O_2}} \\ M_{aa} \frac{c_{aa}}{\beta_{aa} + c_{aa}} \end{pmatrix} \quad (M12)$$

$$\mathcal{M}_+(c) = \begin{pmatrix} M_{CO_2} \\ 0 \\ 0 \end{pmatrix} \quad (M13)$$

The parameters β_i and M_i are compartment specific.

The pH model

The pH model is used in the functions of the O_2 and CO_2 dissociation, which is input to all differential equations of the transport model. The pH is the

negative logarithm of the hydrogen-ion concentration, which is implicitly given as function of the total concentration of carbondioxide c_{CO_2} :

$$pH(c_{CO_2}) = -\log([H^+]) \quad (M14)$$

as the concentration of hydrogen ions $[H^+]$ is found from the following third degree polynomial equation:

$$0 = [H^+]^3 + a_2[H^+]^2 + a_1(c_{CO_2})[H^+] + a_0(c_{CO_2}) \quad (M15)$$

where the coefficients of the polynomial are:

$$\begin{aligned} a_2 &= K_{a,Pr} + [NaOH]_0 + K_{a,CO} \\ a_1 &= K_{a,CO}([NaOH]_0 - c_{CO_2}) + K_{a,Pr}(K_{a,CO} + [NaOH]_0 - [HPr]_0) \\ a_0 &= K_{a,CO}K_{a,Pr}([NaOH]_0 - [HPr]_0 - c_{CO_2}) \end{aligned}$$

The dissociation function

The dissociation functions are specific for both the solutes and the solvents. The vector function for dissociation of the various substances in blood are implicitly given by equations from section 4.4:

Carbondioxide dissociation:

$$c_{CO_2}(p, pH) = c_{CO_2}^{Ery}(p, pH) \frac{c_{Hb}}{c_{Hb}^{Ery}} + c_{CO_2}^{Pla}(p, pH) \left(1 - \frac{c_{Hb}}{c_{Hb}^{Ery}}\right) \quad (M16)$$

$$c_{CO_2}^{Ery}(p, pH) = \alpha_{CO_2}^{Ery} p_{CO_2} (1 + 10^{(pH^{Ery}(p, pH) - pK^{Ery}(p, pH))}) \quad (M17)$$

$$c_{CO_2}^{Pla}(p, pH) = \alpha_{CO_2}^{Pla} p_{CO_2} (1 + 10^{(pH - pK^{Pla}(p, pH))}) \quad (M18)$$

$$pK^{Ery}(p, pH) = 6.125 - \log_{10}(1 + 10^{(pH^{Ery}(p, pH) - 7.84 - 0.06 \cdot s_{O_2}(p, pH))}) \quad (M19)$$

$$pH^{Ery}(p, pH) = 7.19 + 0.77(pH - 7.4) + 0.035(1 - s_{O_2}(p, pH)) \quad (M20)$$

$$pK^{Pla}(p, pH) = 6.125 - \log_{10}(1 + 10^{(pH - 8.7)}) + \alpha_{CO_2}^{Pla} p_{CO_2} \quad (M21)$$

Oxygen dissociation:

$$c_{O_2}(p, pH) = \alpha_{O_2} p_{O_2} + c_{Hb} s_{O_2}(p, pH) \quad (M22)$$

Oxygen saturation:

$$s_{O_2}(p, pH) = \frac{1}{1 + e^{-y(p, pH)}} \quad (M23)$$

$$y(p, pH) = 1.875 + x(p) - x_0(p, pH) + h(p) \tanh(0.5343(x(p) - x_0(p, pH))) \quad (M24)$$

$$h(p, pH) = (3.5 + a(p, pH)) \quad (M25)$$

$$x(p) = \log(p_{O_2}/kPa) \quad (M26)$$

$$x_0(p, pH) = 1.946 + a(p, pH) + 0.055(T/^{\circ}C - 37) \quad (M27)$$

$$a(p, pH) = -0.72(pH - 7.4) + 0.09 \log(p_{CO_2}/5.33kPa) + (0.07 - 0.03x_{Hbf})(c_{dpg}/mmol/l - 5) - 0.368x_{HbCO} - 0.174x_{Hi} - 0.28x_{Hbf} \quad (M28)$$

Anaesthetic dissociation:

$$c_{aa}(p) = \alpha_{aa} p_{aa} \quad (M29)$$

The equations M14 to M29 implicitly define the function $c_b(p)$:

$$c_b(p) = \begin{pmatrix} c_{CO_2}(p_{CO_2}, p_{O_2}, pH) \\ c_{O_2}(p_{CO_2}, p_{O_2}, pH) \\ c_{aa}(p_{aa}) \\ \vdots \end{pmatrix} \quad (M30)$$

Thus the dissociation functions for CO_2 and O_2 depend on the tension of CO_2 and O_2 and on the pH value. We have furthermore based the numerical solution of the differential equation on the assumption that the dissociation of the various anaesthetic agents aa are only depending on the tension of the respective agent and not influencing other substances.

The dissociation of various substances into tissue c_t is a vector function analogue to the blood dissociation, discussed in section 4.4.5.

$$c_t(p) = \begin{pmatrix} c_{CO_2}^{Pla}(p_{CO_2}, pH) \\ c_{O_2}^t(p_{O_2}) \\ c_{aa}^t(p_{aa}) \\ \vdots \end{pmatrix} \quad (M31)$$

The dissociation of oxygen in the tissue $c_{O_2}^t$ is modelled to be independent of the carbondioxide concentration, and thus the expression is less interdependent than the equation defining the blood dissociation.

The dissociation functions are only implicitly given, but solving the equations can be done by finding the carbondioxide concentration, since the pH value depends solely on this, and all the remaining quantities (s_{O_2} , c_{O_2}) depend only on p and pH.

The differential equations of the transport model involve the partially derivative of the dissociation functions. The partial derivatives of the implicit function are found analytically in section 5.2.2.

The transport model in a general form

For practical reasons we have two kind of state variables in the differential equation of the transport model. But to discuss the mathematical properties of the system, this is a confusing and hence inappropriate form. We will therefore rewrite all differential equations in order that the arguments of the all equations are in concentrations.

For that purpose we will introduce two functions γ_b and γ_t , which convert the state variable of the blood transport model x_B to the corresponding concentration in blood and tissue respectively. This is done by compartment, and for compartment j the coordinate function of the γ functions are defined in the following way:

$$\gamma_{bj}(x_{Bj}) = \begin{cases} c_b(x_{Bj}) & \text{when cmpt. } j \text{ has pressure as variable} \\ x_{Bj} & \text{when cmpt. } j \text{ has conc. as variable} \end{cases} \quad (5.7)$$

$$\gamma_{tj}(x_B) = \begin{cases} c_t(x_{Bj}) & \text{when cmpt. } j \text{ has pressure as variable} \\ x_{Bj} & \text{when cmpt. } j \text{ has conc. as variable} \end{cases} \quad (5.8)$$

where x_{Bj} denotes the state vector of compartment j .

Now we can write the differential equation on the nonlinear form:

$$\dot{x}_t = B(x_t, t)\gamma_b(x_t) + C(x_t, t)\gamma_t(x_t) + u(t), \quad (5.9)$$

where $u(t)$ is the external input. B holds the transport relations, and C holds the metabolism. B extends a 14×14 matrix for the 14 compartments, in which every element consists of the state vector of at least 3 substances carried around. Totally we have an 42×42 matrix. The 14×14 matrix contains nonzero elements in the diagonal, and whenever the state variable of another compartment is part of the differential equation, which models blood transport into the compartment. The matrix C has the same size as B , but is a diagonal matrix, as the metabolism in a compartment depends only on the concentration of the tissue.

5.1.3 Interactions of transport and lung model

Interaction between the lung and the transport models occurs only between the gasses in the alveoli, represented by the partial pressures p_p and the gas dissolved in the pulmonary capillaries represented by the tension vector p_{cp} , see equations M4 and M5.

In the final simulator the intention is to letting the lung and the transport model run with different step lengths, and thus some ingenuity will be needed to find a reasonable way to share these values, but we have not done anything to this effect. When we use the two models together we simply run at the same time scale.

5.1.4 External inputs

The external input to the models is in the pressure model the two external pressures of the lung model U_m and U_t , representing the natural and artificial ventilation respectively. The gas model has the composition of inspired air f_e as input. The transport model has inputs from other models of the simulator, as the blood flow is determined by the cardiac output Q and the distribution of the blood flow to the various organs z_i . Furthermore there might be changes in the metabolic rate, either with these as input from the temperature model or in the simulation situation

5.2 Existence, uniqueness, and stability of solutions

In this section we will analyze the model in order to conclude the existence of a solution for particular initial values, which are always positive. In case a solution exists, we will discuss the stability of the solution, when the system has only constant external influences.

5.2.1 The lung model

In the overview section, 5.1, we reduced the lung model, in equation 5.5, to the following form:

$$\dot{p} = A_1 p + B_1 u_1(t) \quad (5.10)$$

$$\dot{f} = A_2(p(t))f + B_2(p(t))u_2(t, p(t)) \quad (5.11)$$

where 5.10 is the pressure model, and 5.11 is the gas model.

Since A_1 and B_1 are constant matrices, the pressure model is linear. Therefore a global unique solution exists for any given initial condition. The solution will be asymptotically stable if all eigenvalues of the matrix A_1 has negative real parts. As the model equations are derived from an electrical network with only passive components, we know that no eigenvalues with positive real parts exist. In order to ensure the eigenvalues to be nonzero, we can by examination of the network, see figure 3.4, ensure that energy in the system will always be lost, and thus that all eigenvalues have negative real parts.

When $p(t)$ is regarded as an external function the gas model is a linear system, with a non-constant matrix A_2 . If each function in A_2 is continuous it can be proved that the system has a global unique solution for a given initial value problem [Far0, Theorem 6.1]. This is the case with our A_2 matrix, in which the only non-differentiable function is $I_+(x)$, which is continuous in 0, even though it is not differentiable in 0. The stability of the system in 5.11 depends on the eigenvalues, which can be considered as functions of time. If the eigenvalues have negative real parts, that are bounded away from zero the system is asymptotically stable.

5.2.2 The transport model

The existence of solutions to the differential equations of the transport model depends on solutions of the submodel equations. In order to ensure existence of solutions to the differential equations, the requirement to the submodels is that solutions exist to all initial values, and that the solutions are \mathbb{C}^1 for positive values. Furthermore the derivative of the dissociation functions $\frac{\partial c}{\partial p}$ are used in the differential equations of the transport model. Thus it is required that these are \mathbb{C}^1 (at least for positive values) as well, which implies that the dissociation functions must be \mathbb{C}^2 . We will discuss the solutions of the submodels first, and then continue with the transport model. Finally we will consider the stability of solutions.

The submodels of the transport model are the metabolic functions, \mathcal{M}_- and \mathcal{M}_+ , and the dissociation functions $c_b(p)$ and $c_t(p)$, which again depends on the pH model. For the metabolic functions, c.f. M12, the requirement of the functions being \mathbb{C}^1 is met for $c \geq 0$. The submodel concerned with dissociation is more complicated, this is the subject for discussion in the following sections. Since the dissociation models depend on the pH model we treat this first.

The pH model

The pH model is a third degree polynomial equation with coefficients a_0 and a_1 described as function of the carbondioxide concentration.

$$g(z) = z^3 + a_2 z^2 + a_1(c)z + a_0(c) = 0 \quad (5.12)$$

The equation $g(z, c)$ determines the relation between $z = [H^+]$ and $c = c_{CO_2}$. As the coefficient of z^3 is 1 and hence positive, the polynomial will tend to $+\infty$ for $z \rightarrow \infty$. Thus if $g(0) < 0$ there must exist at least one positive root. To decide when there is exactly one, we look at the derivative $g'(z) = 3z^2 + 2a_2 z + a_1$. The sum of the roots of $g'(z)$ is $-\frac{2}{3}a_2$. Since $a_2 = K_{a,Pr} + [NaOH]_0 + K_{a,CO}$ is always positive the sum of the roots is always negative. Therefore at least one of the roots is negative. Thus for $g(0) < 0$ the function g cuts the positive half of the axis exactly once. $g(0) = a_0$ and hence the condition for a unique positive solution is

$$a_0 = K_{a,CO} K_{a,Pr} ([NaOH]_0 - [HPr]_0 - c_{CO_2}) < 0 \quad (5.13)$$

equivalent to $[NaOH]_0 - [HPr]_0 - c_{CO_2} < 0$. Our naive chemical interpretation of this limitation is that the total amount of acid must outweigh the total amount of strong base. The limitation seems reasonable when compared to the physiological pH range.

Later, when we find an expression for the derivative of the implicitly given dissociation functions, we will make use of a positive sign of pH function differentiated with respect to the carbondioxide concentration c_{CO_2} . It is our expectation from our knowledge of the physiology, that the pH function is decreasing for increasing c_{CO_2} . However we will mathematically investigate, when it is obtained that the derivative $\frac{\partial pH}{\partial c}$ is negative. Since $pH = -\log(z)$ this implies that $\frac{\partial z}{\partial c} > 0$. Equation 5.12 implies that $0 = \frac{\partial g(z, c)}{\partial c}$, hence we can express $\frac{\partial z}{\partial c}$ by:

$$0 = \frac{\partial g}{\partial c} = \frac{\partial g}{\partial c} + \frac{\partial g}{\partial z} \frac{\partial z}{\partial c} \quad (5.14)$$

Which implies, when $\frac{\partial g}{\partial z} \neq 0$:

$$\frac{\partial z}{\partial c} = - \left(\frac{\partial g}{\partial z} \right)^{-1} \frac{\partial g}{\partial c} \quad (5.15)$$

$$= (3z^2 + 2a_2 z + a_1)^{-1} (zK_{a,CO} + K_{a,CO} K_{a,Pr}) \quad (5.16)$$

By examination of the terms in equation 5.16 we find that all terms except for a_1 is always positive as a consequence of their nature. To ensure that $\frac{\partial z}{\partial c}$ is negative we must therefore require that a_1 is positive.

$$a_1 = K_{a,CO}([NaOH]_0 - c_{CO_2} + K_{a,Pr}(K_{a,CO} + [NaOH]_0 - [HPr]_0) > 0 \quad (5.17)$$

This provides an upper limit on c_{CO_2} . Inserting the parameters given in [Chi0], we find that this upper limit does not influence the physiological range of the carbondioxide concentration. In the allowed range the pH model is found to be C^2 . Now we have ensured the necessary properties of the pH model, and will continue with the dissociation functions.

The dissociation curves

The first problem in the model of the dissociation curves is to ensure that the dissociation curve for CO_2 has a solution, as the definition of c_{CO_2} is implicitly given by the following equation:

$$c_{CO_2} = \varphi_b(p, pH(c_{CO_2})) \quad (5.18)$$

Using the monotonicity of $pH(c_{CO_2})$ and $\varphi_b(p, pH)$ we can prove the existence of a unique solution: The curve $\varphi_b(c_{CO_2})$ is always decreasing as the derivative is negative:

$$\frac{\partial \varphi_b}{\partial c_{CO_2}} = \frac{\partial \varphi_b}{\partial pH} \frac{\partial pH}{\partial c_{CO_2}} < 0 \quad (5.19)$$

The first term is positive for all values of pH, and the second term is found to be negative in the last subsection (5.2.2). Thus for any constant p, we can conclude that there is only one intersection between the curves $c = c_{CO_2}$ and $c = \varphi_b(pH(c_{CO_2}))$. When the pH value is found, the rest of the dissociation functions are given by explicit expressions.

The second problem is finding the partial derivatives of the dissociation curves $\frac{\partial c}{\partial p}$. Even without an explicitly given function for the c_{CO_2} , we can find $\frac{\partial c}{\partial p}$ analytically by use of implicit differentiation in the vector space.

Reordering equation 5.18, we have:

$$F(p, c(p)) = 0 \quad (5.20)$$

Since the differential equations of anaesthetica are assumed to be independent of other gasses and vice versa, the functions split up into two independent

parts; the part for the CO_2 and O_2 , and a part for the anaesthetic agents. Therefore only the first two coordinates of 5.20 are of interest:

$$F = \begin{pmatrix} F_1 \\ F_2 \end{pmatrix} = \left(\begin{pmatrix} \varphi_{\text{CO}_2}(p, pH(c)) \\ \varphi_{\text{O}_2}(p, pH(c)) \end{pmatrix} - \begin{pmatrix} c_{\text{CO}_2} \\ c_{\text{O}_2} \end{pmatrix} \right) = \begin{pmatrix} 0 \\ 0 \end{pmatrix} \quad (5.21)$$

Implicit differentiation yields

$$0 = \frac{\partial F}{\partial p} + \frac{\partial F}{\partial c} \frac{\partial c}{\partial p} \quad (5.22)$$

We want to know the $\frac{\partial c}{\partial p}$. Isolating this term when $\frac{\partial F}{\partial c}$ is evaluated at (p, c) we find, that:

$$\frac{\partial c}{\partial p} = \left(\frac{\partial F}{\partial c} \right)^{-1} \left(-\frac{\partial F}{\partial p} \right) \quad (5.23)$$

We can prove that this matrix has full rank for all $(p, c(p))$ in 5.20 and hence ensure existence of the inverse matrix.

Differentiation of F with respect to p and c yields

$$\begin{aligned} \left(\frac{\partial F}{\partial c} \right) &= \begin{pmatrix} \frac{\partial \varphi_{\text{CO}_2}}{\partial pH} \frac{\partial pH}{\partial c_{\text{CO}_2}} - 1 & \frac{\partial \varphi_{\text{CO}_2}}{\partial pH} \frac{\partial pH}{\partial c_{\text{O}_2}} \\ \frac{\partial \varphi_{\text{O}_2}}{\partial pH} \frac{\partial pH}{\partial c_{\text{CO}_2}} & \frac{\partial \varphi_{\text{O}_2}}{\partial pH} \frac{\partial pH}{\partial c_{\text{O}_2}} - 1 \end{pmatrix} \\ &= \begin{pmatrix} \frac{\partial \varphi_{\text{CO}_2}}{\partial pH} \frac{\partial pH}{\partial c_{\text{CO}_2}} - 1 & 0 \\ \frac{\partial \varphi_{\text{O}_2}}{\partial pH} \frac{\partial pH}{\partial c_{\text{CO}_2}} & -1 \end{pmatrix} \end{aligned} \quad (5.24)$$

The last equality follows because $pH = -\log[H^+]$ and the H^+ concentration is a function of the c_{CO_2} , but not c_{O_2} . Then we only need to convince ourselves, that the first matrix element

$$\frac{\partial \varphi_{\text{CO}_2}}{\partial pH} \frac{\partial pH}{\partial c_{\text{CO}_2}} - 1 \quad (5.25)$$

differs from zero. This is always true, since $\frac{\partial \varphi_{\text{CO}_2}}{\partial pH}$ is positive and $\frac{\partial pH}{\partial c_{\text{CO}_2}}$ is negative. The inverse matrix yields:

$$\left(\frac{\partial F}{\partial c} \right)^{-1} = \begin{pmatrix} A & 0 \\ \frac{\partial \varphi_{\text{O}_2}}{\partial pH} \frac{\partial pH}{\partial c_{\text{CO}_2}} A & -1 \end{pmatrix} \quad (5.26)$$

where

$$A = \left(\frac{\partial \varphi_{\text{CO}_2}}{\partial pH} \frac{\partial pH}{\partial c_{\text{CO}_2}} - 1 \right)^{-1} \quad (5.27)$$

Inserting in equation 5.23, we get following result:

$$\frac{\partial c}{\partial p} = - \begin{pmatrix} A & 0 \\ -\frac{\partial \varphi_{CO_2}}{\partial pH} \frac{\partial pH}{\partial c_{CO_2}} A & -1 \end{pmatrix} \begin{pmatrix} \frac{\partial \varphi_{CO_2}}{\partial p_{CO_2}} & \frac{\partial \varphi_{CO_2}}{\partial p_{O_2}} \\ \frac{\partial \varphi_{O_2}}{\partial p_{CO_2}} & \frac{\partial \varphi_{O_2}}{\partial p_{O_2}} \end{pmatrix} \quad (5.28)$$

$$= - \begin{pmatrix} \frac{\partial \varphi_{CO_2}}{\partial p_{CO_2}} A & \frac{\partial \varphi_{CO_2}}{\partial p_{O_2}} A \\ \frac{\partial \varphi_{CO_2}}{\partial p_{CO_2}} B - \frac{\partial \varphi_{O_2}}{\partial p_{CO_2}} & \frac{\partial \varphi_{CO_2}}{\partial p_{O_2}} B - \frac{\partial \varphi_{O_2}}{\partial p_{O_2}} \end{pmatrix} \quad (5.29)$$

where

$$B = \left(\frac{\partial \varphi_{O_2}}{\partial pH} \frac{\partial pH}{\partial c_{CO_2}} A \right) \quad (5.30)$$

This expression is used for both blood and tissue. In the tissue there is no dependence on CO_2 and pH on the oxygen dissociation. Furthermore the CO_2 dissociation is independent of O_2 . Hence several elements in the matrix $\frac{\partial c_t}{\partial p}$ for tissue turns out to be zero, and we find:

$$\frac{\partial c_t}{\partial p} = - \begin{pmatrix} \frac{\partial \varphi_{CO_2}^t}{\partial p_{CO_2}} A & 0 \\ 0 & -\frac{\partial \varphi_{O_2}^t}{\partial p_{O_2}} \end{pmatrix} \quad (5.31)$$

where the φ^t are the dissociation curves in tissue, which differs from the one in blood. We will not list the expressions for $\frac{\partial c_b}{\partial p}$ and $\frac{\partial c_t}{\partial p}$ here, since they are long and rather uninteresting. They appear as part of the program source code in appendix A.3.

Due to these investigations we can conclude that p determines a unique c , and that $\frac{\partial c}{\partial p}$ is C^1 .

The compartment differential equations

The differential equations forming the compartment model are on the non-linear form (5.9):

$$\dot{x}_t = B(x_t, t)\gamma_b(x_t) + C(x_t, t)\gamma_t(x_t) + u(t), \quad (5.32)$$

To ensure the existence of a local solution it suffices to demand that all functions on the right hand side of 5.32 are C^1 in the interval of interest, which is restricted to positive, nonzero reals. By inspection of the functions in section 5.1, and the derivatives found in section 5.2.2 it is possible to verify that this is the case, provided that the inverse matrices of the expression

$$V_t \frac{dc_t}{dp} + V_b \frac{dc_b}{dp} \quad (5.33)$$

exists and is C^1 .

We have ensured existence of each of the matrices and their inverse each apart, but this does not guarantee existence of the inverse of the linear combination of the matrices. Investigation of the signs of the matrix elements does not ensure that the determinant is non-zero. Thus the inverse matrix does not necessarily exist.

The analogue physiological problem is if O_2 and CO_2 always dissociate in a unique way, or whether the systems include hysteresis, where a solution may depend on the history. Our insight in the involved biochemistry are primarily acquired from the models, and thus we are not sure whether this is a situation to occur in reality. We will leave it to the programmers to control that a singularity does not come into existence in the available range of parameters.

Apart from the existence of the inverse matrix, the differential equations defines a model with a unique local solution. The pH model limits the range of tensions to an interval $]a; b[$, containing the physiological range.

5.2.3 Stability of the transport model

A mathematical investigation of the asymptotical stability of the non-linear transport model would include finding equilibrium points of the system when the external inputs are constant. An equilibrium point is a constant solution to the equations that corresponds to a point where the right hand side of the differential equation vanishes. However, due to the size of the model and the nature of the equations this task is unrealistic. In addition deciding the stability of the equilibrium points would mean finding the Jacobian matrix for all the equations.

In the following we present some intuitive arguments about the stability of the transport model. We are fully aware that these are in no way a mathematical analysis of the model, but since such an analysis is too extensive to carry out, we feel that the intuitive arguments are in place.

A weaker stability than asymptotical stability is *marginal stability*. A system is marginally stable if the state of the system remains bounded for any bounded input [Høh, Def. 17.1]. We find that the nature of the compartment model allows us to argue for marginal stability.

The basic principle of mass balance in our compartmental equations ensures that no state variable can be negative, and that the sum of all the state variables is the total amount of matter in the system. As a consequence each

variable in the system is bounded as long as the total amount of matter in the system remains bounded. There are two ways matter can enter the system, either from the alveoli or from metabolism. The amount of matter entering through the lung membrane will tend to zero as the tension of the substance in the pulmonary capillaries tend to p_A , and hence a bounded p_A cannot infuse an infinite amount of matter. If the ventilation is not eliminated by the lung membrane permeability $\kappa = 0$, there will exist a finite tension that balance any bounded metabolic production. And as the blood flow in the system $Q > 0$ production in the organs exceeding the ventilation will raise the tension in the pulmonary capillaries. Therefore the system would be marginally stable, if the domain of all submodels was \mathbb{R}_+^n . As this is not the case for the pH model, too high metabolic rates for the CO_2 production would introduce CO_2 tensions outside the range of the pH model. In a system with control a high CO_2 production would increase ventilation and blood flow to increase the excretion and thus reduce this problem.

Our intuitive conclusion is that the model will be marginally stable for a range of parameters, and that a control system will extend this range.

Chapter 6

Parameters of the model

The listing in chapter 5 shows that the model contains many parameters. Yet, most of the parameters represent physical or physiological quantities, and must therefore take values that can be estimated independently of the model. However the model contains a few parameters that do not represent meaningful (or measurable) quantities outside the model. In this chapter we will state all the parameters of the models, in order to document our model and further to discuss the principles used when estimates have been made.

Even though most parameters are bound by the quantities they represent, differences in the nature of the parameters exist. We have found that the parameters fall into four rough categories:

Physical: Well defined physical quantities, which only under different circumstances (like a changed temperature) change in accordance to physical laws, but the values are not to be changed from the theoretical values. These are values like the gas constant, R , equilibrium constants for chemical reactions, and air density.

Measurable physiological: Parameters that represent physiological quantities are less well defined than the pure physical parameters, since biological systems show more variation. Thus values like the hemoglobin concentration, the blood and tissue volumes, and the lung dimensions are measurable, but will change from patient to patient.

Non measurable physiological: These are the parameters that in a less direct way represent measurable quantities. Many physiological quantities require measurements in vitro, an example is the pulmonary membrane flux coefficient κ . This quantity is not available because the

equipment for measuring the membrane flux in vitro does not exist, but yet the parameter represents a well defined physiological quantity. The estimate of the non measurable parameters of the model will be discussed in this chapter.

Statistical: The last category are parameters which are not contained in any of the above groups. This is the parameters used for fitting particular curves like for instance some of the parameters in the blood dissociation functions.

For a resume of the parameters of the models, we can conclude that the lung parameters are partly measurable quantities from the literature, partly estimates based on the anatomy of the lungs, see section 6.1.

Most of the parameters of the transport model are physiological measurable parameters directly taken from the literature, see section 6.2. An exception is the dissociation curves for the injected anaesthetic agents, which are estimated on basis of the three compartment models used for describing such agents, see section 6.3.

The metabolic rates of each compartment are calculated on the basis of aggregated values found in the literature and the need to obtain a physiologically correct equilibrium point of the model, see section 6.2.1

The pH model contains physical and physiological measurable quantities.

6.1 Parameters of the Lung Model

The physiological lung parameters are the compliance C and the unstretched volume V_0 for each section of the lung; the resistance, R , estimated from the area A , and the length l of each passage between the lung sections. Further parameters are the external pressure source U_m representing the respirator and the internal pressure source U_i representing the respiratory muscles.

6.1.1 Parameters concerning the pressure sources

The graph of the external pressure source U_m representing the respirator is found in [Bar]. Here typical graphs of the respirator pressure are plotted as functions of time, and we have implemented alike graphs in the model, see chapter 7. The pressure curves oscillate between atmospheric pressure and 3 kPa above this in a continuous but non differentiable way, however,

the precise pressure curve of the respirator depends on the respirator type and the conditions of the patient. In the final simulator the lung model will receive the pressure as input from the respirator, which is used in the operating theatre during the simulations.

According to Rideout [Rid0] the internal pressure source, U_t , representing the respiratory muscle, creates a pressure that is well approximated by a sine curve. The amplitude and the frequency are found so that a physiological tidal volume and ventilatory rate are obtained. The tidal volume at natural ventilation is 0.5-0.8 l, and the frequency is 10-15 breath/minutes.

6.1.2 Parameters concerning the laminar flow

When finding parameters for the $1 + n_a$ resistances, representing the air flow resistances between the lung section, two approaches can be made, either to calculate the resistances from the dimensions of the tubes the air flows through, or find values in the literature.

The first resistance R_0 represents the resistance of the conducting airways of branching generation 0-19, while the remaining parallel resistances represents the resistances of respiratory zone of the lung, branching generation 20-23. Since each generation of the airways consist of 2^g tubes, where g is the generation number, the total resistance of a generation can be calculated from the resistance of each tube in the generation.

When the pressure model was described, see section 3.1, the resistance of a laminar airflow through a tube with length l and radius r was found to be

$$R = \frac{8 l \eta}{\pi r^4} \quad (6.1)$$

where η is the viscosity of the gas. From equation 6.1 the resistance in each generation of tubes in the branched airways is calculated as

$$R = \frac{8 l \eta}{2^g \pi r^4} \quad (6.2)$$

where 2^g is number of tubes in the g 'th generation, see table 6.1. Thus an estimate of the resistances in our model can be calculated as the sum of the serially connected resistances in the generations of the tubes.

Table 6.1 also provides some literature values for resistances of the generations of branching [Wes2].

Our lung compartments represent the upper airways (generation 0-19) and the alveoli (generation 20-23). As resistance between compartment 0 and

<i>g</i>	<i>d</i> [mm]	<i>l</i> [m]	R [kPa s/l]	
			<i>Calc.</i>	<i>Lit.</i>
0	18.00	0.1200	0.00088	0.00680
1	12.20	0.0476	0.00083	0.00700
2	8.30	0.0190	0.00077	0.00740
3	5.60	0.0076	0.00075	0.00790
4	4.50	0.0127	0.00150	0.00830
5	3.50	0.0107	0.00172	0.00760
6	2.80	0.0090	0.00177	0.00610
7	2.30	0.0076	0.00164	0.00440
8	1.86	0.0064	0.00162	0.00330
9	1.54	0.0054	0.00145	0.00230
10	1.30	0.0046	0.00122	0.00130
11	1.09	0.0039	0.00104	0.00100
12	0.95	0.0033	0.00077	0.00050
13	0.82	0.0027	0.00056	0.00025
14	0.74	0.0023	0.00036	0.00020
15	0.66	0.0020	0.00025	0.00020
16	0.60	0.0017	0.00015	0.00015
17	0.54	0.0014	0.00010	
18	0.50	0.0012	0.00006	
19	0.47	0.0010	0.00003	
<i>R</i> ₀ Generation 0–11			0.01521	0.06340
20	0.45	0.0008	0.00001	
21	0.43	0.0007	0.00001	
22	0.41	0.0006	0.00000	
23	0.41	0.0005	0.00000	
<i>R</i> ₁ Generation 12–21			0.002	

Table 6.1: The dimensions of the airways [Gro] and the calculated resistances to airflow in the generations of branching compared to values of the resistances from [Wes2].

the atmosphere we have used the resistance from the upper 12 generations (0–11), to represent the resistance from the atmosphere to the center of the compartment. The resistances in generation 12–21 have been used to estimate the resistance between the center of the central compartment and the center of the alveoli. As it can be seen, the calculated resistances in table 6.1 do not match the values from [Wes2] well in the first generations. Reasons could be that the simplification of the airways to cylindric tubes are

too rough, and that the measured values include some effects of turbulence that increase the resistance. Another reason might be that the resistance of the elastic tubes is not constant during the ventilatory cycle and the standard diameters and lengths are concerning another stage in this cycle, than the resistance from [Wes2]. None of the references discuss the variation of size of the airways with the pressure.

In situations of artificial ventilation, the resistance of the upper airways, R_0 , must include the resistance of the endotracheal tube, since this is inserted through the mouth to the upper airways, to connect the respiratory mask [Bar]. We have used the physiological values found in the literature ([Wes2] and [Rid0]) for the experiments with our model, but performed some fitting as well, to obtain reasonable pV diagrams, see section 7.1.1.

6.2 Parameters of the transport model

The parameters of the transport model are the quantities of the blood and tissue volumes of the body V_b and V_t , the pulmonary membrane permeability κ , the parameters determine the blood flows, which are the cardiac output Q and distribution parameters z_i and λ , and finally all the parameters of the submodels.

The cardiac output and the blood distribution fractions are supposed to be output from the cardio-vascular model, but until the final simulator is available, we have used the standard value 5.2 l/min for cardiac output, and the fractions given in table 6.4. The blood and tissue volumes V_b and V_t are listed in the table too.

The permeability of the membrane connecting the lung and the transport model, κ , is only indirectly a measurable quantity, and it is difficult to distinguish between the effects of a disordered membrane transport, a inhomogeneous perfusion/ventilation ratio or a increased pulmonary shunt. The model is supposed to be usable for investigations of effects of a disordered membrane transport and κ gives the opportunity for differentiating the membrane permeability of substances. We have not found explicit values for κ in the literature, but this has not really constituted a problem, since we have not investigated the effect of membrane transport limitation. Thus the elements of κ has either been 0 or very large to indicate instantaneous equilibrium over the membrane. The model implementation takes advantage of large values of κ to ensure real instantaneous equilibrium, see appendix A.

In the following we treat the remaining parameters of the transport model by submodel.

6.2.1 Fitting the Metabolic Rates

The metabolic rates are compartment specific functions of the concentration in the particular compartment. In each functions for the consuming part of the metabolism \mathcal{M}_- there are two parameters, β and M . M describes the maximum metabolic rate of the compartment, which is valid when the oxygen concentration in tissue is high. β is the concentration where the metabolism is half the maximum value due to lack of available oxygen. For oxygen we have estimated β in such a way that the deviation from the maximum metabolic rate at normal concentrations is 1%. This is done by setting β to 0.01% of the tissue concentration at standard arterial tension.

Values for the metabolic rate can be found in the literature, but not as the per organ metabolism we need, only as the following aggregated values from [Fuk1]:

$$\mathcal{M}_{brain} = 50 \text{ ml/min} \quad (6.3)$$

$$\mathcal{M}_{viscera} = 175 \text{ ml/min} \quad (6.4)$$

$$\mathcal{M}_{muscles} = 35 \text{ ml/min} \quad (6.5)$$

This is metabolic rates at rest when the oxygen supply is sufficient, the sum of these rates is 260, which is the total consumption rate. Under the assumption that the viscera organs have a similar metabolism per volume unit, we have estimated the metabolism of each organ from the aggregated values. A value of the total carbondioxide production has then been distributed between the organs by the same key as the oxygen consumption.

One of the most important properties of the model is that a physiological steady state is obtained when standard input is used. The question is therefore, whether the total metabolic rate from [Fuk1] harmonizes with the difference gas content of arterial and venous blood. The standard physiological values are given in table 6.2.

At normal physiological steady state the tension of CO_2 is 5.3 kPa in systemic arterial blood and 6.1 kPa in systemic venous blood. The tension of O_2 is 13.3 kPa in arteries and 5.3 kPa in veins. When these tensions are found in arterial blood entering the organ compartment, the total metabolic rates for production and consumption (\mathcal{M}_+ and \mathcal{M}_-) of CO_2 and O_2 can be found

	arterial blood	mixed venous blood
p_{CO_2} (kPa)	6.1	5.3
p_{O_2} (kPa)	5.3	13.3
pH	7.4	7.37

Table 6.2: Standard values for pH, CO₂ and O₂ in blood [Nun, p.208]

from the difference in concentrations in the arterial and venous blood and the cardiac output:

$$\mathcal{M}_+ = Qc_{\text{O}_2}(p_{\text{vs}}) - c_{\text{O}_2}(p_{\text{as}}) \quad \mathcal{M}_- = Qc_{\text{CO}_2}(p_{\text{as}}) - c_{\text{CO}_2}(p_{\text{vs}}) \quad (6.6)$$

Inserting the steady state blood tensions p_{as} and p_{vs} , we find that in total $\mathcal{M}_- = 6.15\text{mmol/min}$ of oxygen and $\mathcal{M}_+ = 11.52\text{mmol/l}$ of carbondioxide, which is 258 ml/min and 162ml/min respectively: These quantities are in harmony with the ones given by [Fuk1].

We have therefore set the metabolic rate of the brain compartment to be 50 ml/min. The adipose compartment is assumed not to consume and produce anything. The remaining body compartments are grouped in two, one group containing the muscles and connective tissue and one group containing the viscera organs except the brain. There are still several ways to distribute the aggregated rates of [Fuk1] between these compartments. One possibility is for instance to distribute the total rate in accordance with the fraction of the total blood flow, such that the organs are assumed to be highly perfused because they have a high consumption. This is not a physiologically correct distribution, as the importance of other substances transported with the blood might influence the distribution of blood to organs. We have therefore instead distributed the rates of [Fuk1] with respect to the tissue size of the compartment. Thus for instance the maximum metabolic rate M_{mu} of the muscle compartment are found from the equation:

$$M_{\text{mu}} = 35 \frac{V_{\text{mu}}}{V_{\text{mu}} + V_{\text{co}}} \quad (6.7)$$

6.2.2 Parameters of the pH model

There are four parameters of the pH model. Two are the chemical equilibrium constants, $K_{\text{a,CO}} = 10^{-6.1}$ mole/l, $K_{\text{a,Pr}} = 10^{-7.3}$ mole/l, and not subject to change. The other two parameters are the physiological values of natriumhydroxide and proteinate concentrations, $[\text{NaOH}]_0 = 46.2\text{mmol/l}$, $[\text{HPr}]_0 = 39.8\text{mmol/l}$, from [Chil].

6.2.3 Parameters of the dissociation models

The dissociation functions of the respiratory gasses in blood and tissue contain the same parameters, as we have used the same dissociation functions for tissue as the parts of the blood dissociation, which determine the plasma concentrations.

Symbol	Standard value	Description
$\alpha_{\text{CO}_2}^{\text{Ery}}$	0.195mmol/l/kPa	Solubility of CO ₂ in erythrocytes.
$\alpha_{\text{CO}_2}^{\text{Pla}}$	0.230mmol/l/kPa	Solubility of CO ₂ in plasma.
α_{O_2}	9.83 μ mole/l/kPa	Solubility of O ₂ .
C_{Hb}	9.30mmol/l	Total concentration of hemoglobin.
x_{Hbf}	0	Frac. of Hb that is fetal hemoglobin.
x_{HbCO}	0.005	Frac. of Hb that is carboxyhemoglobin.
x_{Hi}	0.005	Frac. of Hb that is hemoglobin.
C_{DPG}	5.01mmol/l	Conc. of 2,3-diphosphoglycerate.
$C_{\text{Hb}}^{\text{Ery}}$	21.0mmol/l	Conc of Hb in erythrocytes

Table 6.3: Parameters for the dissociation of CO₂ and O₂, from [Sig0].

The blood dissociation models by Siggaard-Andersen used for CO₂ and O₂ have several parameters. The solubility coefficients: $\alpha_{\text{CO}_2}^{\text{Ery}}$, $\alpha_{\text{CO}_2}^{\text{Pla}}$ and α_{O_2} are physical parameters. The remaining parameters are the physiological values of the blood components, see table 6.3. and the blood temperature $T = 37^\circ\text{C}$. All these physiological parameters may be changed for particular simulations if anyone wants to. Even though this does not seem to be the case for all the quantities, we will leave it to the future users, to decide which quantities are relevant to change.

For the anaesthetic agents the dissociation curves are supposed to be either linear with a solubility coefficient α for each solvent. In case the agent is protein binding, the dissociation curves are determined by the concentrations of proteins in the solvent and the equilibrium for the chemical reaction of drugs and proteins [And].

The solubility coefficients of the various inhaled anaesthetic agents are normally stated in the literature, but intravenous anaesthetic agents are in the literature described by a compartment model, with three compartments, originated in the empirical data of the kinetics of anaesthetic agents. Examination of empirical values suggest that a well approximation by a linear combination of three exponential functions. The compartment model can be seen as a way of visualizing the linear combination of three exponential equations [Hul].

For an intravenously given anaesthetic agents, the transport model containing a correct dissociation function for the agent ought to be an appropriate description, as the substance is distributed by the same mechanism as the gasses. If an agent is added to the blood, the substance will be distributed in the body by blood circulation, which we assume is well described in the blood transport model, and diffused into the tissue due to a tension gradient. Hence an injected anaesthetic agent is just a new element in the state vector of the transport model.

Yet, the concept of tension of a dissolved liquid might not be as obvious as the tension of a dissolved gas. Therefore we will state what the meaning of tension is in connection with a liquid dissolved in a liquid. Just like the case of a gas, the tension of a liquid in a liquid is a measure of how well the solvent may hold an amount of the liquid. The lower the tension is with a certain amount dissolved, the better the solvent is to contain the liquid. Thus when distributing a liquid between two solvents, as in an organ compartment, it is not the solubilities in each solvent that matters, but rather the ratio between the solubilities. The three compartment model is a linear model, and thus describes a linear dissociation of the anaesthetic agents. To describe the dissociation of a substance in an organ by the solubilities requires the transport of the agents through membranes to be sufficiently fast, so that equilibrium in the body compartments can be assumed. According to MD. John Jacobsen this is not an unrealistic claim.

The task is therefore to estimate the parameters of the solubility in our model from the parameters of the three compartment model. We intend to do this in accordance with an interpretation of the three compartment model given by [Hul] and [Gib]. In the next section (6.3) we will therefore describe the three compartment models, and then in section 6.4 determine the solubility coefficients of the anaesthetica from the three compartment model.

6.3 The three compartment model

The pharmacokinetics of intravenous agents are usually described by parameters to two or three compartment models, illustrated in figure 6.1 [Olu]. The central compartment represents the blood, and the two other compartments are some kind of tissue compartments. Information about the dynamic of the agents is given in terms of the rates k_{ij} , in which the i and j indicates the flow is from the i 'th to the j 'th compartment. The rate k_{10} is the elimination rate, and model how the agent is eliminated out of the body by metabolism and

excretion. Finally a volume of the central compartment is stated, something we will treat in detail later.

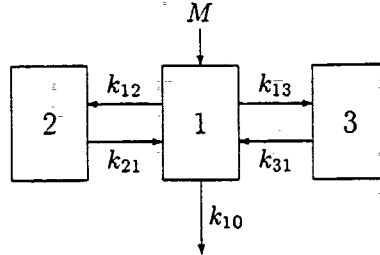


Figure 6.1: The three compartment model of intravenous agents

According to [Hul] and [Gib] the physiological interpretation of this model says that the organs will not obtain an equilibrium state with the arterial blood simultaneously. The different parts of the body receive a share of the total blood flow, which is not controlled from the size of the organ, but rather from the importance of the organ. This means that the kidney and liver will for instance be highly perfused, while muscles and fat deposit receive only a small part of the blood relative to the volumes of these parts.

The concentration of a substance added to the blood will increase fast in the highly perfused organs, while the concentration in low perfused areas will slowly creep to an equilibrium, as illustrated in figure 6.2.

The two peripheral compartments of the three compartment model are a fast and a slow compartment respectively. If the substance dissolves equally in any kind of tissue, the concentration at equilibrium will be the same all over the body, but still the organs reach this point at different stages of the distribution.

6.3.1 The equations and solutions of the 3 compartment model

By considering the flow between the compartments, one reaches the following differential equation, describing the change in the amount of matter in each compartment [Olu]:

$$\begin{pmatrix} \frac{dx_1}{dt} \\ \frac{dx_2}{dt} \\ \frac{dx_3}{dt} \end{pmatrix} = \begin{pmatrix} -(k_{12} + k_{13} + k_{10}) & k_{12} & k_{31} \\ k_{12} & -k_{21} & 0 \\ k_{13} & 0 & -k_{31} \end{pmatrix} \begin{pmatrix} x_1 \\ x_2 \\ x_3 \end{pmatrix} \quad (6.8)$$

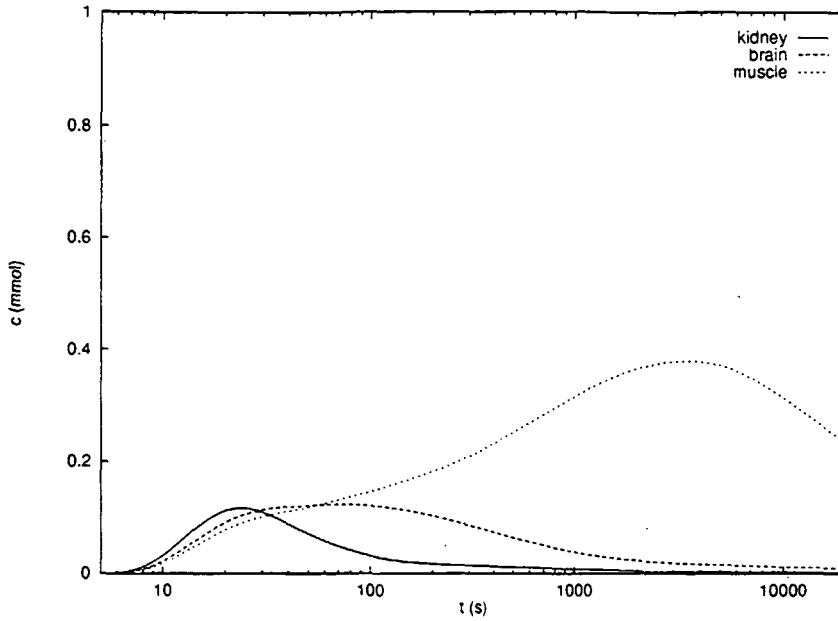


Figure 6.2: Curves showing the amount of substance distributed by blood flow to different perfused organs.

where x_i is the amount of matter in the i 'th compartment.

The initial conditions corresponding to an instantaneous injection of the drug M into the blood are $x_1(0) = M$ and $x_2(0) = x_3(0) = 0$.

We find the following solution to the system

$$\begin{pmatrix} x_1 \\ x_2 \\ x_3 \end{pmatrix} = K \begin{pmatrix} e^{\lambda_1 t} \\ e^{\lambda_2 t} \\ e^{\lambda_3 t} \end{pmatrix} \quad (6.9)$$

where K is the matrix

$$\begin{pmatrix} \frac{M(\lambda_1^2 - (k_{21} + k_{31})\lambda_1 + k_{21}k_{31})}{(\lambda_1 - \lambda_2)(\lambda_1 - \lambda_3)} & \frac{M(\lambda_2^2 - (k_{21} + k_{31})\lambda_2 + k_{21}k_{31})}{(\lambda_2 - \lambda_3)(\lambda_1 - \lambda_2)} & \frac{M(\lambda_3^2 - (k_{21} + k_{31})\lambda_3 + k_{21}k_{31})}{(\lambda_3 - \lambda_2)(\lambda_1 - \lambda_3)} \\ -\left(\frac{M(k_{21}(k_{31} - \lambda_2))}{(\lambda_2 - \lambda_3)(\lambda_1 - \lambda_2)} + \frac{M(k_{21}(k_{31} - \lambda_2))}{(\lambda_2 - \lambda_3)(\lambda_1 - \lambda_3)}\right) & \frac{M(k_{21}(k_{31} - \lambda_2))}{(\lambda_2 - \lambda_3)(\lambda_1 - \lambda_2)} & \frac{M(k_{21}(k_{31} - \lambda_2))}{(\lambda_2 - \lambda_3)(\lambda_1 - \lambda_3)} \\ -\left(\frac{M(k_{31}(k_{21} - \lambda_2))}{(\lambda_2 - \lambda_3)(\lambda_1 - \lambda_2)} + \frac{M(k_{31}(k_{21} - \lambda_2))}{(\lambda_2 - \lambda_3)(\lambda_1 - \lambda_3)}\right) & \frac{M(k_{31}(k_{21} - \lambda_2))}{(\lambda_2 - \lambda_3)(\lambda_1 - \lambda_2)} & \frac{M(k_{31}(k_{21} - \lambda_2))}{(\lambda_2 - \lambda_3)(\lambda_1 - \lambda_3)} \end{pmatrix}$$

and $\lambda_1, \lambda_2, \lambda_3$ are the eigenvalues of the matrix in 6.8, solving the characteristic polynomial:

$$\lambda^3 + (k_{12} + k_{21} + k_{13} + k_{31})\lambda^2 + (k_{10}k_{31} + k_{10}k_{21} + k_{12}k_{31} + k_{13}k_{21} + k_{21}k_{31})\lambda + k_{10}k_{21}k_{31} = 0$$

To obtain a curve of the concentration in the blood from the above solution 6.9, the volume of the blood compartment has to be known. The variables

can be changed from amounts to concentrations by dividing the amount by the volume V_i of the respective compartment.

$$c_i(t) = \frac{x_i(t)}{V_i} \quad (6.10)$$

The volume V_i is subject to some confusion in the literature, and thus we find it relevant to clarify some definitions of volumes used in connection with compartment models.

Apparent volume

An apparent volume is a virtual volume of a compartment, associated with a measurement. It is the volume that the injected dose must be divided by to obtain the concentration that can be measured after the injection of the drug, see equation 6.10. This need not be the same as the physical volume of the compartment, e.g. the volume of the blood [Hul].

Our interpretation of an apparent volume is that the drug is supposed to combine with something in the compartment, to form a compound, that is not included when the concentration is measured. A very fast chemical reaction that is linear would satisfy such an interpretation. Linearity of a chemical reaction is reasonable if the concentration of the drug is very small compared to the concentration of the substance it combines with.

However the literature is not quite clear in the interpretation of the apparent volume, since the apparent volume in the literature [Gib. Hul] may be ascribed to an insufficient mixing of the blood. In our view this interpretation of the apparent volume is not a useful quantity, since it will depend on the exact circumstances of measurement. The mixing of the blood is closely related to the transport of drug to the organ tissue, and thus the effect of distribution in the body is accounted for twice, both in the body compartments (2, 3) and in the apparent volume. A model with more compartments is based on an assumption of instantaneous mixing in smaller areas is therefore supposed to offer a better description of the distribution.

We find that the latter interpretation is a confusion with the volume of distribution, as described in the following.

Volume of distribution

The volume of distribution is a term from compartmental theory that describes the volume the blood compartment should have if the blood concen-

tration of the matter in a steady state situation reflected a distribution of matter only into the blood.

Thus the ratio of the distribution volume V_d and the real blood volume V_b expresses the ratio between the amount of substance injected, M , and the amount of substance present in the blood, when equilibrium between blood and tissue is obtained in a situation where the total content in the three compartment is constant. This can be written

$$\frac{V_b}{V_d} = \frac{x_{1e}}{M} \quad (6.11)$$

where x_{1e} is the amount of matter in the central compartment at equilibrium. The distribution volume can be expressed by the parameters of the three compartment model, and enters in fact the solution of the differential equations for the three compartment model. In a situation of equilibrium the amounts of drug in the three compartments must satisfy

$$x_{1e} = \frac{k_{21}}{k_{12}} x_{2e} = \frac{k_{31}}{k_{13}} x_{3e}$$

Since the total amount of matter in the model is the sum of the matter in each compartment the equilibrium situation satisfies

$$M = x_{1e} \left(1 + \frac{k_{12}}{k_{21}} + \frac{k_{13}}{k_{31}} \right)$$

Inserting this in equation 6.11 yields the volume of distribution:

$$V_d = V_b \left(1 + \frac{k_{12}}{k_{21}} + \frac{k_{13}}{k_{31}} \right) \quad (6.12)$$

in which V_d is the distribution volume, and V_b is the blood volume.

The volume of distribution is found directly from the solution of the three compartment model, by setting the elimination k_{10} to 0, and examining the solution. In this system one of the eigenvalues becomes zero, since they are the solutions to the following characteristic polynomial:

$$\lambda(\lambda^2 + (k_{12} + k_{21} + k_{13} + k_{31})\lambda + k_{12}k_{31} + k_{13}k_{21} + k_{21}k_{31}) = 0$$

Inserting $\lambda_1 = 0$ in the solution we find for the amount of drug in the central compartment:

$$x_1(t) \rightarrow M \frac{k_{21}k_{31}}{\lambda_2\lambda_3}, \quad t \rightarrow \infty$$

Since the product of the roots λ_2 and λ_3 equals the constant term in the second degree polynomial, $(\lambda - \lambda_1)(\lambda - \lambda_2) = \lambda^2 - (\lambda_2 + \lambda_3)\lambda + \lambda_2\lambda_3$ and hence $\lambda_2\lambda_3 = k_{12}k_{31} + k_{13}k_{21} + k_{21}k_{31}$, we find by use of equation 6.12, that:

$$x_1(t) \rightarrow M \frac{k_{21}k_{31}}{k_{21}k_{31}(1 + \frac{k_{12}}{k_{21}} + \frac{k_{13}}{k_{31}})} = M \frac{V_b}{V_d}, \quad t \rightarrow \infty$$

The concentration C_1 in the blood is found

$$C_1 = \frac{M}{V_b} \frac{V_b}{V_d} = \frac{M}{V_d}$$

for $t \rightarrow \infty$.

The volume of distribution can be seen as the apparent volume of the total model. In our opinion the confusion of the interpretation of an apparent volume in a multicompartment model might arise from a mix-up of the apparent volume for compartment 1 with the apparent volume of the total system, the distribution volume. If the dissociation functions of the intravenous agent are being deduced from parameters of a three compartment model, the interpretation of the volumes in this model ought to be unambiguous. In next section (6.4) we will describe how to find the solubility coefficients of the anaesthetics from the parameters of the three compartment model.

6.4 Solubility of intravenous anaesthetics

In the blood transport model we have assumed that the diffusion from the blood into the tissue does not depend on the amounts found in the two solvents, but on the tensions. The tension relates to the concentration by the solubility α , which we assume to be constant for the anaesthetic agents:

$$c = \alpha p \quad (6.13)$$

The amount of matter in a compartment is

$$x = cV = \alpha pV \quad (6.14)$$

in which x is the amount, c the concentration, V the volume, α the solubility coefficient, and p the tension. Thus we get

$$p = \frac{x}{\alpha V} \quad (6.15)$$

The parameters k_{ij} of the 3 compartment model are given as specific parameters for substances. In systems without elimination ($k_{10} = 0$), the equilibrium among the three compartments is found from the k_{ij} 's.

$$x_{1e}k_{12} = x_{2e}k_{21} \text{ and } x_{1e}k_{13} = x_{3e}k_{31} \quad (6.16)$$

where x_{ie} is the amount of matter in the i 'th compartment at equilibrium.

Since the physiological interpretation of the three compartment model is that compartments 2 and 3 represent tissue, the physiological meaning of an equilibrium situation is that the blood has a constant concentration of drug, and that the content of compartments 2 and 3 are distributed in the tissue of the body in some way.

Thus the equilibrium situation of the three compartment model must correspond to a situation where an equilibrium exist over the membranes dividing the blood and the tissue. In our model this is equivalent to a situation with the tension being uniform throughout the body. Using equation 6.15 we find that the tension of all compartments in the equilibrium situation is

$$p = \frac{x_{1e}}{V_1\alpha_1} = \frac{x_{2e}}{V_2\alpha_2} = \frac{x_{3e}}{V_3\alpha_3} \quad (6.17)$$

and hence we deduce that

$$\frac{\alpha_1}{\alpha_2} = \frac{k_{21}V_2}{k_{12}V_1} \quad (6.18)$$

$$\frac{\alpha_1}{\alpha_3} = \frac{k_{31}V_3}{k_{13}V_1} \quad (6.19)$$

where α_1, α_2 and α_3 is the solubility coefficient of compartments 1, 2 and 3, and the volumes are real volumes.

The task of fitting parameters for our model is to find the solubilities for the eight tissue compartments and the blood. The equations 6.18 and 6.19 give the ratio between the solubility of the blood and two different sections of the body, which we term "fast" and "slow". A fast compartment is one that is fast to reach equilibrium with the blood because the blood perfusion is high relative to the size of the organ, while a slow compartment has a low relative perfusion.

To find which organs are fast and which are slow in the blood transport model, we examine the differential equation governing the change of tension of the anaesthetic agent in an organ compartment:

$$\frac{dp}{dt} = (V_t \frac{dc_t}{dp} + V_b \frac{dc_b}{dp})^{-1} (z_i Q (c_b(p_{as}) - c_b(p)) + \mathcal{M}_+ - \mathcal{M}_-) \quad (6.20)$$

The solubility of the anaesthetic agent is assumed to be constant, thus the dissociation functions $c(p) = \alpha p$ are independent of the presence of oxygen and carbondioxide, and thus the term $\frac{dc}{dp}$ is simply the solubility coefficient α . From equations 6.18 and 6.19 we know that the ratio between α_b and α_t is constant.

Thus for the anaesthetic agent equation 6.20 in a system without elimination becomes

$$\frac{dp}{dt} = \frac{z_i Q(\alpha_b p_{as} - \alpha_b p)}{(V_t \alpha_t + V_b \alpha_b)} = \frac{z_i Q(p_{as} - p)}{(V_t \psi + V_b)} \quad (6.21)$$

for $\psi = \frac{\alpha_t}{\alpha_b}$. It can be seen that the equation does not depend on the actual level of the solubilities, but only on the ratio between them.

All body compartments has inflow of blood only from the arterial blood pool, and thus the content of drug in the inflowing blood will be equal in all body compartments. Thus any differences in the behaviour of the body compartments must come from differences in how the drug supply is relative to the compartment size. From equation 6.21 it can be seen that the behaviour depends on the term $\frac{z_i}{V_t \psi + V_b}$ (and the metabolism, which is not the concern right now). To acquire an overview of how the different organ compartments behave, we have calculated this term for different ratios of solubilities, see table 6.4.

	Standard parameters			Perfusion vs. size		
	z	V_t [l]	V_b [l]	$1000 \frac{z}{V_t \psi + V_b}$		
				$\psi = 1$	$\psi = 10$	$\psi = 100$
Liver	0.283	2.973	1.106	69.380	9.178	0.948
Kidney	0.222	0.270	0.051	691.589	80.698	8.207
Heart	0.048	0.307	0.040	138.329	15.434	1.561
Brain	0.135	1.300	0.105	96.085	10.301	1.038
Remaining	0.041	0.217	0.015	176.724	18.764	1.888
Connective	0.101	8.182	0.653	11.432	1.225	0.123
Muscles	0.107	26.773	0.700	3.895	0.399	0.040
AdiPOSE	0.062	14.786	0.562	4.040	0.418	0.042

Table 6.4: Perfusion vs. size in the organ compartments at different ratios between solubilities in blood and tissue.

From the table it can be seen that the kidney compartment is the best perfused organ, but all the organs receive better perfusion than the muscles, connective and adiPOSE tissue. Based on the figures, we have decided to

partition the compartments into two groups: the viscera organs, (liver, kidney, heart, brain, and remaining) as fast, and the slow "tissue", (muscle, connective and adipose tissue).

Estimating the solubility coefficients of these compartments we let the fast compartments correspond to the compartment in the three compartment model with the highest k_{1i} . We assume this is compartment 2, and let the slow compartments correspond to compartment 3. Since the actual level of the solubility does not affect the equation for each organ, cf. 6.21 we arbitrarily set the blood solubility $\alpha_b = 1$. Then using equation 6.18 the solubility of the tissue in the viscera organs become

$$\alpha_{\text{fast}} = \frac{V_1 k_{12}}{V_{\text{fast}} k_{21}} \quad (6.22)$$

where V_1 is the blood volume and V_{fast} is the total volume of the viscera organ compartments. The solubility of the slow compartment is estimated by

$$\alpha_{\text{slow}} = \frac{V_1 k_{13}}{V_{\text{slow}} k_{31}} \quad (6.23)$$

The final parameter for the anaesthetics, the metabolic rate, is estimated from the same as the elimination rate k_{10} . Thus we have used the information from the three compartment model to estimate parameters for the anaesthetic agent. If more specific information of the dissociation on a specific agent is available, we propose that this information is used, however.

6.5 Conclusion

The models of the respiratory system contain the parameters, which are needed for the requested scenarios. We expect that the physiological ranges of the parameters are sufficient to simulate the effect of the required disorders of the respiratory system with an acceptable model output. Further the models suggest other scenarios by the presence of several parameters, which through the physiological literature we realized are of importance for the system modelled. An example is the components of the blood, which are as important as the ventilation for the transport of gasses between the atmosphere and the tissue. Another example is the level of detail in the description of the blood flow. The partition of the body into fourteen compartments enables simulations, in which the status of blood in specific parts of the body is measured, or scenarios with changes in the size and metabolic rates of specific organs.

Chapter 7

Testing the model

In this section we are testing the models of the respiratory system. The aim of this chapter is to give an overview of the possibilities in simulations of the respiratory system with the models presented in this thesis. The simulations we will present are thus not considered to be a complete description of the behaviour of the models under all circumstances, but rather a highlight of some interesting behaviours.

First the lung model is tested in order to produce some characteristic pV -diagrams found in [Bar], within the estimated range of parameters found in chapter 6. These diagrams are output from the pressure model, which is a submodel of the lung model. The other part of the lung model, the gas model, shows the partial pressures in the expired air and the alveoli under different circumstances.

The evaluation of the blood transport model is made, first by testing the submodels of the blood transport system and afterwards the blood transport model is used for simulations of distribution of respiratory gasses and anaesthetics. We show the dynamics of the blood transport model, with and without metabolism. For respiratory gasses we describe the influence of the Bohr-Haldane effect. For the anaesthetic agent thiopentone we compare the dynamics of drug distribution when the model is configured with estimated solubilities and when it is configured with explicit solubilities from the literature.

7.1 The lung model

The lung model consists of the pressure model and the gas model, and we will test each submodel individually.

7.1.1 The pressure model

Based on their experience with equipment that displays diagrams of the respiratory mask pressure and the lung volume during anaesthesia the MDs of the SIMA group has requested that our lung model can produce these pV diagrams. The technique of measurement is described in [Bar], which also shows some characteristic diagrams.

For comparing the output of the model with the diagrams of [Bar] we have used an approximation of a respirator pressure curve for input, see figure 7.1.1. The inaccuracies of our piecewise linear approximation are a problem

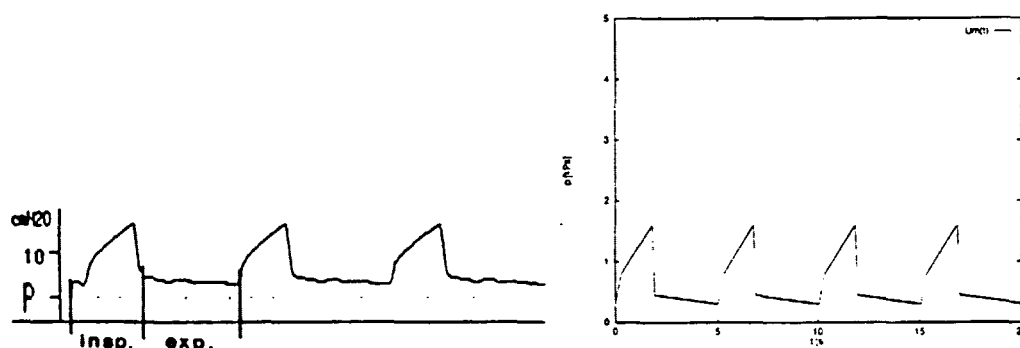


Figure 7.1: The respirator pressure from [Bar], and our approximation.

only during testing, since the pressure will be measured on a real respirator in the final simulator. The purpose of our tests is to demonstrate the nature of changes in the diagrams for different configurations, and for this we find the approximation adequate. With the pressure curve shown in 7.1.1 as the pressure function $U_m(t)$ and the parameters from table 7.1 we have produce a pV diagram of a normal lung, see figure 7.1.1.

	R	C	V_0
Central cmpt.	1.00	0.02	0.1
Alveoli cmpt.	0.02	0.80	2.7

Table 7.1: The parameters of the standard lung

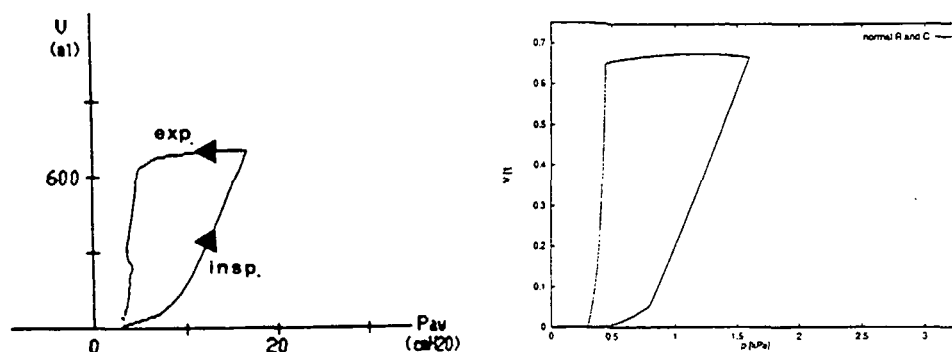


Figure 7.2: The model generated pV diagram for normal lung, and the diagram from [Bar].

The effect of a low compliance can be seen in figure 7.3. The characteristic effect is that the tidal volume is lower than in the normal lung, and thus that the loop is more flat. Another significant display is the “duck tail” at the end of the expiration. The pressure falls to zero, but since the lung contains a small amount of air relative to the resistance, the air leaves easily, and the last of the expiration the pressure inside the lung is almost equal to the external pressure.

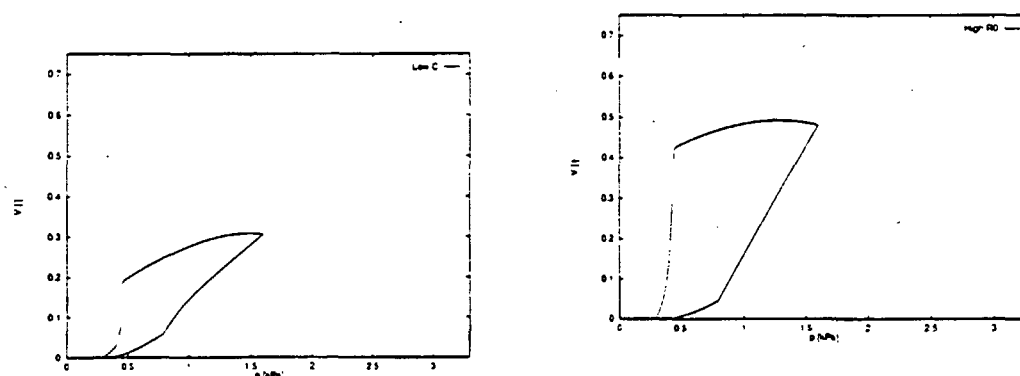


Figure 7.3: pV diagram generated with low compliance $C_1 = 0.5 * C_{1, \text{std}}$

Figure 7.4: pV diagram generated with high airways resistance $R_0 = 2 * R_{0, \text{std}}$

Increasing the resistance of the upper airways hampers the flow of air in and out of the lung, see figure 7.4. Thus the tidal volume decreases, since less air enters during inspiration. The “duck tail” effect observed with low compliance does not occur.

7.1.2 The gas model

The interesting aspect of the gas model is its ability to renew the air in the alveoli. To show the dynamics of the ventilation we have set the gas flow over the lung membrane constant at a level that matches normal metabolism (260ml O_2 and 160ml CO_2 pr minute), and started the model with a high level of carbondioxide and a low level of oxygen in the alveoli.

In figures 7.5 and 7.6 can be seen the behaviour of the partial pressures of CO_2 and O_2 in both the central and the alveolar compartment. The standard parameters from table 7.1 and the pressure curve from figure 7.1.1 are used. The central compartment shows large variation, since the partial pressures tend towards the partial pressures of the atmosphere during inspiration and the partial pressures of the alveoli during expiration. The variation in the alveoli are much less, which is not surprising since the alveoli make up most of the lung volume, and the alveolar volume is about 6 times the tidal volume. The graphs show how the excess carbondioxide is eventually removed, and the oxygen level increased to the normal levels.

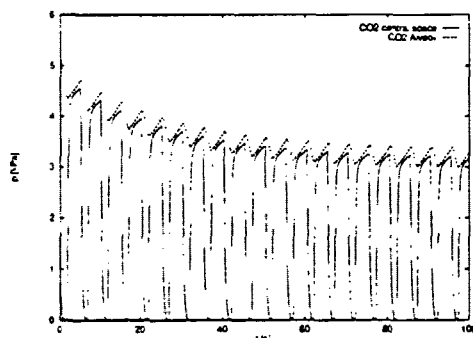


Figure 7.5: p_{CO_2} in a normal lung

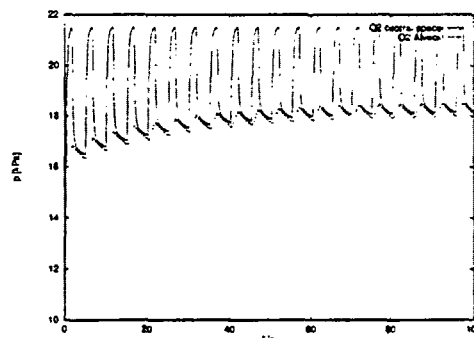


Figure 7.6: p_{O_2} in a normal lung

When the same test is run on the lung with half compliance, the result is very different. The ventilation of this lung is not sufficient to remove the carbondioxide or supply the oxygen. Normally this would be counteracted by the respirator by an increased pressure, but the graphs in figures 7.7 and 7.8 illustrate the effect of a poor ventilation. The level of CO_2 raises and the O_2 level drops.

A final view of the dynamics of our gas model can be found in figure 7.9, where the respirator pressure is shown together with the carbondioxide partial pressure in the central compartment. During the inspiration a gas analyzer in the respiratory mask will not detect any CO_2 , since it receives air from the

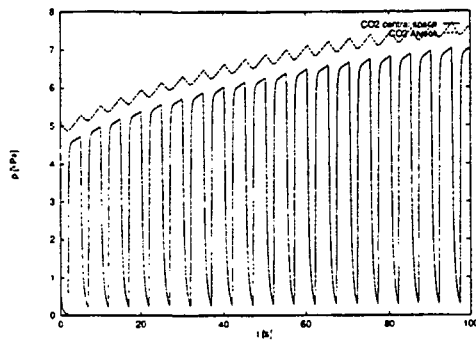


Figure 7.7: p_{CO_2} in a lung with low compliance

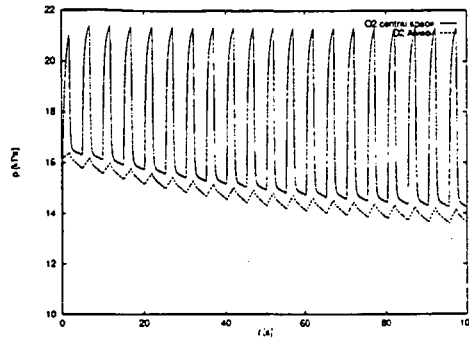


Figure 7.8: p_{O_2} in a lung with low compliance

atmosphere. When expiration starts, at the peak of the respirator pressure curve, the analyzer will start to receive air from the central compartment. This air will show the characteristic increase in carbondioxide level, when the air from the alveoli has filled the central compartment to an extent where most of the air expired originates in the alveoli. Thus the volume expired before the increase is the anatomical dead space.

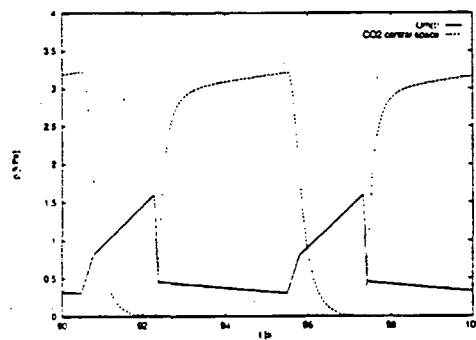


Figure 7.9: The respirator pressure U_m and the CO_2 pressure in the central compartment.

7.2 The pH model

The pH value is plotted as a function of the carbondioxide concentration in figure 7.10. We do not have any curves from the literature for comparison, which shows pH as a function of CO_2 concentration, but only the venous and

arterial point. The curve is a bit displaced from the two physiological points, but was accepted by the MDs from the SIMA group as a proper model of the pH value in blood.

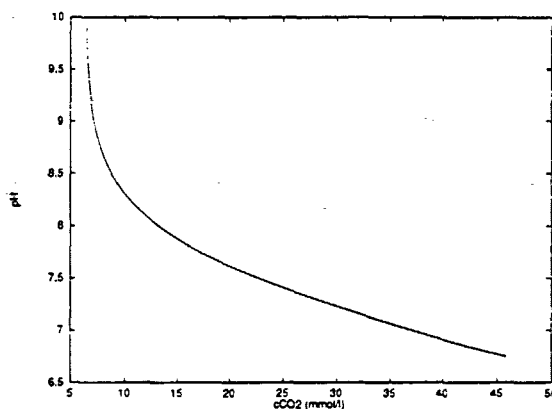


Figure 7.10: The pH curve.

7.3 The dissociation curves

In this section we show output of the models of the dissociation curves of Siggaard-Andersen, [Sig0], under different conditions. The output is compared with data from [Nun]. Other literature, [Wid, Gro, Wes2], has been consulted as well, but is found to be in agreement with [Nun].

The dissociation curves are curves of the gas concentration in blood as a function of the tension of the gas, but since the respiratory gasses dissociate into blood in a non-simple way, due to chemical reactions, the curves depend on several other parameters. This section has two aims. One aim is to run scenarios with the models, which produce dissociation curves under different circumstance, and discuss whether the models of [Sig0] are in accordance with the literature. Another aim is to evaluate the importance of the different effects included in the model.

7.3.1 Dissociation of carbondioxide

The influence of the pH value

The models [Sig0] are developed to be used for analyzing measured data. The pH value of blood is a parameter of the models, which is usually mea-

sured. Thus adapting the models of the dissociation curves from [Sig0], we have added the model of pH in blood developed by Chiari et al. [Chi1]. The graph in figure 7.11 shows the dissociation curve of carbondioxide with constant pH value 7.4, compared to the curve with a dynamic pH varying with the carbondioxide concentration. The intersection of the curves shows the concentration of carbondioxide at which pH 7.4 is found. Both curves are plotted with constant oxygen tension.

Obviously the interaction of carbondioxide with the hydrogen ions is the main reason for the non linearity of the CO_2 dissociation. The higher tension of p_{CO_2} , the lower pH value, which limits the solubility of the carbondioxide. In conclusion to figure 7.11 we can say that the pH dependence in the CO_2 dissociation curve is very important, and that the model with constant pH value is not adequate.

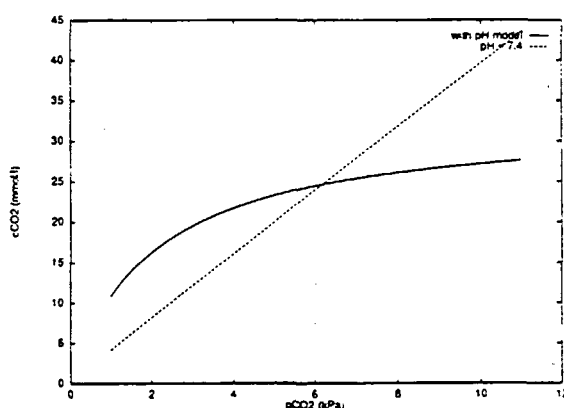


Figure 7.11: The carbondioxide model of MD Siggard Andersen, with and without the pH model

The influence of the oxygen content

In figure 7.12 we have varied the tension of oxygen from 13.3 kPa (normal arterial tension) to 2 kPa, so that the saturation of hemoglobin with oxygen is lowered from approximately 100%, to a saturation which at pH 7.8 is about 40%, according to the model of O_2 dissociation. A small shift of the curve to the left at low oxygen saturation is found. According to the values at table 7.2 from [Nun], the difference in CO_2 carriage of venous and arterial blood is about 1.8 mmol/l. According to [Nun] about one third of the reported difference is due to the Haldane effect, which is the difference in the quantity

Whole blood	Arterial blood Hb 95 % sat.	Mixed venous blood Hb 70% sat.	Arterial/venous difference
pH	7.4	7.367	-0.033
p_{CO_2} [kPa]	5.3	6.1	+0.8
c_{CO_2} [mmol/l]	21.5	23.3	+1.8

Table 7.2: Normal values for carbondioxide in blood

of CO_2 carried, at constant p_{CO_2} , in oxygenated and reduced blood. The rest of the difference is caused by the change in p_{CO_2} in arterial and venous blood.

Thus the difference in carbondioxide concentration in arterial blood at $(p_{\text{CO}_2}, p_{\text{O}_2}) = (5.3\text{kPa}, 13.3\text{kPa})$ and in mixed venous blood $(p_{\text{CO}_2}, p_{\text{O}_2}) = (6.1\text{kPa}, 5.3\text{kPa})$ ought to be about 1.8 mmol/l and is in the model found to be about 1.2 mmol/l. We do not consider this discrepancy to be crucial for the models, as the Haldane effect is rather small and thus not significant for the behaviour of the model.

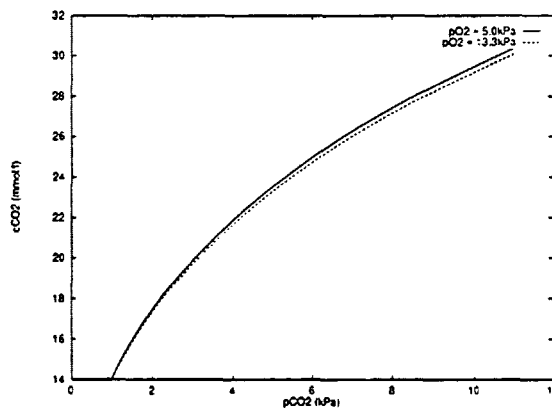


Figure 7.12: The Haldane effect yields different dissociation of carbondioxide for changed oxygen tensions

7.3.2 Dissociation of oxygen

The curves of oxygen dissociation are under normal circumstances dominated by the hemoglobin carriage, as only a negligible part of the oxygen is dissolved into the blood. Therefore there are no visible difference in the curve form of the oxygen dissociation curve and the oxygen saturation curve of hemoglobin when a normal content of hemoglobin is found in the blood. In this section

we will show the saturation curves for scenarios with normal hemoglobin content in blood rather than the concentration curve, since these are more frequently used in the literature.

When we plot the oxygen saturation curve under different circumstances it is not always possible to change one parameter at a time, as some parameters of the model influence each other. Normally the literature does not treat this problem when graphs illustrating changes in one parameter are shown. These curves have no direct physiological interpretation and thus we do not have the exact information in order to reproduce the graphs. It is under consideration of this fact that the comparisons of our model with the literature have been made.

The influence of the pH value

We have investigated the influence of a change in the pH value on the oxygen saturation curve. The pH value changes with the carbondioxide concentration, which can be calculated as a function of different tension of carbondioxide and oxygen. Hence a change in pH might either be caused by a variation in the CO_2 tension, or by some other change that will in turn change the balance between oxygen and carbondioxide. Hence without information about the cause of the change in pH, it is not possible in a unique way to deduce the CO_2 tension along the curves.

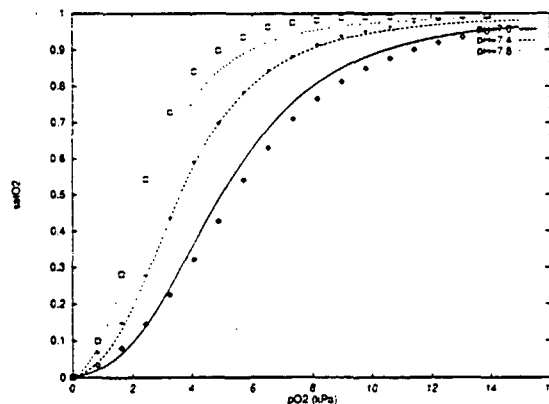


Figure 7.13: The oxygen dissociation with different pH values. Points from [Nun]

Figure 7.13 shows the saturation of hemoglobin as a function of the oxygen tension for different values of pH. The carbondioxide tension is constantly

5.3kPa. The curve is shifted to the left with increased pH values. Compared with the points from [Nun, p. 265] the curves lie a little too close, but the graphs in figure 7.13 are qualitatively in agreement. It is not stated which values of p_{CO_2} the curves from [Nun] represent.

The saturation curves of our model are shown for other values of p_{CO_2} in figure 7.14. We have plotted the dissociation curves for oxygen at various tensions

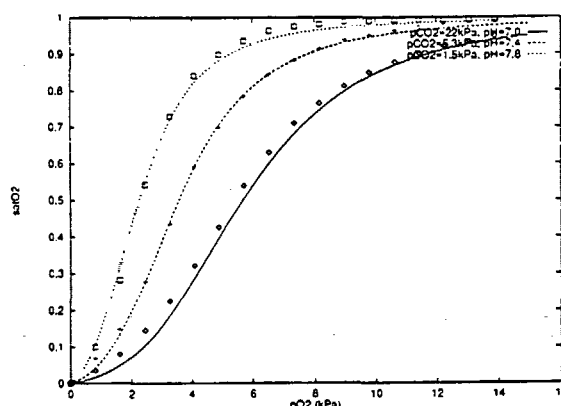


Figure 7.14: The oxygen saturation curves with adjusted p_{CO_2} . Points from [Nun]

of carbondioxide, which correspond to the pH values when no other effects are taken into account. This situation is not physiologically realistic, as the carbondioxide tension is found to exceed a physiological range. The drastic changes of the pH values shown in the graphs are only found in situations with other disturbances of the pH value. The curves coincide better with the points from [Nun].

Influence of the hemoglobin status

Other parameters relevant for changes in the model of oxygen dissociation are the concentration of hemoglobin in blood, and the fraction of hemoglobin bound with carbon monoxide. The remaining parameters of the model are not subject to changes in the simulator, according to MD John Jacobsen, and we have not found any data usable for comparison in the literature. The concentration of hemoglobin is normally 7.0 mmol/l corresponding to a content of 14.4 g/dl. At lower concentrations the blood is called anaemic, and the oxygen carriage is reduced. Another way to obtain a reduction in oxygen carriage is by an increased fraction of hemoglobin in combination

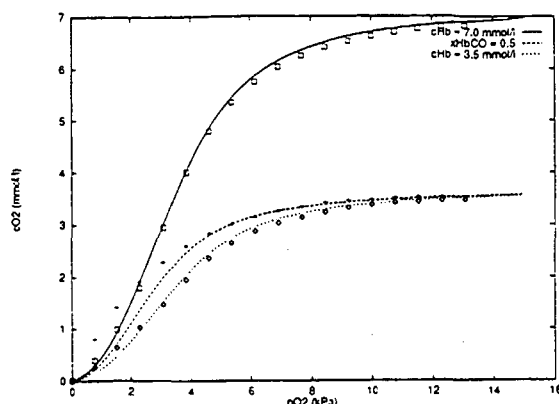


Figure 7.15: Oxygen concentration in normal, anaemic, and CO poisoned blood. Points from [Nun].

with carbon monoxide. The presence of carbon monoxide will displace the hemoglobin from combination with oxygen.

In figure 7.15 the dissociation curves of the two cases are shown. We have plotted the concentration of oxygen in blood as a function of the oxygen tension at a 50% reduction of the hemoglobin concentration and at a fraction of carboxyhemoglobin at 50% of the total hemoglobin concentration respectively. The output of the model for anaemic blood is in good agreement with the graph from [Nun]. It is seen how the concentration of oxygen in the blood is found to be half of the concentration at a normal content of hemoglobin in the blood. The reduction of oxygen carriage by means of a high level of carboxyhemoglobin is not identical with the graph from [Nun]. In [Nun] it is stated, that the leftward shift is due to a change in level of c_{DPG} (concentration of 2,3-diphosphoglycerate), which is found when carbon monoxide is present. We have not modelled the influence of the c_{DPG} by the carbon monoxide and hence the model does not produce a realistic output of oxygen tensions below 4 kPa, under CO poisoning.

7.4 The blood transport model

The transport model keeps track of both anaesthetic agents and respiratory gasses. When we are testing the model we will present the respiratory dynamic of the respiratory gasses and the anaesthetic agents separately.

7.4.1 The blood transport of respiratory gasses

In this section we present output of the transport model concerning the respiratory gasses. The dynamic of the model is presented step by step taking one effect into account at a time. First we will show the simplest possible version of the transport model. The simulation does not show a physiological situation. The initial simulations are made with the metabolism set to zero and with constant partial pressures in the alveoli of 13.3 kPa in oxygen tension and 5.3 kPa in carbondioxide tension (this is standard arterial values), and without pulmonary shunt.

The oxygen and carbondioxide tension is initiated to 10 kPa, in all other compartments in order to show how the oxygen is distributed into the compartments and carbondioxide is removed.

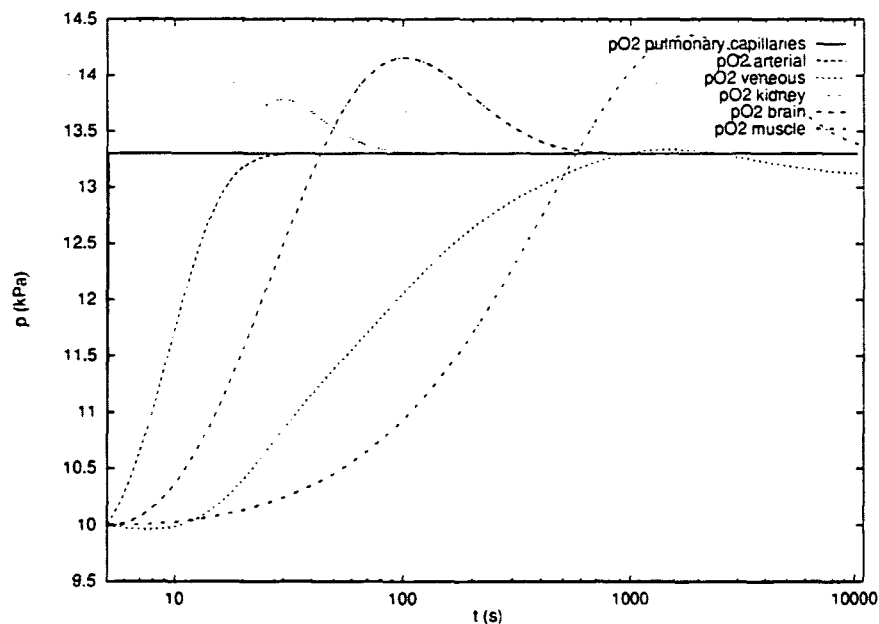


Figure 7.16: Oxygen tension in various compartments without metabolism

Figures 7.16 and 7.17 show the curves of oxygen tension and carbondioxide tension respectively for venous and arterial blood pools, for several selected organs, and the constant curves of the pulmonary capillaries. Since the metabolism is zero, all tensions will tend to the same value as the pressure in the alveoli, and hence the graphs show how the compartments in different stages reach the tension of the capillaries.

The arterial compartment is the only compartment connected directly to the pulmonary compartment and hence the increase in oxygen and decrease in

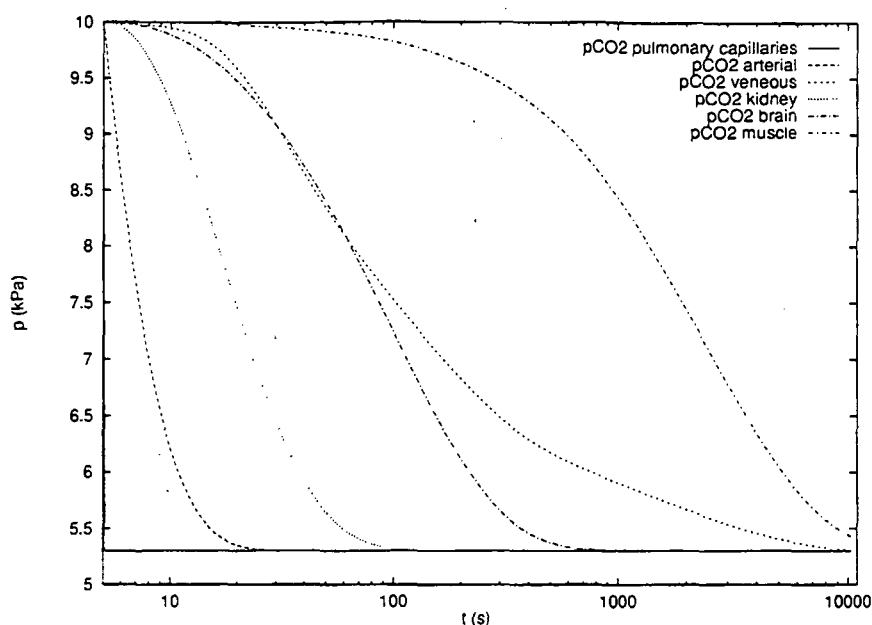


Figure 7.17: Carbondioxide tension in various compartments without metabolism

carbondioxide begin in the arterial pool. The venous pool does not change until the tensions in the flow out of the bodycompartments change.

The stages of the body compartment depend on the perfusion compared with the size of the compartment. Thus at first the kidney compartment has the highest increase in O_2 and decrease in CO_2 tension. Afterwards follows the brain compartment and at last the low perfused muscle compartment. The perfusion of the muscle compartment is much lower than the viscera compartments and therefore the change of the tensions in the venous blood is higher than the muscle compartment, even though part of the blood flow to the venous pool arrives from the muscle compartment.

When the oxygen tensions of the compartments increase towards the tension of the pulmonary compartment, it is seen that the tension of the compartment increases above the oxygen tension of the compartment from which the inflowing blood came. This might seem strange but it is explained by the Bohr effect, which causes the shift of the dissociation curves of oxygen at different tensions of carbondioxide.

The Bohr effect

Because the body compartments have a higher tension of carbondioxide than the arterial blood, the ability of the blood to carry oxygen is lower in these compartments and thus a lower concentration is still found in the outflowing blood than in the inflowing blood, even though there is a higher oxygen tension in the compartment than in the inflowing blood.

The Bohr effect is seen in the overshoot of tensions in all the body compartments and the venous pool, but in this section we will take a close look at what happens in the kidney compartment during the first 2 minutes. In figure 7.18 we have plotted the curves of oxygen and carbondioxide tension in the arterial and kidney compartment from figure 7.16 and 7.17 at a linear time scale.

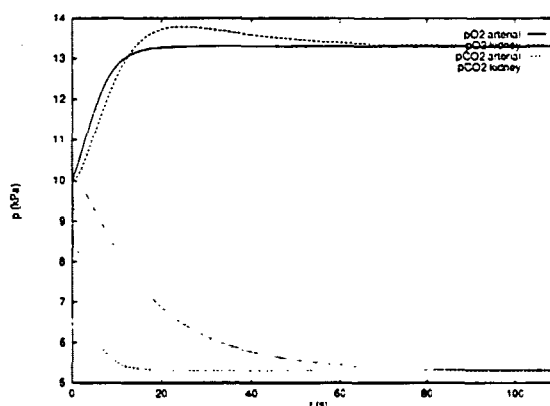


Figure 7.18: Oxygen and carbondioxide tension in arterial pool and kidney.

The two oxygen curves intersect at about 12 seconds at an oxygen tension about 13 kPa. The concentrations of oxygen in the two compartments at the moment of the two curves intersection are found in figure 7.19. Even though there is the same tension of oxygen the two compartments, the shift of the oxygen dissociation curve by the difference in p_{CO_2} result in different concentrations of the blood. Thus the concentration of oxygen in the kidneys is still lower than in the arterial blood and the total amount of oxygen in the kidneys still increases, as more oxygen is brought with the blood to the compartment, than the amount removed by the outflowing blood.

The oxygen curve for the kidneys peaks at the moment when the concentration equals the concentration of arterial blood. This happens because the concentration of carbondioxide is reduced significantly.

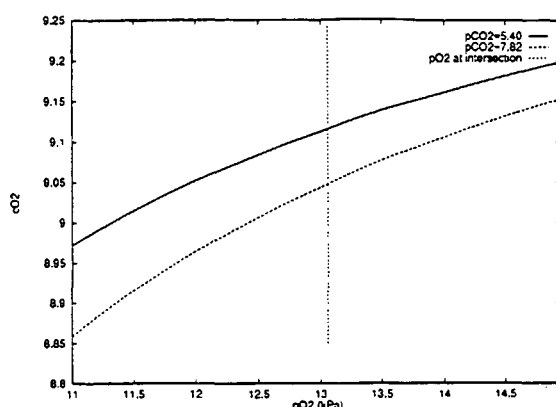


Figure 7.19: Oxygen concentrations in the two compartments are marked at the moment of intersection of the tension curves

The Bohr effect causes the oxygen tension of all the body compartments and the venous blood pool to oscillate in figure 7.16. When the tension in the venous blood is seen to decrease below the tension of oxygen in the body compartment again, it is the same effect in reverse.

The steady state of the respiratory model

We will now introduce the metabolic functions, and thus regard oscillations towards a more realistic equilibrium than in the previous shown graphs. In chapter 6 metabolic rates of the transport model was found for each compartment. This was done in agreement with the literature, and further calculated in such way that a physiological steady state of the model is obtained. In this section we have turned the metabolic rates on and in figure 7.20 and 7.21 it is seen how the state of the system reach the steady state.

The Bohr effect is still causing oscillations in the curves of the oxygen tension (figure 7.21), especially for the kidney compartment. The equilibrium of the gas tension of the various compartments are no longer identical, because the metabolic rates of the compartments differs. The high equilibrium tension of oxygen in the kidney compartment reflects that the metabolic rates have been assigned in accordance to the size of the compartment and not with respect to the blood perfusion. A small compartment with a high perfusion content will therefore reach a high tension of oxygen at equilibrium, and for the same reason the carbondioxide tension of the kidneys is low.

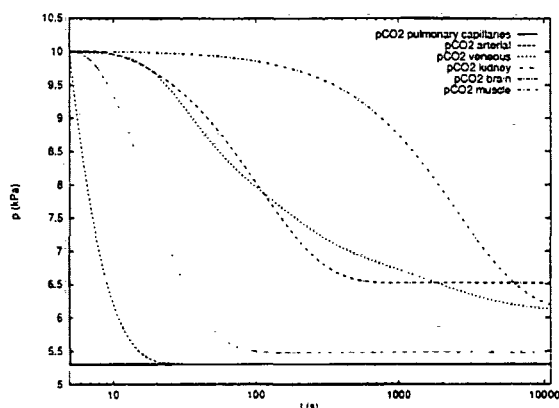


Figure 7.20: Carbondioxide tensions in various compartments with metabolism.

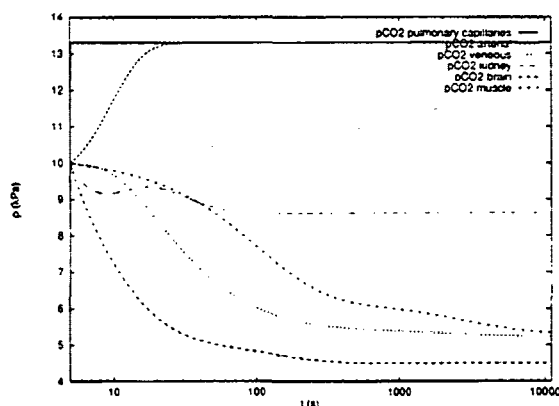


Figure 7.21: Oxygen tensions in various compartments with metabolism.

7.4.2 The blood transport of anaesthetics

In section 6.4 we proposed a method for estimating the solubility coefficients of anaesthetic agents from parameters of a three compartment model of pharmacokinetics. We estimate the solubilities in two groups, the slow and the fast compartments. The fast compartments are the viscera organs, and the slow compartments are the muscles, connective and adipose tissue.

We have tested our method for the drug thiopentone. For this drug we have both the ratio between the solubilities in each organ, from [Hul] and parameters from a previous simulator version, see table 7.3.

The distribution of the drug in the body can be seen in figure 7.23. At $t = 5$ we have placed 1mmol thiopentone in the central venous pool. From here the drug is distributed first to the fast viscera organs, but eventually to the

	α_t	Est. α_t	
Liver	1.7	fast	1.8
Heart	1.5		
Kidney	1.5		
Remaining	1.5		
Brain	1.4	slow	1.5
Muscle	1.5		
Connective	1.5		
AdiPOSE	11.0		

Table 7.3: Relative solubilities for thiopentone from [Hul] and estimated from PAWI data.

larger compartments of muscles, fat and connective tissue. The final balance will be with most of the drug in the adiPOSE compartment, which has appr. 30% of the total volume and a solubility that is 11 times as high as the solubility in blood. The final equilibrium is when the tensions are equal in all the compartments. This can be seen on the tension curves for the same run, see figure 7.22.

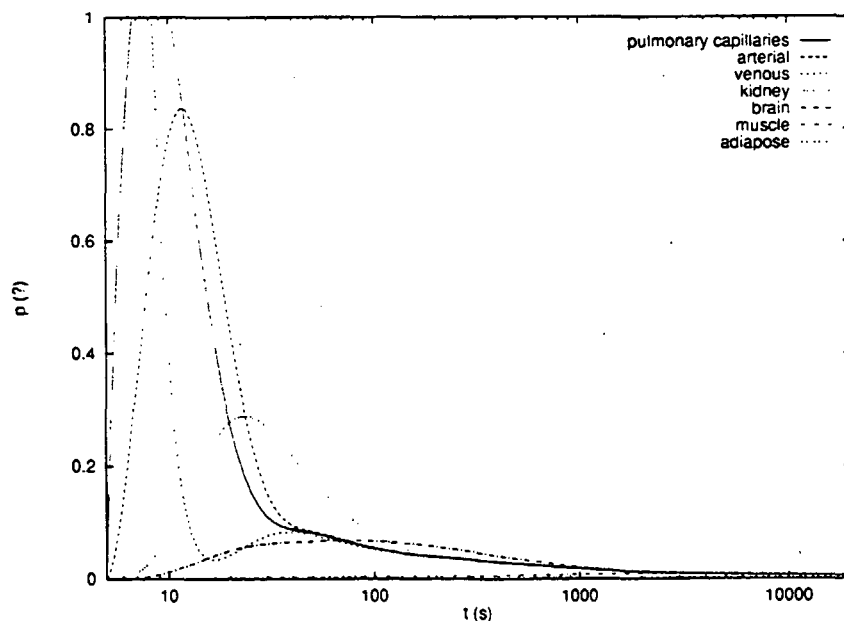


Figure 7.22: The tensions during distribution of drug, cf. 7.23. The unit of this curve are not well defined, as we only know the ratio between the solubility coefficients.

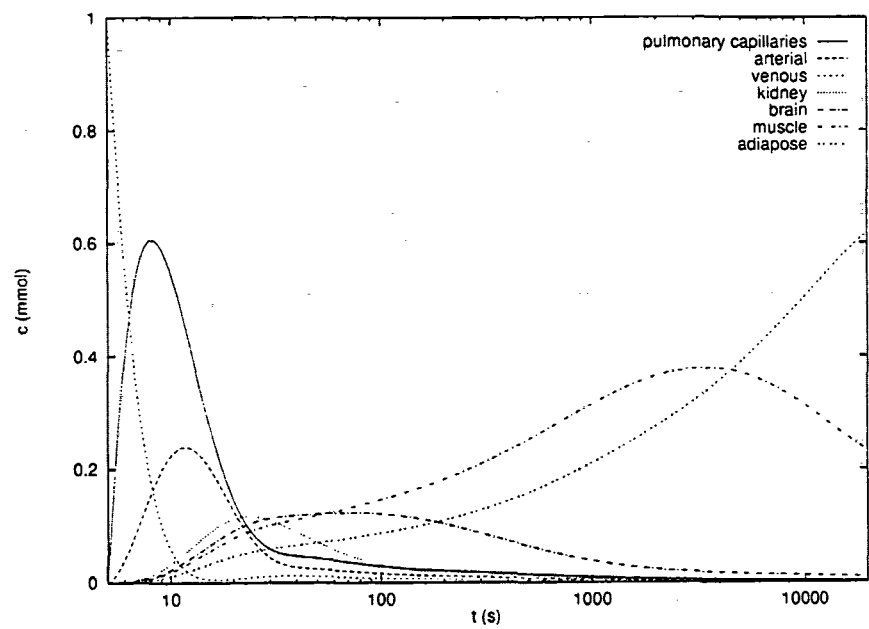


Figure 7.23: Drug distribution in selected compartments after initial injection of 1mmol thiopentone in central venous pool.

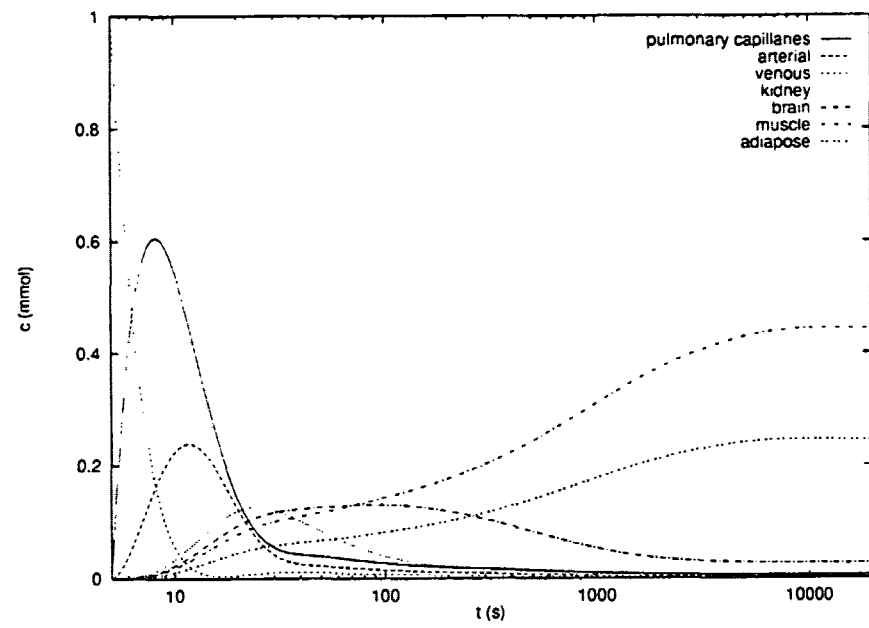


Figure 7.24: Distribution of 1mmol thiopentone with estimated solubilities.

Our estimates of the solubilities differ a lot from the real values of [Hul], see table 7.3. However the graphs of the tissue distribution are in better agreement, see figures 7.23 and 7.24. The final distribution is different though. With the correct solubilities most of the drug ends in the adipose compartment, but with the estimated solubilities it splits between the adipose, muscle and connective compartments. This reflects that the estimated solubilities does not differentiate the tissue of the slow compartments, and thus the drug will be distributed by organ size. With the solubilities from [Hul] the volume of distribution of the slow compartments is 215l, while for the estimated values it is only 75l.

During anaesthesia the distribution of the drug is most critical in the initial stage, and hence we find that our estimates looks usable, especially for drugs that have their primary effect in the viscera organs, in situations when correct solubilities are not available.

7.5 Conclusion

The simulations presented in this chapter all shows that the required output of the model is obtained within a physiological change in parameters.

Even with the assumptions we have made during the construction of the lung model it behaves reasonably like the physiological system.

The tests of the blood transport model has given us an impression of which modelled effects are important for the dynamics of the respiratory system. The Bohr effect is clearly identified in the output of the blood transport model, while the Haldane effect is not directly observable. The metabolic functions and the ventilation determine the level of a steady state in arterial and venous blood and the distribution of the metabolic rates of the organs determine the tension in these organs and the peripheral venous pools. The dissociation functions of the drugs determine the pharmacokinetics, and hence the final distribution of drug in the various organs. However, right after an injection the distribution will initially be influenced more by the perfusion of the organs than by their ability to dissolve the drug.

Chapter 8

Discussion and conclusion

In this final chapter we will discuss whether the result of our modelling is a satisfactory solution of the assigned task.

Initially we will assess how the model meets the requirements, a subject that has already been partially treated in the conclusions in the previous chapters.

Then we will discuss where in the modelling our contributions are most significant, and where we mainly depend on the works of others. For the parts of our model that are adapted from the literature, we will discuss the choices behind these model, and how they promote our goals.

As a perspective on the future of the model, we consider the maintainability and extendability of the model.

The problems of extracting the requirement of the model from the SIMA group are discussed, to address the question of whether the final model is really what the MDs and the SIMA group need. Furthermore we will discuss application of the model in addition to use in the training sessions in the simulator.

Finally we state a brief conclusion of the thesis as a whole.

8.1 Evaluating the model

Since our modelling is done in response to a request from the SIMA group, the process has involved regular cooperation to ensure that our product ended up being what the SIMA group wanted.

The cooperation with the SIMA group has submitted to the form normally used in the group, implying that during the period of our work we have

produced 2–3 deliverables that have been assessed by a group of at least a mathematician, a medical doctor, and a computer programmer. By these evaluations the SIMA group has maintained an overview of the direction of our work, and the progress we were making, but on the other hand it has still been our responsibility to decide the course of the modelling. We have kept more or less regular meetings with the SIMA MDs, to clarify medical issues, and to present to them our modelling of different stages in order to discuss the possibilities of courses the modelling could take. These discussions of possible courses have touched both whether we were neglecting important physiological relations, and whether the values of the parameters we proposed were accessible as measurable physiological quantities.

During the modelling process we have developed both our own and the MDs view of what the model should be able to do. By showing the model to the group at various stages we have sparked their imagination and their awareness of what was within reach of the modelling as well. This has resulted in a list of requests that is larger and with more visions than the vague requirements we originally received.

The model we present in this thesis will without any doubt meet the requirements of the SIMA group. The models contain parameters that allow the requested scenarios to be simulated, and the output of the model behaves in accordance with the expectations. The model is well suited for simulation of anaesthetic sessions, since it includes the important physiological connexions of short and medium time periods. For simulation of longer scenarios, like intensive care, the slower mechanism of kidney elimination of excess base or acid from the blood will be needed to obtain realistic output. Furthermore a control system will be important for simulation of situations where the natural heart and respiration functions of the patient is not disabled by anaesthesia.

The application of the model is not restricted to reproducing a certain behaviour in the simulations. An expectation that we share with the MDs of the SIMA group is that by using the model the MDs can improve their insight in the dynamics of the respiratory gasses by investigation of the quantities that are not measurable in real life. This may for instance be the actual concentration of gasses in the organs under different circumstances, or the effects of changing the perfusion/ventilation ratio in different ways, which is in real life only seen as a change in the gas content of the blood and the expired air.

8.2 Model contributions

In our view the foremost contribution of our modelling is the way we have managed the interactions between multiple substances. This is done by two basic ideas, the vector state variables, and the trick of transforming the state variable of the compartmental mass balance equation to tension.

In the use of vectors as state variables our model differs from the models found in the literature. Using exactly the same model for each respiratory gas and anaesthetic agent has the advantage that it reduces the overall complexity of the model, by exploiting the similarities in transportation mechanism. As a mode of thought the vectors have also proved useful, since they have continuously drawn our attention to the fact that the gasses may influence each other.

The technique of converting the mass balance by means of the derivative of the dissociation curve is especially elegant when used in combination with the vector variables. For vector variables the derivative $\frac{\partial c}{\partial p}$ is a matrix with the diagonal elements representing the solubility, either constant or a function of p , and non-diagonal elements representing interactions between dissociation of substances. An alternative approach is to use the concentration as state variable, and find the tension via the inverse of the dissociation function. This approach is suggested by Chiari et al. in [Chi0]. However, they refrain from carrying out the idea, as the inverse of their dissociation curve is hard to find. In our method the Jacobian matrix can be found, even in situations when the dissociation function is not explicitly stated.

We have adapted a model of the dissociation of carbondioxide and oxygen in blood, that was not originally developed for use in a transport model, but to be used with measured values [Sig0]. To do this we have added a pH model, to calculate the pH value from the blood carbondioxide contents.

The choice of dissociation model was rather easy since it was the only model we have encountered that models the Bohr and Haldane effects. Since the descriptions in the literature of the respiratory physiology had stressed that these effects are important for the transport of respiratory gasses, especially in situations with respiratory problems, we found it crucial to catch these effects in our model.

We discovered our pH model [Chi1] during our investigation of the dissociation curves for carbondioxide [Chi0], and found that it directly answered our need to know the pH value from the blood content of carbondioxide. We do not have the biochemical insight to determine whether our pH model will be able to cooperate with a future model of the electrolytes and fluid balance.

But since pH is one of several issues covered by the balance of ions, we find it reasonable to let the ion model treat this problem.

The model of the metabolism, by a Michaelis-Menten kinetic reaction, is directly from [And]. Our distribution of the metabolic rates between the organs show that it is possible to obtain a reasonable steady state situation with this metabolism, at least under normal conditions.

Our model of the pressures in the lung is a combination of two models, [Gal, Rid0]. The difference is that our model partitions the lung in a different way, to enable simulation of the requested lung scenarios.

The basic principle of our gas model is similar to the approach used in [Rid0], but to realize the basic assumptions of the model we choose to create our own model. During this we have investigated the effect of diffusion, and found that in a model of our level of detail the effect is captured in the assumption of instantaneous mixing inside our compartments.

8.2.1 Nature of variables and parameters

Modelling an object from reality is a process of selecting which effects and relations to include in the model, and which to neglect. When the detailing stops at some level the effects that are still unaccounted for are normally captured by some sort of statistically determined parameters. Taking this into account somewhat widens the discussion of the nature of our variables and especially parameters.

When we identified the problem of this thesis in section 1.1, we stated that we intended to model by use of physiologically recognizable variables and parameters.

We find that we have adhered to this principle, but due to the nature of modelling this is only true to level of detail. Beyond this level the parameters are of a more statistical nature.

The blood transport model is a good example of these levels of detail. The model itself is based on the principle of mass balance and a partition of the body where the tension is uniform throughout each section. Thus on this level the model has very direct interpretations to the variables, and the parameters like cardiac output and blood fractions to various organs. To actually state the equations of the mass balance, we need to know the relation between tension and concentration. Such a dissociation function is in itself a well defined physiological relation. However the model of the dissociation of oxygen and carbondioxide has not a direct physiological interpretation of

each parameter in the model. In the models there are several constants, that are the result of fitting the model to measured data. According to MD Siggaard-Andersen attempts to model the saturation curve for oxygen in terms of hemoglobin binding sites, a more directly interpretable way, have not yet resulted in useful models.

Our conclusion is that our model on the upper level adhere to our principle of physiological variables and parameters. The levels where this is not true are in the submodels, but it should be possible to change or replace the submodels without destroying the overall structure of the model. Thus we have confidence in the description of the physiology offered by the model, but are aware that improvements are possible.

This naturally leads to the next section where we reflect on the fact that the model is intended for a *real* project, and will thus still be subject to development in the future.

8.2.2 Maintainability and extendability

Since our model is a part of a larger frame, the SIMA project, we expect that future needs will arise to change or extend our model. During our modelling we have tried to design the model in a way that would support such developments. In the cause of this we have imagined some more or less likely changes and extensions.

First we have the control system, which is to be part of the simulator, but which is not made yet. It is in a way an extension of the respiratory model, since it regulates both on the ventilation and the blood flow.

If the simulator is to be used for simulation of intensive care, as well as anaesthesia, the long term effects of respiratory disturbances may need more thought, especially concerning the metabolic response to long-term disturbances of the acid/base balance of the blood.

If the model was to deal with substances that did not support the assumption of instant equilibrium in our organ compartments, a solution could be to split the organs into two compartments, and introduce a membrane transport matrix like the one representing the pulmonary membrane.

Modelling compartments with non-constant volumes is relevant in situations when bleeding or blood transfusions occur. This would change the compartment equations, as the inflow and the outflow would no longer be the same. Furthermore it may be necessary to model different composition of blood at

various parts, and thus to include the transport of blood components like hemoglobin in the transport vectors.

All our submodels are candidates of future replacement or improvement. The pH model could be replaced with a model including a balance of the electrolytes of the blood. The dissociation curves for anaesthetics could be extended with protein binding. Extension of the metabolic model could incorporate more chemical insight in the mechanisms of the involved processes.

8.3 Conclusion

As a final conclusion we are well satisfied with our model. The model describes the interactions of the respiratory system in a way that is in agreement with the theoretical basis of physiology.

We are confident that the model is what the SIMA group needs for the simulation of anaesthetic situations with the range of complications we have included in the list of requirements for the model. Due to the general physiological principles the model is based on, we believe that reasonable responses can be expected, even with combinations of parameter values that have not yet been tested. Furthermore due to the general physiological principles the models may be useful for research purposes.

Should the future reveal more requirements to the model, or more scenarios to simulate, we expect it to be fairly easy to incorporate these extensions.

In a broader view of modelling biological systems, we want to emphasize our contribution of the method for converting mass balance equations to tension variables by means of the derivative of the dissociation function. Even though the mathematics of this is not advanced beyond the level of our initial university course of analysis, we have not found the method used in any of the literature we have surveyed. And the technique has the advantage that the derivative of the dissociation function may be obtainable in situations when the inverse of the function cannot be expressed analytically.

Appendix A

The implementation

The contents of this section is a documentation of our implementation of the model. The information is primarily meant for the programmers that will later incorporate our model in the simulator software, but may serve as a useful source of details on precisely how the models are run for other readers as well. The source code for our model implementation is later in the appendix, A.3. Even though numerical analysis techniques has not been a primary concern in this project, a short description of the methods used are included in this section as well.

A.1 The implemetation

All implementations are in C++, and the numerical differential equation solver used is a Runge-Kutta-Fehlberg adapted from 'Numerical Recipes in C' [Pre], see section A.2.1. For solving the equations of the pH model and the dissociation curves, we have used the Newton-Raphson method, see section A.2.2.

The interface to the solver is a class template that can be configured to handle a differential equation system of a number of equations. As a special feature the type of the system variables of the equations are configurable as well, and thus the equations may have any user defined data type as system variables, as well as built-in data types like double. This option is used to write differential equations with vectors as system variables in our models.

For this use we have developed a general vector class, defining vector variables with addition, scalar multiplication, and a square matrix class with addition, scalar multiplication, and multiplication of a matrix and a vector.

A general base class for compartment models have been derived from the solver class, and used as a base class for the transport model, but not for the lung model, as this proved easier to implement directly on top of the solver class.

A.1.1 The transport model implementation

The transport model is a derived class from a 14 compartment instantiation of the general model class with three dimensional vectors as the base data type: `Model<vvec<double,3>,14>`. The model class receives an array of compartment pointers, where each compartment is a derived class from the class `cmpt`. The role of the compartment class is to unify the most basic features each compartment has, thus the compartment class has a function to calculate the derivative, and another to set its state variable to a new value. The hierarchy of compartment classes are shown in figure A.1.

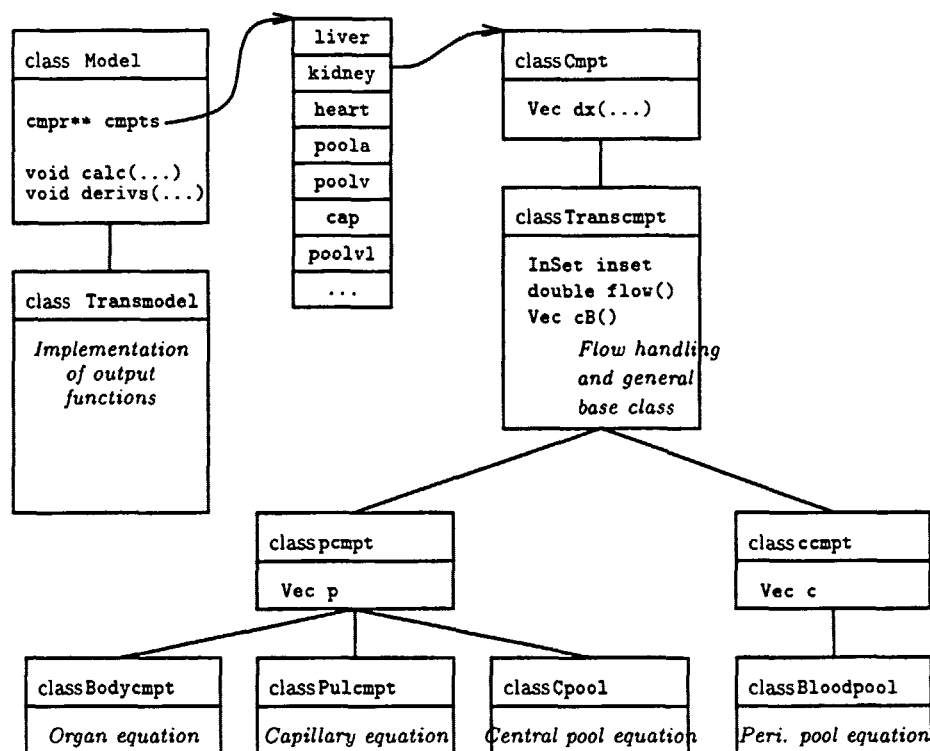


Figure A.1: The relations between the main classes.

Class Transcmt

The knowledge of connections and flows between compartments are included in the transport compartment class `Transcmt`, as well as an interface to the pH model and the blood dissociation curves. The class serves as a common base class for all compartment classes, and defines functions that are common to all our compartments.

Connections between compartments are represented as a set of connections, in which each element holds a compartment and a fraction in a structure called `In`. The semantics on an `In` is that it represents an inflow to a compartment, the compartment identifier telling which compartment, and the fraction telling how much of the outflow of that compartment that goes to here.

Based on the set of `In` structures the class implements the flow system; a function `double flow()` returning the current flow through the compartment. The default implementation is to return the sum of inflows defined by the `In`-set, but the derived central blood pool class `Cpool` redefines this function, to avoid an infinite recursive definition. The `Cpool`'s are the central compartments through which cardiac output flows.

The blood concentration is returned by the function `cB()`, which is implemented in the derived classes `pcmpt` and `ccmpt`. By combining the blood concentration function and the flow function the amount of matter transported into the blood can be calculated, which is done in the function `sumI()`.

The pH model and the dissociation curves are both implemented by a numerical solution to the involved equations. The method used in both cases is Newton-Raphson, see section A.2.2. Solving the dissociation curve means solving the pH model as well, as the pH level depends on the concentration of CO_2 . Fortunately the dissociation curves only depends on the concentration through the pH value. Hence the CO_2 concentration can be found independent of the O_2 concentration, and thus a two dimensional Newton-Raphson is not needed. When finding the CO_2 concentration, each proposed value can be used in the pH model to find the corresponding pH value, and the sought concentration is then the one that satisfies $c_{\text{CO}_2} = \varphi_{\text{CO}_2}(p, \text{pH}(c_{\text{CO}_2}))$.

The pH function and the dissociation curves are defined in the modules `ph.cc` and `phi.cc`. These are used by the implementations in the class hierarchy to calculate pH and concentrations from the value of the compartment variable.

Class pcmt and class ccmt

These classes define the state variable for the compartment; a pressure vector in pcmt and a concentration vector in ccmt.

The blood concentration function i is redefined in these classes, to return the current concentration.

Specialized compartment classes

Derived from pcmt and ccmt are the final specialized compartment classes. The differential equations are implemented as the function $dx()$. There are four different compartment types:

Pulcmt: The pulmonary compartment with blood flow from the central venous pool, and gas exchange to the lung model. To speed model calculations the latter has been implemented as a 'cheat', where high permeability coefficients are treated as instantaneous equilibrium between the blood and the alveoli. This is done to prevent the step size regulation of the Runge-Kutta-Fehlberg algorithm to reduce stepsize enough to find the precise curve of this equalizing.

Cpool: A central blood pool with only a blood part. Pressure is used as a state variable, not because it is needed to find equilibrium between different phases of gas, but because the arterial and venous tension is wanted as an output variable. An alternative implementation would be to use concentration as the state variable, and then find the pressure when needed by solving the equation $c = cB(p)$. We have chosen to change the state variable, as this is similar to what is done in the other pressure compartments, and does not involve multidimensional root finding.

Bodycmt: Organ compartments with a single inflow from the arterial pool.

Bloodpool: The only type of concentration based compartments, used for the local venous pools.

A.1.2 The lung model implementation

The lung model is implemented directly on top of the differential equation solver class rkf. This was done because the interactions between the compartments are heavier than is the case with the transport model.

The implementation combines the pressure and the gas model to a single model with a state variable that consists of a fraction vector and a scalar pressure. This is implemented as a vector with the pressure added as an extra component, a data type named `xpvec`. The `rkf` class requires a function to calculate the derivative in a point (t, x) . As the functions for the derivatives are already generalized to a variable number of alveoli compartments, the implementation also enables easy variation of the number of branches.

A.2 Numerical Methods

A.2.1 The Runge-Kutta-Fehlberg adaptation

The Runge-Kutta-Fehlberg method is a differential equation solver, and is here described in two parts; the Runge-Kutta method and the Fehlberg part. The implemented Runge-Kutta is of order five, which means that for every timestep, a weighted average of the differential quotient in 6 points are used for the calculation of the new state. The error committed by this method is proportional to the stepsize in fifth power; Δt^5 . Hence the category fifth order.

The general form of a fifth order Runge-Kutta-Fehlberg formula is

$$k_1 = hf(x_n, y_n) \quad (\text{A.1})$$

$$k_2 = hf(x_n + a_2h, y_n + b_{21}k_1) \quad (\text{A.2})$$

$$\dots \quad (\text{A.3})$$

$$k_6 = hf(x_n + a_6h, y_n + b_{61}k_1 + \dots + b_{65}k_5) \quad (\text{A.4})$$

$$y_{n+1} = y_n + c_1k_1 + c_2k_2 + c_3k_3 + c_4k_4 + c_5k_5 + c_6k_6 \quad (\text{A.5})$$

The Fehlberg part of the method optimizes the stepsizes by an estimate of the error. This is done comparing two estimates of the new state calculated with different weighting of the differential quotients in the 6 points.

$$y_{n+1} = y_n + c'_1k_1 + c'_2k_2 + c'_3k_3 + c'_4k_4 + c'_5k_5 + c'_6k_6$$

For the adaption to the vector class, we have defined the difference of these states as the sum of differences in each variable.

A.2.2 The Newton-Raphson method

The Newton-Raphson method is used for solving equations of the form $0 = g(x)$, by successive approximation with the expression

$$x_{n+1} = x_n - \frac{g(x_n)}{g'(x_n)},$$

until $|g(x_{n+1}) - g(x_n)| < \varepsilon$ for some zero criteria ε .

Problems with the method occur in points when $g'(x) = 0$, but otherwise the algorithm normally terminates fairly fast.

We use this method for finding the root of the polynomial in the pH model, even though a general formula for the root of a third degree polynomial is available. This is because the general solution may involve complex number as intermediate results, even though the root itself is a real number. Aside from this practical problem the numerical stability of the Newton-Raphson might be better, than using the explicit expression, as the general formula involves the difference between two complicated expressions, where underflow in the calculations may affect the resulting small value significantly.

A.3 Program source listing

The following is a source code listing of our model implementation.

File: cmpt.h

```
//
// The compartment base class
//
#include <iostream.h>
#include "rkf.h"
#include "vec.h"

class Cmp {
public:
    virtual Vec dx(double t, double dt) = 0;
    virtual void x(const Vec&) = 0;
};

class Cid {
    static Cmp* cmpts;
    int idx;
    // Cmp* cp;
public:
    Cid(int i) { idx = i; }
    operator Cmp* () { return cmpts[idx]; }
    Cmp* operator->() { return cmpts[idx]; }
    int operator==(const Cid& cid) const { return idx == cid.idx; }
    static void x_cmpts(Cmp* cpp) { cmpts = cpp; }
};

template <class C, int n> class Model : public rkf<C, n> {
    Cmp* cmpts;
```

```

double ddtinc;
void cmptinit(const vvec<C,n>& x)
{
    for (int i = 0; i < n; i++)
        cmpts[i] = x[i];
}
void derive(double t, double dt, const vvec<C,n>& x, vvec<C,n>& dxdt)
{
    int i;
    cmptinit(x);
    for (i = 0; i < n; i++)
        dxdt[i] = cmpts[i] - dx(t, dt);
}
public:
    Model(Cmpt* cpp, double ddti = 1) { cmpts = cpp; ddtinc = ddti; }
    virtual void initdisp() {}
    virtual void disp(double t, int mm = 0) = 0;
    void initx(const vvec<C,n>& x)
    {
        yinit(x);
        cmptinit(x);
    }
    // disp() is called each ddt
    void calc(double t1, double t2, double ddt = 10, double cdt = 5)
    {
        stepsize(cdt);
        initdisp();
        disp(t1);
        for (double t = t1; t < t2; t += ddt) {
#ifdef __GNUC__
            try {
#endif
                odeint(t, t+ddt);
#ifdef __GNUC__
            }
            catch(StepUError sufe)
            {
                cerr << "Step underflow in rkf\n";
                // do the appropriate thing
            }
            catch(StepSzError sse)
            {
                cerr << "Step size error in rkf\n";
            }
            catch(HConcError hce)
            {
                cerr << "Error in pH model: " << hce << "\n";
            }
        }
        disp(t+ddt);
        ddt = ddtinc;
    }
};

```

File: trans.h

```

#ifdef _TRANS_H
#define _TRANS_H
#include <iostream.h>
#include "cmpt.h"
#include "vec.h"
#include "set.h"

const int ncmpt = 14;

#ifdef __GNUC__
ostream& operator<<(ostream& o, const HConcError& err)
{
    return o
        << "(x=" << err.x << ",gH=" << err.gH << ",dgH/dx=" << err.dgHdx << ")";
}
#endif

// The blood transport model
class Transmodel : public Model<Vec,ncmpt> {
    set<Cid> plot;
public:
    Transmodel(Cmpt* cmpts, set<Cid> p, double ti=1)

```

```

: Model<Vec,ncmpt>(cmpts, ti) { plot = p; }
void calc(double t1, double t2, double ddt=10, double cdt=5)
{
    Model<Vec,ncmpt>::calc(t1, t2, ddt, cdt);
}
void initdisp();
void disp(double t, int mm = 0);
};

class In {
    double z;
    Cid cid;
public:
    // In(double frac, Cid id) : cid(id) { z = frac; }
    In(Cid id, double frac) : cid(id) { z = frac; }
    int operator==(const In& in) const { return cid == in.cid; }
    double flow();
    Vec xflow();
};

class Transcmt : public Cmpt {
    double VB; // the volume of the blood part of compartment
    double VT; // the volume of the tissue part of compartment
    double Temp; // Core temperature
    set<In> inset; // inflows as fractions from compartments
public:
    Transcmt(double vb, double vt, const set<In>& is, double T=37);
    virtual Vec dx(double t, double dt) = 0;
    virtual void x(const Vec& c) = 0;
    virtual const Vec& cB() = 0; // phi blood
    virtual const Vec& q_x() = 0;
    virtual double pH();
    virtual double T();
    Vec sumI(); // the inflowing amount in concentration
    virtual double flow(); // the blood flow through compartment
    double q_VB();
    double q_VT();
    double q_T();
};
#endif

```

File: scmpt.h

```

//
// Specialized compartments for the TC model
//
#include "trans.h"
#include "ph.h"
#include "phi.h"

class pcmpt : public Transcmt {
    Vec p; // uniform compartment pressure
    Vec c; // blood conc c = cB(p)
    double curpH; // current pH = pH(c[CO2]);
public:
    pcmpt(double vb, double vt, const set<In>& is)
        : Transcmt(vb,vt,is) {}
    Mat dcB() { return dcdp(p, curpH, c[CO2]); }
    const Vec& pB() { return p; }
    const Vec& cB() { return c; }
    const Vec& q_x() { return p; }
    void x(const Vec& np) { p = np; c = ::cB(p); curpH = pH(); }
    double q_pH() { return curpH; }
    virtual Vec dx(double t, double dt) = 0;
};

class ccmpt : public Transcmt {
    Vec c; // blood conc c = phiB(p)
public:
    ccmpt(double vb, double vt, const set<In>& is) : Transcmt(vb,vt,is) {}
    void x(const Vec& nc) { c = nc; }
    const Vec& q_x() { return c; }
    virtual Vec dx(double t, double dt) = 0;
    const Vec& cB() { return c; }
};

class Bodycmpt : public pcmpt {
    Vec mr; // metabolic rate
    Vec beta; // metabolic increase const.
};

```

```

double aanaT; // alpha ana tissue [mmol/(l kPa)]
public:
static int mh = 0; // malign hyperthermia activated
Bodycmt(double vb, double vt, const Vec& r, Cid cid, double z,
double aat) : pcmt(vb, vt, set<In>(In(cid,z)))
{
    mr = r;
    aanaT = aat;
    beta[02] = 0.0005; // mmol/l rather low
    beta[ANA] = 0.004; // mmol/l, from Model 10
}
double cTana() { return pB()[ANA]*aanaT; }
double cTco2() { return ::cTco2(pB()[CO2]); }
Vec cT();
//Bodycmt(double vb, set<In> in) : pcmt(vb,0,0,in) {}
Vec metabolism(double t)
{
    Vec meta = q_VT()*mr;
    // Malign Hyperthermia
    if (mh && t > 0)
        meta += (t < 4) ? 2.5*t : 10;
    meta[02] += ao2*pB()[02]/(beta[02]*ao2*pB()[02]);
    meta[ANA] += aana*pB()[ANA]/(beta[ANA]*aana*pB()[ANA]);
    return meta;
}
Mat dcT()
{
    Mat dc = ::dcTdp(pB());
    dc[ANA][ANA] = aanaT;
    return dc;
}
virtual Vec dx(double t, double dt);
};

class Pulcmt : public pcmt {
    vmatrix<double,3> perma;
    lung* lungp;
    Vec pa;
    // from mech lung compartmentmodel, if available.
public:
    Pulcmt(double vb, Vec perm, Cid cid, double z, const Vec& p)
        : pcmt(vb,0, set<In>(In(cid,z))),perma(perm)
    { pa = p; lungp = 0; }
    virtual Vec dx(double t, double dt);
    Vec pa() const { return lungp ? lungp->pa(1) : pa; }
    Vec dpeq(int i); // change when instant equilibrium with alveoli
    const vmatrix<double,3>& perm() { return perma; }
    void initlung(lung* lp) { lungp = lp; }
};

class Cpool : public pcmt {
    double Qc; // the Cardiac Output
public:
    Cpool(double VB, double qc, const set<In>& is) : pcmt(VB,0,is) { Qc=qc; }
    double flow() { return Qc; }
    virtual Vec dx(double t, double dt);
    double pANA(double nana)
    {
        return nana/(q_VB()*aana);
    }
};

class Bloodpool : public ccmt {
public:
    Bloodpool(double VB, const set<In>& is) : ccmt(VB, 0, is) {}
    virtual Vec dx(double t, double dt);
};

```

File: lm.h

```

// the lung model
#ifdef _LM_H
#define _LM_H
#include <iostream.h>
#include "rkf.h"
#include "vec.h"

enum { dead, alvi, NPCHPT };

```

```

#define PRESS NGAS

#define NSAWN 10

const double pi = 3.1415725;

typedef vvec<double, NGAS+1> xpvvec;
typedef vvec<xpvvec, NPCMPT> pulvec;

ostream& operator << (ostream& o, const xpvvec& xp);

class Pulcmpt;

class lung : public xvec<xpvvec, NPCMPT> {
    vvec<double, NPCMPT> R; // flow resistance
    vvec<double, NPCMPT> C; // compliance
    vvec<double, NPCMPT> VO; // unstressed volume
    vvec<double, NPCMPT> l; // tube length
    vvec<double, NPCMPT> A; // total tube area
    double RT; // Gas constants
    Pulcmpt* pulcap; // the pulmonary capillaries
    double patm; // barometric pressure = 101.3 kPa
    double a; // amplitude of pe
    double w; // angular velocity
    xpvvec xpe; // x distribution of mask air
    // double D; // diffusion coefficient [m^2/s]
    double VT; // Tidal volume for tidal()
    double pmin; // Min pressure for tidal()
    double tmax; // Max resp. cycle length
    double dp1, dp2; // slopes for tidal() pressure curve
    enum { T_ASC, T_DSC, T_EXP } state; // tidal() variables
    double t0, t1; // tidal() var: length of increasing pressure period
    double pmax; // " : max pressure
    double vmin;
    int nflg;
    int nv; // how many full rounds
    int nsav; // sav() number of points
    double ps[NSAWN]; // sav() parameters, nsav points
    double ts[NSAWN]; // sav() turn points, w fractions
    double sav(double t); // sav tooth generator
    double tidal(double t); // constant tidal volume generator
    virtual double ut(double t) { return 0; }
    //virtual double um(double t) { return a*(sin(w*t)+1) + patm; }
    virtual double um(double t) { return sav(t) + patm; }
    // mask pressure:
    virtual xpvvec pe(double t) { xpe[PRESS] = um(t); return xpe; }
    static xpvvec pp(const xpvvec& xp) { return xp = xp[PRESS]; }
    static Vec parp(const xpvvec& xp)
    {
        Vec pp;
        double p = xp[PRESS];
        for (int i = 0; i < NGAS; i++)
            pp[i] = xp[i]*p;
        return pp;
    }
    xpvvec dfflow(int i, const xpvvec& xp, const xpvvec& xpx, double R);
    init();
    int prsasn(char*, double*);
    int prsiasn(char*, int*, double*, int maxi = NPCMPT);
    int prsasnvec(char*, xpvvec*);
    int prsiasnvec(char*, int*, xpvvec*, int maxi = NPCMPT);
public:
    lung() { pulcap = 0; nflg = nv = -1; init(); }
    void readfile(char* fn);
    lung(char* fn) { init(); readfile(fn); }
    void dispparam();
    virtual ~lung() {}
    void derive(double t, double dt, const pulvec& xp, pulvec& dxdt);
    virtual void disp(double t, int mm = 0);
    virtual void initdraw(double t0, double t1) {}
    virtual void draw(double t) {}
    void calc(double t0, double t1, double ddt);
    Vec pA(int i) { return parp(qy()[i]); }
    xpvvec dfven(int i, const pulvec& xp)
    {
        return dfflow(i, xp[i], xp[0], R[i]);
    }
    xpvvec dfven(int i) { return dfven(i, qy()); }
    double dp(int i)
    {
        return (qy()[0][PRESS]-qy()[i][PRESS] - um(qx()))/(R[i]*C[i]);
    }
    Vec dpA(int i)

```

```

{
    Vec v;
    double p = qy()[i][PRESS];
    xpvect xp;
    xp = pdriven(i); //dp(i)=qy()[i];
    for (int i = 0; i < NPCMPT; i++)
        v[i] = xp[i];
    return v;
}
double um() { return um(qx()); }
double _V();
double V() { return _V() - vmin; }
double Vdot();
void znflg(int i) { nflg = i; }
void initpulcap(Pulcmpt* pc) { pulcap = pc; }
};
#endif

```

File: pv.h

```

// pV drawing lung model
#include "win.h"
#include "lm.h"

class lung : lung {
    Win* win;
public:
};

class pV : public lung {
    VI* win;
    int first;
    int values;
public:
    pV(int v = 1) { values = v; }
    virtual ~pV() {}
    void initdraw(double, double);
    void draw(double t);
    void disp(double t);
};

class VV : public lung {
    VI* win;
    int first;
    int values;
public:
    VV(int v = 1) { values = v; }
    virtual ~VV() {}
    void initdraw(double, double);
    void draw(double t);
    void disp(double t);
};

```

File: rs.h

```

// The Total Respiratory System
#include "trans.h"
#include "lm.h"

class rs {
    double ddtinc;
    Transmodel* tm;
    lung* lm;
public:
    rs(Transmodel* t, lung* l, double di=1) : tm(t), lm(l) { ddtinc = di; }
    void calc(double x1, double x2, double ddt, double cdt);
};

```

File: phi.h

```

// Dissociation curves

```

```

#include "ph.h"
#include "vec.h"
// concentration in blood: dissociation curves
extern double cHb; // 9.3; // Blood Hb conc, mmol/l
extern double cHbery; // 21; // Ery Hb conc, mmol/l
extern double ksi; // cHb/cHbery;
extern double xHi; // 0.005;
extern double xHbco; // 0.005; // Fraction
extern double ctHb; // 9.30; // Total Hb conc: mmol/l
extern double xHbf; // 0 fraction
extern double cDPG; // conc diphosphoglycerate
// anaesthetics dissociation curve parameters
extern double aana; // G " " fat solubility
extern double aana; // G " " tissue solubility
extern double cBpr0; // G total anaes. binding protein conc in blood
extern double cBpr0; // " " in non fat tissue
extern double Ke; // G protein equilibrium [PrAna] = Ke[Pr][Ana]
extern double aana; // G alpha anaesthetics blood part solubility
extern double aco2; // 0.00983; // Solubility O2 in blood: mmol/(l kPa)
extern double aplaco2; // 0.230; // Solubility: alpha[plasma, co2] mmol/(l kPa)
extern double aseryco2; // 0.195; // Solubility: alpha[ery, co2] mmol/(l kPa)

double cplasma(const Vec& p, double pH);
double _phiCO2(const Vec& p, double pH, double ksi = 9.3/21);
double cCO2(const Vec& p, double c = 22, double ksi = 9.3/21);
double cO2(const Vec& p, double pH);
Mat dcdp(const Vec& p, double ph, double c);
Mat dcTdp(const Vec& p);
double cTana(double p);
double cTco2(const Vec& p);
double dcTana(double p);
double so2(const Vec& p, double pH);
Vec cB(const Vec& p, double oldc = 22);
Vec cT(const Vec& p);

```

File: ph.h

```

// pH model interface
#ifdef _ph_h
#define _ph_h

class HConcError {
public:
    double z, gH, dgHdz;
    HConcError(double z, double gh, double dgh) { z = z; gH = gh; dgHdz = dgh; }
};

extern double cna; // [Na+]: mmol/l
extern double cpro; // [HPr]0: mmol/l
extern double Ka1; // 7.9433e-7; // Ka: CO2 + H2O <-> H+ + HCO3- (pK=6.1)
extern double Ka2; // 5.0119e-8; // Ka: Pr <-> H+ + Pr- (pK=7.3)

double pH(double c);
double dpHdc1(double c);
#endif

```

File: rkf.h

```

//
// Frontend for the Runge-Kutta-Fehlberg algorithm
//
#ifdef RKF_H
#define RKF_H
#include <math.h>
#include "vec.h"

class StepSzError {
public:
    StepSzError() {}
};

class StepUFEError {
    double x, err;
public:
    StepUFEError(double v, double e) { x = v; err = e; }
};

```

```

};

template <class C, int n> class rkf {
    double x; // current x value
    vvec<C,n> y; // current y value
    vvec<C,n> dydx;
    vvec<C,n> yerr;
    vvec<C,n> yout;
    vvec<C,n> yscale; // scaling of errors
    double eps; // limit
    int mnok, mnbad;
    double h1; // stepsize
    double hmin; // minimum allowable stepsize
    double hact; // The actual stepsize
    double hnext; // next proposed stepsize
    double TINY; // = 1.0e-30;
    double SAFTY; // = 0.9;
    double PGROW; // = -0.2;
    double PSHRINK; // = -0.25;
    double ERACON; // = 1.89e-4;

public:
    rkf(double dx=0.1, double e=1e-8, double dxmin=1e-15)
    {
        mnok = mnbad = 0;
        x = 0;
        eps = e;
        h1 = dx;
        hmin = dxmin;
        TINY = 1.0e-30;
        SAFTY = 0.9;
        PGROW = -0.2;
        PSHRINK = -0.25;
        ERACON = 1.89e-4;
    }
    virtual ~rkf()
    {
    }
    rkf<C,n>& operator=(const rkf<C,n>& b)
    {
        x = b.x; // current x value
        y = b.y; // current y value
        dydx = b.dydx;
        yerr = b.yerr;
        yout = b.yout;
        yscale = b.yscale; // scaling of errors
        eps = b.eps; // limit
        mnok = b.mnok;
        mnbad = b.mnbad;
        hmin = b.hmin; // minimum allowable stepsize
        hact = b.hact; // The actual stepsize
        hnext = b.hnext; // next proposed stepsize
        return *this;
    }
    void stepsize(double h) { h1 = abs(h); }
    void yinit(const vvec<C,n>& yinit) { y = yinit; }
    virtual void derive(double t, double dt, const vvec<C,n>& y, vvec<C,n>& dydt) = 0;
    /* 5th order Runge-Kutta-Fehlberg method Num Res (2ed) p 719 */
    void rkfk(double h)
    {
        int i;
        const double a2= 0.2, a3= 0.3, a4= 0.6, a5= 1.0, a6= 0.875,
            b21= 0.2, b31= 3.0/40.0, b32= 9.0/40.0,
            b41= 0.3, b42= -0.9, b43= 1.2,
            b51= -11.0/54.0, b52= 2.5, b53= -70.0/27.0, b54= 35.0/27.0,
            b61= 1631.0/55296.0, b62= 175.0/512.0, b63= 575.0/13824.0,
            b64= 44275.0/110592.0, b65= 253.0/4096.0,
            c1= 37.0/378.0, c3= 250.0/621.0, c4= 125.0/594.0,
            c6= 512.0/1771.0, dc5= -277.0/14336.0;
        const double dc1= c1-2825.0/27648.0, dc3= c3-18575.0/48384.0,
            dc4= c4-13525.0/55296.0, dc6= c6-0.25;
        vvec<C,n> ak2,ak3,ak4,ak5,ak6;
        derive(x+a2*h,(1-a2)*h,y+b21*h*dydx,ak2);
        derive(x+a3*h,(1-a3)*h,y+h*(b31*dydx+b32*ak2),ak3);
        derive(x+a4*h,(1-a4)*h,y+h*(b41*dydx+b42*ak2+b43*ak3),ak4);
        derive(x+a5*h,(1-a5)*h,y+h*(b51*dydx+b52*ak2+b53*ak3+b54*ak4),ak5);
        derive(x+a6*h,(1-a6)*h,y+h*(b61*dydx+b62*ak2+b63*ak3+b64*ak4+b65*ak5),ak6);
        yout = y+h*(c1*dydx+c3*ak3+c4*ak4+c6*ak6);
        yerr = h*(dc1*dydx+dc3*ak3+dc4*ak4+dc5*ak5+dc6*ak6);
    }
    void rkqs(double h)
    {
        int i;
    }

```



```

double errmax, htemp, xnew;
for(;;) {
    rkck(h);
    errmax = norm(yerr/yscale)/eps;
    if(errmax>1.0) {
        htemp=SAFTY*h*pow(errmax,PSHRINK);
        if(h>0.0)
            (htemp>0.1*h) ? h=htemp : h = 0.1;
        if(h<0.0)
            (htemp<0.1*h) ? h=htemp : h = 0.1;
        xnew = x+h;
        if(xnew==x)
#ifdef __GNUC__
            { cerr << "Step underflow" << x << ", " << errmax << "\n";
              return; }
#else
            throw StepUPErr(x, errmax);
#endif
        derivs(x,h,y,dydx);
    } else {
        if(errmax>ERRCON)
            hnxt=SAFTY*h*pow(errmax,PGROW);
        else
            hnxt=5.0*h;
        x += (hact=h);
        y = yout;
        return;
    }
}
// develop from x1 to x2
void odeint(double x1, double x2)
{
    int i;
    double h;
    x=x1;
    h = (x2>x1) ? h1 : -h1;
    mnok = mnbad = 0;
    for(;;) {
        derivs(x,h,y,dydx);
        yscale=abs(y)+abs(dydx*h)+vvec<C,n>(C(TINY));
        if ((x+h-x2)*(x+h-x1) > 0.0)
            h=x2-x;
        rkqs(h);
        (hact == h) ? ++mnok : ++mnbad;
        if ((x-x2)*(x2-x1) >= 0.0) {
            h1=abs(hnxt);
            return;
        }
        if (abs(hnxt) <= hmin)
#ifdef __GNUC__
            { cerr << "Step size error " << x << "\n";
              return; }
#else
            throw StepSzError();
#endif
        h=hnxt;
    }
}
double singlestep(double x1, double maxh)
{
    int i;
    double h = min(h1,maxh);
    x=x1;
    derivs(x,h,y,dydx);
    yscale=abs(y)+abs(dydx*h)+vvec<C,n>(C(TINY));
    rkqs(h);
    return hact;
}
double qx() { return x; }
const vvec<C,n>& qy() { return y; }
const vvec<C,n>& qdydx() { return dydx; }
};
#endif

```

File: trans.cc

```

//
// the Transport model

```

```

#include <iostream.h>
#include "trans.h"
#include "ph.h"

double In::flow() { return x*((Transcmt*)(Cmpt*)cid)->flow(); }
Vec In::Xflow() { return flow()*((Transcmt*)(Cmpt*)cid)->cB(); }

Transcmt::Transcmt(double vb,double vt, const set<In*>& is, double T)
: inset(is)
{
    VT=vt; VB=vb; Temp=T;
}

double Transcmt::pH() { return ::pH(cB()[CO2]); } // pH in the blood part
double Transcmt::T() { return Temp; }
double Transcmt::q_VB() { return VB; }
double Transcmt::q_VT() { return VT; }
double Transcmt::q_T() { return Temp; }

```

File: scmpt.cc

```

#include <iostream.h>
#include <stdio.h>
#include "ln.h"
#include "scmpt.h"

//template <class S, class R> R sum(set<S>, const R& (&f)(const S&));

Vec Transcmt::sumI()
{
    // sum all the inflows
    const member<In*>* ip;
    Vec res = 0;
    for (ip = inset.members(); ip; ip = ip->tail())
        res += ((In*)(*ip))->Xflow();
    return res;
}

double Transcmt::flow()
{
    const member<In*>* ip;
    double res = 0;
    for (ip = inset.members(); ip; ip = ip->tail())
        res += ((In*)(*ip))->flow();
    return res;
}

Vec Cpool::dx(double, double)
{
    return invers(q_VB()-dcB())*(sumI() - flow()*cB());
}

Vec Bodycmt::dx(double t, double)
{
    Vec I, O, M;
    double f;
    Mat m = (q_VT()-dcT()*q_VB()-dcB());
    m.invers();
    I = sumI();
    O = cB();
    f = flow();
    M = metabolism(t);
    //printf(stderr,"I=%f f=%f O=%f fO=%f M=%f\n",I[ANA],f,O[ANA],fO[ANA],M[ANA]);
    Vec v = (I-f*O+M);
    v = m*v;
    return v;
}

Vec Bodycmt::cT()
{
    Vec c;
    c[CO2] = cTco2();
    c[O2] = ac2+pb()[O2];
    c[ANA] = cIana();
    return c;
}

// really dc/dt, as system variable for this cmt is c, not p.
Vec Bloodpool::dx(double, double)

```

```

{
    return (sumI() - flow()*cB())/q_VB();
}

Vec Pulcmpt::dppequ(int i)
{
    return 0.5*(invers(q_VB()*dcB())*(sumI()-flow()*cB()) + lungp->dpA(i));
}

// If permea[i] >= 100, assume instant equilibrium of gas i
//   calculated if lung model is present
//   believed true since initiation of p[i], otherwise.
Vec Pulcmpt::dx(double, double dt)
{
    Vec d;
    Vec dpeq;
    if (lungp)
        dpeq = dppequ(alv1);
    d=invers(q_VB()*dcB())*(sumI() - flow()*cB()*permea*((pA()-pB())));
    for (int i = 0; i < NGAS; i++)
        if (permea[i][i] >= 100)
            d[i] = dpeq[i];
    return d;
}

```

File: lm.cc

```

//
// The complete lung model
#include <stdio.h>
#include <stdlib.h>
#include <iostream.h>
#include <fstream.h>
#include <math.h>
#include <ctype.h>
#include "lm.h"
#include "scompt.h"

ostream& operator << (ostream& o, const xpvect& xp)
{
    return o << "(" << xp[CO2] = xp[PRESS] << "," << xp[O2] = xp[PRESS] << ")";
}

const double platm = 101.3; // iatm = 101.3 kPa

lung::init()
{
    patm = platm; // kPa
    RT = 8.31451*310;
    a = 1; // kPa
    w = 1; // 2pi*1/6 s^-1
    xpe[CO2] = 0;
    xpe[O2] = 0.21;
    xpe[PRESS] = patm;
    //D = 1.76e-5; // m^2/s
    //R[0] = 0.055; // kPa s / l
    R[0] = 0.20; // kPa s / l
    C[0] = 0.10; // l / kPa
    A[0] = pow(0.018/2.2)*pi; // A tranchea [m^2]
    l[0] = 0.20; // m
    // V0 = V0[iatm] - iatm*C
    V0[0] = 0.1-platm*C[0]; // l
    R[1] = 0.0010;
    C[1] = 1.10;
    A[1] = 500000*pow(0.0005/2.2)*pi; // Generation 19 [m^2]
    l[1] = 0.25; // m
    V0[1] = 2.7-platm*C[1]; // l
    // sav tooth function initialize
    nsav = 3;
    ps[0] = 0.0;
    ps[1] = 1.47; // kPa
    ps[2] = 0.2;
    ts[0] = 0.9/3.2;
    ts[1] = 0.1/3.2;
    ts[2] = 2.2/3.2;
}

xpvect lung::dflow(int i, const xpvect xp, const xpvect xpx, double R)
{

```

```

xpvect df;
double Dp;
double p = xp[PRESS];
if ((Dp = xpx[PRESS] - p) > 0) {
    df = Dp*(xpx - xp)/(22.39*R);
    df[PRESS] = 0;
} else
    return df; // 0
return df*RT/((C[i]*p+V0[i])*p);
}

void lung::derive(double t, double dt, const pulveck xp, pulveck dxdt)
{
    int i;
    xpvect xp0 = xp[0];
    // p part
    double dpdt[NPCMPT];
    double x = 0;
    double u = ut(t);
    pe(t);
    double z;
    for (i = 1; i < NPCMPT; i++) {
        x += (xp0[PRESS]-xp[i][PRESS] - u)/R[i];
        dpdt[i] = z/C[i];
    }
    dpdt[0] = (xp[PRESS]-xp0[PRESS])/(R[0]-C[0]) - x/C[0];
    // frac part
    // carr << "d" << t << " " =";
    //xpvect dfd = dfdiff(xp0, xpe, A[0], 1[0]);
    xpvect dff = dfflow(0, xp0, xpe, R[0]);
    for (i = 1; i < NPCMPT; i++) {
        // contribution to cmpt 0
        //dfd += dfdiff(xp0, xp[i], A[i], 1[i]);
        dff += dfflow(0, xp0, xp[i], R[i]);
        double p = xp[i][PRESS];
        xpvect dm;
        dxdt[i] = dfven(i, xp);
        if (pulcap) {
            Vec dpp = RT/((C[i]*p+V0[i])*p);
            *pulcap->perm()=(pulcap->pb()-parp(xp[i]));
            Vec dfvp = pulcap->dppequ(i); // ventilation*perfusion rate
            for (int k = 0; k < NGAS; k++)
                if (pulcap->perm()[k][k] < 100)
                    dxdt[i][k] += dpp[k];
            else
                dxdt[i][k] = (dfvp[k]-dpdt[i]-xp[i][k])/p;
        } else {
            // membrane diffusion, to match metabolism
            // in not-present body model
            double m = 1.8e-3-0.083*RT/((C[i]*p+V0[i])*p);
            dxdt[i][CO2] += m;
            dxdt[i][O2] -= m;
        }
    }
    //dxdt[0] = dfvot(xp0[PRESS], C[0], V0[0], dfd, dff);
    dxdt[0] = dff;
    // fill in the derivative for the pressure model
    for (i = 0; i < NPCMPT; i++)
        dxdt[i][PRESS] = dpdt[i];
}

double lung::sav(double t)
{
    double T = (2*pi*w);
    int n = (int)(t/T);
    if (n > nv) {
        vmin = _V();
        nv = n;
    }
    t -= floor(t/T)*T;
    t /= T;
    int i;
    double tt;
    for (i = 0, tt = 0; i < nsav-1 && t > (tt + ts[i]); i++)
        tt += ts[i];
    return ps[i] + (t-tt)*(ps[(i+1)*nsav] - ps[i])/ts[i];
}

double lung::tidal(double t)
{
    //t -= floor(t/w)*w;
    double p;
    switch (state) {

```

```

    case T_ASC:
        pmax = (t-t0)*dp1;
        if (V() < VT)
            return pmax;
        state = T_DSC;
        t0 = t;
        // fall through
    case T_DSC:
        p = pmax - (t-t0)*dp2;
        if (p > pmin)
            return p;
        state = T_EXP;
        t1 = t;
        // fall through
    case T_EXP:
        if (t - t0 >= tmax)
            state = T_ASC;
        return pmin;
    }
}

void lung::disp(double t, int mm)
{
    double p0= qy()[0][PRESS];
    double p1= qy()[1][PRESS];
    xpvac pp0= pp(qy()[0]), pp1= pp(qy()[1]);
    if (nflg < 0 || nflg == nv) {
        if (!mm)
            cout << t;
        cout << '\t' << pe(t)[PRESS]-piatm << '\t' << V() << '\t'
            << p0 << '\t' << pp0[CO2] << '\t' << pp0[O2] << '\t'
            << p1 << '\t' << pp1[CO2] << '\t' << pp1[O2];
        if (!mm) {
            cout << '\n';
            cout.flush();
        }
    }
}

void lung::calc(double t, double t1, double ddt)
{
    initdraw(t, t1);
    disp(t);
    for (; t < t1; ) {
        odeint(t, t+ddt);
        draw(t);
        disp( t += ddt);
    }
}

double lung::_V()
{
    int i;
    double Q = 0;
    for (i = 0; i < NPCMPT; i++)
        Q += C[i]*qy()[i][PRESS] - C[i]*piatm;
    return Q;
}

double lung::_Vdot()
{
    int i;
    double Vd = 0;
    for (i = 0; i < NPCMPT; i++)
        Vd += C[i]*qdydx()[i][PRESS];
    return Vd;
}

void lung::readfile(char* fn)
{
    ifstream in(fn);
    char buf[1024];
    int ok, i, lno=0;
    char* s;
    double v;
    xpvac vv;
    pulvec xp = qy();
    double v0[NPCMPT];
    for (i = 0; i < NPCMPT; i++)
        v0[i] = V0[i]+piatm*C[i];
    // fix initial values
    while (in.getline(buf,1024)) {
        lno++;

```

```

for (s = buf; isspace(*s); s++)
;
switch (*s) {
case ' ': continue;
// parameters
case 'R': if (ok = prsiasgn(s+1, &i, &v)) R[i] = v; break;
case 'C': if (ok = prsiasgn(s+1, &i, &v)) C[i] = v; break;
case 'V': if (ok = prsiasgn(s+1, &i, &v)) v0[i] = v; break;
case 'A': if (ok = prsiasgn(s+1, &i, &v)) A[i] = v; break;
case 'I': if (ok = prsiasgn(s+1, &i, &v)) I[i] = v; break;
//case 'D': if (ok = prsiasgn(s+1, &v)) D = v; break;
// generators
case 'a': if (ok = prsiasgn(s+1, &v)) a = v; break;
case 'u': if (ok = prsiasgn(s+1, &v)) u = v; break;
case 'n': if (ok = prsiasgn(s+1, &v) && (int)v > 1 && (int)v < NSAWM)
    nsaw = (int)v; break;
// initial values
case 'p':
    switch (s[i]) {
    case 'e': if (ok = prsiasgn(s+2, &v)) xpe[PRESS] = v; break;
    case 's': if (ok = prsiasgn(s+2, &i, &v, nsaw)) ps[i] = v; break;
    default:
        if (ok = prsiasgn(s+1, &i, &v, 3))
            xp[i][PRESS] = v;
    }
    break;
case 't':
    if (ok = prsiasgn(s+1, &i, &v, nsaw)) ts[i] = v; break;
case 'f':
    if (*s == 'e') {
        if (ok = prsiasgnvec(s+2, &vv)) {
            vv[PRESS] = xpe[PRESS];
            xpe = vv;
        }
    } else if (prsiasgnvec(s+1, &i, &vv)) {
        vv[PRESS] = xp[i][PRESS];
        xp[i] = vv; break;
    }
    break;
default:
    ok = 0;
}
if (!ok)
    cerr << fn << ": syntax error line " << lno << "\n";
}
yinit(xp);
for (i = 0; i < NPMPT; i++)
    v0[i] = v0[i]-plam*C[i];
double t = 0;
for (i = 0; i < nsaw-1; i++)
    t += ts[i];
ts[i] = 1 - t;
}

int lung::prsiasgn(char* s, double *vp)
{
    for (; isspace(*s); s++)
        ;
    if (*s != ' ')
        return 0;
    char* p;
    *vp = strtod(s, &p);
    return s != p;
}

int lung::prsiasgn(char* s, int* ip, double *vp, int maxi)
{
    int i = 0, found = 0;
    while (*s >= '0' && *s <= '9') {
        i += 10;
        i += *s - '0';
        found = 1;
    }
    if (found && i < maxi) {
        if (prsiasgn(s, vp)) {
            *ip = i;
            return 1;
        }
    }
    return 0;
}

int lung::prsiasgnvec(char* s, xpvect* vp)

```

```

{
    char* p;
    for (; isspace(*s); s++)
        ;
    if (*s++ != ' ')
        return 0;
    for (int i = 0; i < NGAS; i++) {
        for (; isspace(*s); s++)
            ;
        if (*s == (i ? ' ' : '('))
            s++;
        for (; isspace(*s); s++)
            ;
        if (*s == ',' || (i == NGAS-1 && *s == ' '))
            (*vp)[i++] = strtod(s, &p);
        else
            return 0;
    }
    return 1;
}

int lung::prsaasgnvec(char* s, int* ip, xpvect* vp, int maxi)
{
    int i = 0, found = 0;
    while (*s >= '0' && *s <= '9') {
        i += 10;
        i += *s++ - '0';
        found = 1;
    }
    if (found && i < maxi) {
        if (prsaasgnvec(s, vp)) {
            *ip = i;
            return 1;
        }
    }
    return 0;
}

void lung::dispparam()
{
    int i;
    cout << "s pe = " << xpe[PRESS] << "\n";
    cout << "s fe = " << xpe << "\n";
    //cout << "s D = " << D << "\n";
    cout << "s a = " << a << "\n";
    cout << "s v = " << v << "\n";
    cout << "sSav p t\n";
    for (i = 0; i < nsav; i++)
        cout << "s " << ps[i] << "\t" << ts[i] << "\n";
    cout << "s Cmpt R C VO A[e-6] l p f\n";
    for (i = 0; i < NPCMPT; i++)
        cout << "s\t" << i << "\t" << R[i] << "\t" << C[i] << "\t"
            << VO[i] + C[i]*plam << "\t" << A[i]*1e6 << "\t" << l[i] << "\t"
            << qy()[i][PRESS] << "\t" << qy()[i] << "\n";
}

```

File: main.cc

```

//
// main: Blood transport model
//
#include <GetOpt.h>
#include <iostream.h>
#include <fstream.h>
#include <stdio.h>
#include "rs.h"
#include "scmpt.h"

enum { cap, poola, poolv, kidney, brain, heart, liver, muscles, conn,
        adia, rest, poolvv, poolvl, poolva, local_ncmpt };
Cmpt* cmpts[ncmpt];
char* cmptnam[] =
{ "cap", "poola", "poolv", "kidney", "brain",
  "heart", "liver", "muscles", "conn",
  "adia", "rest", "poolvv", "poolvl", "poolva" };

Cmpt* Cid::cmpts = cmpts;

enum { F_CHMPT3 };

```

```

void initcmpts(int flgs);

enum { O_P, O_CB, O_CT, O_X, N_OUT };
char* outnam[] = { "p", "cB", "cT", "x" };
int out; // bits: 1 << O_x
int outana = 0;

ostream& operator<<(ostream& os, const Vec& v)
{
    if (outana)
        os << v[ANA];
    else
        os << "(" << v[C02] << ", " << v[02] << ")";
    return os;
}

int Bodycmpt::mh = 0;

int main(int argc, char* argv[])
{
    if (local_ncmpt != ncmpt) {
        cerr << "Illegal configuration:\nmodel size (" << ncmpt
              << ") differs from number of compartments (" << local_ncmpt << ")\n";
        exit(1);
    }
    int i;
    int mhflg = 0;
    int flgs = 0;
    int ss = 0; // select staty state starting point
    double t0 = 5;
    double tmax = 20000;
    double ddt = 0.1;
    double cdt = 0.05;
    double dddt = 1.1;
    double nana = 0; // amount of anaesthetica placed in venous pool
    char* lungfile = 0;
    GetOpt getopt(argc, argv, "3a:cCxpmt:d:l:l:");
    while ((i = getopt()) != EOF) switch (i) {
        case '3': flgs |= (1 << F_CMPT3); break;
        case 't': tmax = atof(getopt.optarg); break;
        case 'd': ddt = atof(getopt.optarg); break;
        case 'l': dddt = atof(getopt.optarg); break;
        case 'a': outana++; nana = atof(getopt.optarg); break;
        case 's': ss++; break;
        case 'c': out |= (1 << O_CB); break;
        case 'C': out |= (1 << O_CT); break;
        case 'x': out |= (1 << O_X); break;
        case 'p': out |= (1 << O_P); break;
        case 'm': mhflg++; break;
        case 'L': lungfile = getopt.optarg; break;
        default:
            cerr << "usage: " << "\n";
            exit(1);
    }
    if (!out)
        out = (1 << O_P);
    if (mhflg)
        Bodycmpt::mh++;
    if (ddt < cdt)
        cdt = ddt;
    // create transport model
    initcmpts(flgs);
    vvec<Vec, ncmpt> x0;
    TransportModel tm(cmpts,
        set<Cid>(poola, poolv).ins(cap).ins(muscles).ins(kidney)
        .ins(brain).ins(adia), dddt);
    if (ss) {
        x0[cap] = mkv(5.3, 13.3);
        x0[poola] = mkv(5.3161, 12.4566);
        x0[poolv] = mkv(6.13678, 5.17942);
        x0[kidney] = mkv(5.49209, 8.41225);
        x0[brain] = mkv(6.53507, 4.4601);
        x0[heart] = mkv(6.28108, 4.91597);
        x0[liver] = mkv(6.9572, 3.86156);
        x0[muscles] = mkv(6.1229, 5.26527);
        x0[conn] = mkv(5.56972, 7.6418);
        x0[adia] = mkv(5.31614, 12.4566);
        x0[rest] = mkv(6.10728, 5.30375);
        x0[poolvv] = mkv(25.2272, 6.37059);
        x0[poolvl] = mkv(24.5604, 7.60013);
        x0[poolva] = mkv(23.7613, 9.08395);
    } else {

```



```

    x0[cap] = ((Pulcmpt=cmts[cap])>>pA());
    x0[poola] = x0[kidney]=x0[brain]=x0[heart]=x0[liver]
        =x0[conn]=x0[adia]=x0[rest] = x0[poolv]= mkv(10,10,0);
    x0[poolvv]=x0[poolvl]=x0[poolva] = cB(mkv(10, 10, 0));
    x0[muscles] = mkv(10,10,0);
}
if (outana)
    x0[poolv][ANA] = ((Cpool=cmts[poolv])>>pANA(nana);
tm.initx(x0);
// create lung model
pulvac p;
double platm = 101.3;
Vec pcp = tm.qy()[cap];
p[0][CO2] = 0.004;
p[0][O2] = 0.10;
p[0][PRESS] = platm;
p[1][CO2] = pcp[CO2]/platm;
p[1][O2] = pcp[O2]/platm;
p[1][PRESS] = platm;
lung lm;
lm.yinit(p);
lm.stepsize(0.1);
// link lung to transport, and vice versa
lm.initpulcap((Pulcmpt=cmts[cap]));
((Pulcmpt=cmts[cap])>>initlung(&lm);
// create the combined model
rs resp(tm, lm, ddt);
cout << "s Blood transport model: "
    << t0 << "-" << tmax << " s" << ddt << "[" << ddt << "]"<< "\n";
if (Bodycmt::mh)
    cout << "s Malign Hyperthermia activated\n";
resp.calc(t0, tmax, ddt, cdt);
}

void initcmts(int flgs)
{
    // Cardiac Output
    const double Qc = 0.083; // 1/s **** check value
    // Blood volumes, [Model 10, Lerou]
    const double Vbvein = 1.427;
    const double Vba = 0.2*Vbvein;
    const double Vbvt = 0.8*Vbvein;
    const double Vbv = 0.126*Vbvt;
    const double Vbv1 = 0.364*Vbvt;
    const double Vbva = 0.111*Vbvt;
    const double Vbvv = 0.399*Vbvt;
    // Pulmonary shunt
    const double lambda = 0.02; //0.02;
    // Organ Blood and Tissue volumes
    const double Vtkid = 0.27;
    const double Vbkid = 0.051;
    const double Vthea = 0.307;
    const double Vbhea = 0.040;
    const double Vtbra = 1.3;
    const double Vbbra = 0.105;
    const double Vtliv = 2.973;
    const double Vbliv = 1.106;
    const double Vtmus = 26.773;
    const double Vbmus = 0.700;
    const double Vtcon = 8.182;
    const double Vbcon = 0.653;
    const double Vtadi = 14.786;
    const double Vbadi = 0.562;
    const double Vtres = 0.217;
    const double Vbres = 0.015;
    const double Vblun = 0.530;
    const double Vt = Vtkid+Vthea+Vtbra+Vtliv+Vtres;
    // blood flow fractions
    const double zbra = 0.135;
    const double zkid = 0.222;
    const double zliv = 0.283;
    const double zhea = 0.048;
    const double zmus = 0.107;
    const double zcon = 0.101;
    const double zadi = 0.062;
    const double zres = 0.041;
    const double zorg = zbra + zkid + zliv + zhea + zadi + zmus + zcon + zres;
    // Thiopentale: alpha ana tissue, from Hull
    double aabra = 1.4;
    double aakid = 1.5;
    double aaliv = 1.7; // adj. since our liver includes stomach
    double aahea = 1.5;
    double anmus = 1.5;

```

```

double aacon = 1.5;
double aaadi = 11.0;
double aares = 1.5;
if (flgs & (1 << F_CMPT3)) {
    // k12/k21 // slow
    double aaslow = 14.308*5.2/(Vtmus*Vtadi*Vtcon);
    // k13/k31 // fast
    double aafast = 1.781*5.2/Vt;
    aabra = aakid = aaliv = aashea = aares = aafast;
    aamus = aacon = aaadi = aaslow;
}
Cid::x_cmpts(cmpts);
// hack up for missing lung model
Vec pa = mkv(5.3,13.3,0);
#define mkIn(x) In(x,1)
cmpts[cap] = new Pulcmpt(0.53,mkv(100,100,0),poolv,1-lambda,pa);
cmpts[poola] = new Cpool(Vba, Qc,
    set<In>(In(cap, 1), In(poolv, lambda)));
cmpts[poolv] = new Cpool(Vbv, Qc,
    set<In>(mkIn(poolvv)).ins(mkIn(poolvl)).ins(mkIn(poolva))
    .ins(In(poola, /-1-xorg=/0)));
double xv = 175.0/260.0; // from Fukui;
double xbra = 50.0/260.0;
double xl = 35.0/260.0;
const double co2prod = 6.15/60; // (mmol/s) CO2 prod [Nun]
const double o2con = -11.52/60; // (mmol/s) O2 consumption [Nun]
Vec Mv = mkv(co2prod*xv, o2con*xv, 0)/(Vtkid*Vthea*Vtliv*Vtres);
Vec Mbra = mkv(co2prod*xbra, o2con*xbra, 0)/Vtbra;
Vec Ml = mkv(co2prod*xl, o2con*xl, 0)/(Vtmus*Vtcon);
Vec lmr; // standard metabolic rate, liver
// lmr[AFA] = -26.5/60/1000/Vtliv; // from 'model 10'
cmpts[kidney] = new Bodycmpt(Vbkid, Vtkid, Mv, poola, zkid,aakid);
cmpts[heart] = new Bodycmpt(Vbhea, Vthea, Mv, poola, zhea,aashea);
cmpts[brain] = new Bodycmpt(Vbbra, Vtbra, Mbra, poola, zbra,aabra);
cmpts[liver] = new Bodycmpt(Vbliv, Vtliv, Mv+lmr, poola, zliv,aaliv);
cmpts[muscles] = new Bodycmpt(Vbmus, Vtmus, Ml, poola, zmus,aamus);
cmpts[conn] = new Bodycmpt(Vbcon, Vtcon, Ml, poola, zcon,aacon);
cmpts[adia] = new Bodycmpt(Vbadi, Vtadi, mkv(0,0,0), poola, zadi,aaadi);
cmpts[rest] = new Bodycmpt(Vbres, Vtres, Mv, poola, zres,aares);
cmpts[poolvv] = new Bloodpool(Vbv,
    set<In>(mkIn(kidney)).ins(mkIn(heart)).ins(mkIn(brain))
    .ins(mkIn(liver)).ins(mkIn(rest)));
cmpts[poolvl] = new Bloodpool(Vbvl,
    set<In>(mkIn(muscles), mkIn(conn)));
cmpts[poolva] = new Bloodpool(Vbva, set<In>(mkIn(adia)));
}

void terminate()
{
    cerr << "exception not caught.\n";
    exit(1);
}

void Transmodel::initdisp()
{
    cout << "S";
    for (int o = 0; o < N_OUT; o++)
        if (out & (1 << o))
            cout << '\t' << outnam[o];
    cout << "\n";
    cout << "S";
    for (int i = 0; i < ncmpt; i++)
        if (plot.in(i))
            cout << '\t' << cmptnam[i];
    cout << "\n";
}

void Transmodel::disp(double t, int mm)
{
    int outp;
    if (!mm)
        cout << t;
    for (int o = 0; o < N_OUT; o++) {
        if (!(out & (1 << o)))
            continue;
        outp = o;
        for (int i = 0; i < ncmpt; i++)
            if (plot.in(i)) {
                Transcmpt* p = ((Transcmpt*)::cmpts[i]);
                Vec x;
                switch (i) {
                    // blood only
                    case cap:

```

```

        case poola:
        case poolv:
            x = (outp == 0_P) ? p->q_x()
                : ((outp == 0_X) ? p->q_VB() : 1.0)*p->cB();
            break;
        // conc only
        case poolvv:
        case poolvl:
        case poolva:
            x = ((outp == 0_X) ? p->q_VB() : 1.0)*p->q_x();
            break;
        // both tissue and tension
        case kidney:
        case brain:
        case heart:
        case liver:
        case muscles:
        case conn:
        case adia:
        case rest:
            switch (outp) {
                case 0_CB: x = ((Bodycmt*)p)->cB(); break;
                case 0_CT: x = ((Bodycmt*)p)->cT(); break;
                case 0_X: x = p->q_VT()*((Bodycmt*)p)->cT(); break;
                case 0_P: x = p->q_x(); break;
            }
            break;
        }
        cout << '\t' << x;
    }
    if (!mm) {
        cout << '\n';
        cout.flush();
    }
}

```

File: ph.cc

```

//
// Chiari et al: pH model
//
#include <math.h>
#include <iostream.h>
#include "ph.h"

double cna = 46.2e-3; // mol/l
double cpro = 39.8e-3; // mol/l
double Ka1 = 7.9433e-7; // pov(10,-6.1); Ka: CO2 + H2O <-> H+ + HCO3- (pK=6.1)
double Ka2 = 5.0119e-8; // pov(10,-7.3); Ka: Pr <-> H+ + Pr- (pK=7.3)

#ifdef __GNUC__
inline double abs(double x) { return x >= 0 ? x : -x; }
#endif

static double gH(double z, double cco2)
{
    return ((z + Ka2*cna*Ka1)*z + Ka1*(cna-cco2)+Ka2*(cna-cpro*Ka1))*z
        + Ka1*Ka2*(cna-(cco2*cpro));
}

static double dgHdz(double z, double cco2)
{
    return (3*z + 2*(Ka2*cna*Ka1))*z + Ka1*(cna - cco2)+Ka2*(cna - cpro + Ka1);
}

static double dgHdc(double z, double cco2)
{
    return -Ka1*(z*Ka2);
}

static double H(double c)
{
    double z, dz;
    const double e = 1e-20;
    for (z = 0.000001; abs(dz = gH(z, c)/dgHdz(z, c)) > e; z += dz)
        ;
    if (z < 0)
        ;
#ifdef __GNUC__

```

```

        throw HConcError(z, gH(z,c), dgHdz(z,c));
    } else
    { cerr << "pH error: "<<z<<"", "<<gH(z,c)<<"", "<<dgHdz(z,c)<<"\n";
      return 1e-14; }
    }
}

// c in mmol/l
double pH(double c)
{
    return -log10(H(c/1000));
}

// dpH/dc
double dpHdc(double c)
{
    c /= 1000;
    double z = H(c);
    return (1/log(10))/H(c)=dgHdc(z,c)/dgHdz(z,c)/1000;
}

```

File: phi.cc

```

#include <math.h>
#include <stdio.h>
#include <stdlib.h>
#include <iostream.h>
#include "ph.h"
#include "phi.h"

//double ctHb = 9.30; // Total Hb conc: mmol/l
double aplace2=0.230; // Solubility:alpha[plasma, co2] mmol/(l kPa)
double aeryco2=0.195; // Solubility:alpha[ery, co2] mmol/(l kPa)
double cHb=9.3; // Blood Hb conc, mmol/l
double cHery=21; // Ery Hb conc, mmol/l
double ksi=cHb/cHery;
double cDPG=5.01; // mmol/l
double ao2 = 0.00983; // Solubility O2 in blood: mmol/(l kPa)
double xHi = 0.005; // Fraction
double xHbf = 0;
double xHbco = 0.005;
// blood solubility of anaesthetic agent
double aana = 1; // mmol / (l kPa)
// Thiopental:
if 0
double g2 = 14.308; //(5.2/49.741); // k12/k21 // slow
double g3 = 1.781; //(5.2/5.067); // k13/k31 // fast
double aanaf = (g2*(14.786+8.182+26.773)-g3*(14.786+26.773))/14.786;
double aanat = g3;
//else
double aanaf = 11;
double aanat = 1.5;
#endif
// protein binding, not configured!
double cSpr0 = 0;
double cpr0 = 0;
double xfat = 0;
double Ke = 1; // virtual!, change when cpr0 != 0
double T = 37; // Temperature celcius

// Siggaard Andersen: phi CO2
inline double alog(double x) { return pow(10,x); }

double pKpla(const Vec& p, double ph)
{
    return 6.125-log10(1+alog(ph-8.7));
}

double pHery(const Vec& p, double ph)
{
    return 7.19+0.77*(ph-7.4) + 0.035*(1-(so2(p, ph)));
}

double pKery(const Vec& p, double ph)
{
    return 6.125-log10(1+alog(pHery(p,ph) - 7.84-0.06*so2(p, ph)));
}

```

```

// CO2 concentration in plasma
// Eqn (3) [ 4 - 7 ]
// c is co2 conc for pH calculation
double cplasma(const Vec& p, double ph)
{
    return aplaco2*p[CO2]*(1 + alog(ph-pKpla(p,ph)));
}

// Eqn (11) [ 12 - 14 ]
double cery(const Vec& p, double ph)
{
    return aceryco2*p[CO2]*(1+alog(pHery(p,ph)-pKery(p,ph)));
}

// p in Pa
// eqn (8) [ 9 ]
double _phiCO2(const Vec& p, double ph, double ksi)
{
    return cery(p, ph)*ksi + cplasma(p, ph)*(1-ksi);
}

// primitive numeric---works!
double d_phidc(double c1, const Vec& p, double ph, double c)
{
    double dc=1e-9;
    return (_phiCO2(p,pH(c+dc))-c1)/dc;
}

// iterate the correct c value in the phi, pH equation
// p in kPa, proposed start value c in mmol/l
double cCO2(const Vec& p, double c, double ksi)
{
    double dc;
    int i = 100;
    const double e = 1e-10;
    double ph = pH(c);
    double c1 = _phiCO2(p,ph,ksi);
    for (; abs(dc=(c1-c)/(d_phidc(c1,p,ph,c)-1)) > e && --i;) {
        ph = pH(c + dc);
        c1 = _phiCO2(p,ph,ksi);
    }
    return c;
}

//
// Siggard Andersen phi function for O2
//
double a(const Vec& p, double ph)
{
    return -0.72*(ph-7.4)+0.09*(log(p[CO2]/5.33))
        +(0.07-0.03*xHbf)*(cDPG-5)
        -0.368*xHbco-0.174*xH1-0.28*xHbf;
}

double b()
{
    return 0.055*(T-37);
}

double xx(const Vec& p)
{
    return log(p[O2]);
}

double x0(const Vec& p, double ph)
{
    return 1.946*a(p,ph)*b();
}

double h(const Vec& p, double ph)
{
    return 3.5*a(p,ph);
}

double Th(const Vec& p, double ph)
{
    return tanh(0.5343*(xx(p) - x0(p,ph)));
}

double y(const Vec& p, double ph)

```

```

{
    return 1.875*xx(p)-x0(p,ph)+h(p,ph)*Th(p,ph);
}

double so2(const Vec& p, double ph)
{
    return 1/(1+exp(-y(p,ph)));
}

double c02(const Vec& p, double ph)
{
    double cHbfree = cHb*(1-xHbco-xHi);
    return ao2*p[02]+cHbfree*so2(p, ph);
}

Vec cB(const Vec& p, double oldc)
{
    Vec c;
    c[C02] = cC02(p, oldc);
    c[02] = c02(p, pB(c[C02]));
    c[ANA] = aana*p[ANA];
    return c;
}

double cTco2(const Vec& p)
{
    return cC02(p, 22, 0);
}

Vec cT(const Vec& p)
{
    Vec c;
    c[C02] = cTco2(p);
    c[02] = ao2*p[02];
    return c;
}

// Derived:
Vec dsdp(const Vec& p, double ph)
{
    Vec z;
    register double ey = exp(-y(p,ph));
    register double n2 = pow(1+ey,2);
    register double c2 = pow(cosh(0.5343*(xx(p)-x0(p,ph))),2);
    register double ch = h(p,ph);
    z[C02] = ey/n2*(0.09/p[C02])*(-1+ch*(-0.5343/c2)+Th(p,ph));
    z[02] = ey/n2/p[02]*(1+ch*0.5343/c2);
    z[ANA] = 0;
    return z;
}

double dsdpB(const Vec& p, double ph)
{
    register double ey = exp(-y(p,ph));
    register double n2 = pow(1+ey,2);
    double dThdpB = 0.72*0.5343/pow(cosh(0.5343*(xx(p) - x0(p,ph))),2);
    return ey/n2 *(0.72*h(p,ph)+dThdpB*Th(p,ph)+(-0.72));
}

double dphi1dp1(const Vec& p, double ph)
{
    double alogpla = alog(ph-pKpla(p,ph));
    double dplaa = aplaco2*(1+alogpla);
    return dplaa;
}

double dphi1dp1(const Vec& p, double ph)
{
    Vec ds = dsdp(p, ph);
    double ksi = cHb/cHbery;
    double dpBery = -0.035*ds[C02];
    double phery = pBery(p,ph);
    double pkery = pKery(p,ph);
    double so = so2(p,ph);
    double alogph = alog(phery-7.84-0.06*so);
    double dpKery = 0.095*ds[C02]/(1+alogph)*alogph;
    double alogery = alog(phery-pkery);
    double alogpla = alog(ph-pKpla(p,ph));
    double dery = aeryco2*(1+alogery
        + p[C02]*log(10)*alog(phery-pkery)*(dpBery-dpKery));
    double dplaa = aplaco2*(1+alogpla);
    return ksi*dery*(1-ksi)+dplaa;
}

```

```

double dphi1dp2(const Vec& p, double ph)
{
    double ds = dsdp(p,ph)[02];
    double so = so2(p,ph);
    double phery = pKery(p,ph);
    double alogery = alog(phery-7.84-0.06*so);
    double dpHery = -0.035*ds;
    return ksi*aeryco2*p[02]*log(10)*alog(phery-pKery(p,ph))
        *(dpHery+alogery/(1+alogery)*(dpHery-0.06*ds));
}

double dphi2dp1(const Vec& p, double ph)
{
    return cHb*dsdp(p, ph)[02];
}

double dphi2dp2(const Vec& p, double ph)
{
    return ao2+cHb*dsdp(p,ph)[02];
}

Vec dphidpH(const Vec& p, double ph)
{
    Vec x;
    double ds = dsdpH(p, ph);
    double dpHery = 0.77-0.035*ds;
    double phery = pKery(p,ph);
    double alogph = alog(phery-7.84-0.06*so2(p,ph));
    double dpKery = -alogph/(1+alogph)*(dpHery-0.06*ds);
    double dcery = aeryco2*p[02]*log(10)*alog(phery-pKery(p,ph))
        *(dpHery - dpKery);
    double H = alog(ph-8.7);
    double dpKpla = -H/(1+H);
    double dcplas = aplaco2*p[02]*log(10)*alog(ph-pKpla(p,ph))*(1-dpKpla);
    x[02] = ksi*dcery*(1-ksi)*dcplas;
    x[02] = cHb*ds;
    return x;
}

Mat dcdp(const Vec& p, double ph, double c)
{
    Mat dc;
    Vec ddpH = dphidpH(p,ph);
    double A = 1/(ddpH[02]*dpHdc1(c)-1);
    double B = A*(ddpH[02]*dpHdc1(c));
    dc[ANA][ANA] = aana;
    dc[02][02] = -dphi1dp1(p,ph)*A;
    if 0
        cout << "dcdp:\t(" << p[02] << ", " << p[02] << ", " << p[ANA] << ")"
            << "\t<< c << "\t<< ph << "\t<< A << "\t<< dc[02][02]
            << "\t<< dphidpH(p,ph)[02] << "\t<< dpHdc1(c) << "\t<< dphi1dp1(p,ph)
            << "\t" << "\n";
    #endif
    dc[02][02] = dphi2dp1(p,ph)-dphi1dp1(p,ph)*B;
    dc[02][02] = -(dphi1dp2(p,ph)*A);
    dc[02][02] = dphi2dp2(p,ph)-dphi1dp2(p,ph)*B;
    return dc;
}

void tcdp()
{
    Vec p1;
    double p, A, c, ph, dc;
    p1[02] = 5.3;
    cout << "sp c pH A dc didpH dpHdc didp1 dcdp11\n";
    for (p = 1; p < 15; p+=0.1) {
        p1[02] = p;
        c = cB(p1)[02];
        ph = pH(c);
        Vec ddpH = dphidpH(p1,ph);
        A = 1/(ddpH[02]*dpHdc1(c)-1);
        dc = -dphi1dp1(p1,ph)*A;
        cout << p << "\t(" << p1[02] << ", " << p1[02] << ", " << p1[ANA] << ")"
            << "\t<< c << "\t<< ph << "\t<< A << "\t<< dc
            << "\t<< dphidpH(p1,ph)[02] << "\t<< dpHdc1(c) << "\t<< dphi1dp1(p1,ph)
            << "\t" << dcdp(p1, ph, c)[02][02] << "\n";
    }
}

double dphi1TdpH(const Vec& p, double ph)
{
    double H = alog(ph-8.7);

```

```

double dpKpla = -H/(1+H);
return aplaco2*p[CO2]=log(10)*alog(ph-pKpla(p,ph))=(1-dpKpla);
}

Mat dcTdp(const Vec& p)
{
    Vec c = cT(p);
    double ph = pH(c[CO2]);
    Mat dc;
    double A = 1/(dphi1TdpH(p, ph)*dpHdc1(c[CO2])-1);
    dc[CO2][CO2] = -dphi1Tdp1(p,ph)*A;
    dc[O2][O2] = ao2;
    return dc;
}

```

File: pv.cc

```

#include <iostream.h>
#include "pv.h"

void PV::initdraw(double, double)
{
    if (win = new VJ)
        win->axes(-0.3, 0, 1.5);
}

void PV::draw(double t)
{
    if (!win)
        return;
    if (first) {
        win->move(um()-101.3, V());
        first = 0;
    } else
        win->draw(um()-101.3, V());
}

void PV::disp(double t)
{
    if (values && t >= 2)
        cout << t << "\t" << um() << "\t" << um()-101.3 << "\t" << V() << "\n";
}

void VV::initdraw(double, double)
{
    if (win = new VJ)
        win->axes(-1.2, 1, -1, 1);
}

void VV::draw(double t)
{
    if (!win)
        return;
    if (first) {
        win->move(V(), Vdot());
        first = 0;
    } else
        win->draw(um()-101.3, V());
}

void VV::disp(double t)
{
    if (values)
        cout << t << "\t" << um() << "\t" << um()-101.3 << "\t" << V() << "\n";
}

```

File: rs.cc

```

#include <iostream.h>
#include "rs.h"

// step the two models in unison
void rs::calc(double x1, double x2, double ddt, double cdt)
{

```



```

double h2;
double x=x1;
pulvec puly, npuly;
double h = cdt;
int disp = 1;
for (;;) {
    if (disp) {
        cout << x;
        lm.disp(x,1);
        tm.disp(x,1);
        disp = 0;
        cout << '\n';
        cout.flush();
    }
    puly = lm.qy();
    h = lm.singlestep(x,h);
    npuly = lm.qy();
    lm.yinit(puly);
    h2 = tm.singlestep(x,h);
    if (h2 < h)
        lm.singlestep(x,h = h2);
    else
        lm.yinit(npuly);
    x += h;
    if ((x+h-(x1+ddt))*(x+h-x1) > 0.0) {
        disp++;
        x1 = x;
        ddt += ddtinc;
    }
    if ((x-x2)*(x2-x1) >= 0.0)
        break;
}
cout << x;
lm.disp(x,1);
tm.disp(x,1);
disp = 0;
cout << '\n';
cout.flush();
}

```

Appendix B

Glossary

This chapter contains definitions of the physiological and medical vocabulary, that has caused us trouble during the preparation of this report.

Acid 1) Molecule capable of releasing a hydrogen ion. 2) A solution having a concentration of hydrogen ions, which is higher than that of pure water.

Acidosis Any situation in which arterial hydrogen ion concentration is elevated.

Alkalosis Any situation in which arterial hydrogen ion concentration is reduced.

Alveolar deadspace The volume of air in unperfused alveoli, which thus remains unexchanged with the blood.

Alveoli The blind-ended terminal sacs of the airways where majority of gas exchange takes place and majority of the lung volume resides.

Anatomical deadspace The volume of air in the conducting zone, which is expired without exchange of gasses with the blood.

Apnoe A short pause or a stop of breathing in the expiratory position

Bohr effect The influence of CO₂ on the dissociation curve for O₂.

Bronchi Airways between the trachea and the alveoli.

Carbamino A complex of protein (mainly hemoglobin) and carbon dioxide.

Carbonic anhydrase An enzyme found in red blood cells which accelerates the equilibrium of the reaction $\text{CO}_2 + \text{H}_2\text{O} \leftrightarrow \text{H}_2\text{CO}_3$.

DPG 2,3-Diphosphoglycerate, found in red cells, shifts the O_2 dissociation curve to the right.

Erythrocyte Red blood cell.

Haldane effect The influence of O_2 on the dissociation curve for CO_2 .

Hemoglobin A protein found in red blood cells by which most of the oxygen in blood is carried

Henderson-Hasselbalch equation Yields the equilibrium condition of CO_2 and bicarbonate, and hydrogen ions.

Hypoxia Lack of oxygen in tissue.

Lactic acid Three-carbon molecule formed in absence of oxygen. Dissociates to form lactate and hydrogen ions.

Metabolic acidosis Acidosis due to any cause other than accumulated CO_2

Metabolic alkalosis Alkalosis due to any cause other than excessive respiratory removal of CO_2 .

Myoglobin A protein binding molecule found in the muscle fibres.

Obstructive pulmonary disorder A disordered ventilatory function due to an obstruction of the airways.

Pulmonary The adjectival form of "lungs".

Respiratory acidosis Increased arterial hydrogen ion concentration due to CO_2 retention

Respiratory alkalosis Decreased arterial hydrogen ion concentration due to excessive respiratory removal of CO_2 .

Restrictive pulmonary disorder A disordered ventilatory function due to impaired respiratory movement.

Spirometer An instrument for measuring lung volumes.

Total deadspace The anatomical and alveolar deadspace.

Tidal volume That volume of air passing into or out of the lungs during each breath.

Trachea Single airway connecting larynx with bronchi.

Vein A vessel that returns blood to the heart.

Ventilation Air exchange between air and alveoli.

Appendix C

Symbol list

<i>Symbol</i>	Description
Lung model	
p	pressure
f	fraction vector
R	resistance
C	compliance
V	volume
V_0	unstretched volume
U_m	respirator generated pressure at mouth
U_t	pressure generated by respiratory muscles in thorax
R	the gas constant
T	absolute temperature
κ	lung membrane flux coefficient
n_a	number of alveoli branches
n	amount of substance by number of moles
g	generation of airway branching
r	radius
l	length
ρ	density of gas or fluid
η	viscosity of gas or fluid
I	current
J	flux
U	voltage
Q	charge
Blood transport model	
x	amount of matter
\mathcal{M}_+	metabolic production rate
\mathcal{M}_-	metabolic consumption rate

Symbol	Description
Q	cardiac output
z_i	fraction of cardiac output to compartment i
λ_i	fraction of cardiac output to capillary branch i
λ	pulmonary shunt
c	concentration
c_b	blood concentration
c_t	tissue concentration
c_i	concentration in blood of compartment i
p	pressure vector
V_b	volume of blood part of compartment
V_t	volume of tissue part of compartment
κ	lung membrane flux coefficient
Metabolism	
β	reference concentration when metabolism is half M
\mathcal{M}	metabolic rate
\mathcal{M}_+	metabolic rate, production
\mathcal{M}_-	metabolic rate, consumption
M	maximum metabolic rate
pH and dissociation	
$[z]$	concentration of substance z
α	solubility coefficient
α_{O_2}	solubility coefficient of O_2
$\alpha_{CO_2}^{Ery}$	solubility coefficient of CO_2 in erythrocytes
$\alpha_{CO_2}^{Pla}$	solubility coefficient of CO_2 in plasma
α	solubility coefficient of anaesthetic agent
c_{Hb}	concentration of hemoglobin
c_{Hb}^{Ery}	concentration of hemoglobin in erythrocytes
c_{CO_2}	concentration of CO_2
c_{O_2}	concentration of O_2
$c_{CO_2}^{Ery}$	concentration of CO_2 in erythrocytes
$c_{CO_2}^{Pla}$	concentration of CO_2 in plasma
s_{O_2}	oxygen saturation of hemoglobin
K_a	equilibrium constant for chemical reaction
pH	pH in plasma
pH^{Ery}	pH in erythrocytes
pK^{Pla}	pK in plasma
pK^{Ery}	pK in erythrocytes
x_{Hbf}	fraction of fetal hemoglobin
x_{HbCO}	fraction of carboxyhemoglobin
x_{Hi}	fraction of hemoglobin
Miscellaneous	
μ	the set of model parameters

<i>Symbol</i>	Description
x_L	state variable of the lung model
x_B	state variable of the blood transport model
n_a	number of alveoli and capillary branches
n_s	number of substances in a compartment vector
γ_b	function that converts the state vector to blood concentrations
γ_t	function that converts the state vector to tissue concentrations

Bibliography

- [Alo] Alonso, Marcelo & Finn, Edward J: *Fundamental University Physics* Vol 1, Mechanics and Thermodynamics, Addison-Wesley Publ. Company, 1979.
- [Atk] Atkins, P. W: *Physical Chemistry* Oxford University Press, 1990.
- [And] Andreassen, Trine; Christensen, Blørn; Green, Christine; Hansen; Anja S & Helmgaard, Lisbeth: *Model 10—en matematisk model af intravenøse anæstetikas farmakokinetik*. IMFUFA tekst 274, IMFUFA, Roskilde Universitetscenter, Danmark, 1994.
- [Bar] Bardoczky, Gizella; Vries, Jaap de; Meriläinen, Pekka; Schofield, Jim & Tuomaala, Lauri: *Side stream spirometry* Datex Division Instrumentarium Corp, Helsinki, Finland.
- [Bro] Brown, Stanley S (ed.): *Chemical diagnosis of disease* Elsevir, Amsterdam, 1979.
- [Bis] Bischoff & Dedrick: *Thiopental Pharmacokinetics* Journal of Pharmaceutical Science, vol 57, No 8: 1346-1351, 1968.
- [Chi0] Chiari, L; Avanzolini, G; Gnudi G. & Grandi, F: *A non-linear simulator of the human respiratory chemostat*. Powers & Hart (ed): *Computer Simulations in Biomedicine*, Computer Mechanics Publications, Southampton, Boston, 1995.
- [Chi1] Chiari L; Avanzolini, G; Grandi, F & Gnudi, G: *A simple model of the chemical regulation of acid-base balance in blood* Engineering advances, ed. by Sheppard et al: Proc. of the 16th Int. Conf. of the IEEE-EMBS, 1025-1026, 1994.
- [Duf] Duffin, J: *A mathematical model of the chemoreflex control of ventilation* Resp. Physiol. Vol 15:277-301, 1972.

- [Eva] Evans, John W; Wagner, Peter D. & West, John B: *Conditions for reduction of pulmonary gas transfer by ventilation-perfusion inequality* Journal of Applied Physiology, Vol 36, May 1974.
- [Far0] Farlow, Stanley J.: *An introduction to differential equations and their applications*, McGraw-Hill, Inc. 1994.
- [Fin] Fincham, W.F. & Tehrani, F.T: *A mathematical model of the human respiratory system* J Biomed Eng 5: 125-133, 1983.
- [Fre] Frellesen, Lars (ed.), Andreasen, Viggo & Jensen, Per Føge: *SIMA anaesthesia simulator requirements specification* Unpublished working paper, SIMA group, IMFUFA, Roskilde University, May 17, 1995.
- [Fuk0] Fukui, Yasuhiro & Smith, N. Ty: *Interactions among ventilation, the circulation, and the uptake and distribution of Halothane—Use of a hybrid computer multiple model*. Anesthesiology 54:119-124, 1981.
- [Fuk1] Fukui, Yasuhiro: *A Study of the Human Cardiovascular-Respiratory System using Hybrid Computer Modelling*. Ph. D. thesis, University of Wisconsin; 1972.
- [Gab1] Gaba, David M.: *Dynamic Decision-making in Anesthesiology: Use of realistic Simulation for Training*. NATO Advanced research Workshop: Advanced Models of Cognition for Medical Training and Practice, June, 1991.
- [Gal] Galster, Gert: *Source code for a model of pulmonary mechanics*. Unpublished. Bisbebjerg Hospital, København, 1995.
- [Gib] Gibaldi, Milo & Perrier, Donald: *Pharmacokinetics. (Drugs and the pharmaceutical sciences; v. 15) Second edition*. Marcel Dekker, inc., New York, 1982.
- [Gol] Golden, James F; Clark, John W. & Stevens, Paul M: *Mathematical modeling of pulmonary airway dynamics* IEEE-TBME, vol 20, no 6: 397-404, 1973.
- [Gra] Granger, Wesley M; Miller, David A; Ehrhart, Ina C. & Hofman, Wendel F: *The effect of blood flow and diffusion impairment on pulmonary gas exchange: A computer model*. Computers and Biomedical Research 20, 497-506 (1987).

-
- [Gro] Grodins F. S. & Yamashiro S. M. *Respiratory function of the lung and its control* New York, 1978.
- [Hop] Hoppenstaedt, Frank C. & Peskin, Charles S: *Mathematics in medicine and the life sciences, kap. 6: Gas Exchange in the Lungs*. Springer-Verlag, New York, 1992.
- [Hor] Hornbein, Thomas F.: *Regulation of breathing (Lung biology in health and disease vol. 17, part 1 + 2*. 1981.
- [Hul] Hull, C.J: *Pharmacokinetics and pharmacodynamics* Br. J. Anaesth. Vol 51, p.579, 1979.
- [Høh] Høholt, Tom; Jensen, Helge Elbrønd & Nielsen, Frank: *Lineære differential ligninger* Matematisk Institut, Danmarks Tekniske Højskole, 1984.
- [Jac] Jackson, Andrew C & Milhorn, Howard T: *Digital Computer Simulation of Respiratory Mechanics* Computers and Biomedical Research, Vol 6, p 27-56, 1973.
- [Jac0] Jacquez, John A.: *Compartmental Analysis in Biology and Medicine. Second edition*. University of Michigan Press, 1985.
- [Jac1] Jacquez, John A. & Simon, Carl P.: *Qualitative Theory of Compartmental Systems*. SIAM Review, Vol 35, No. 1, pp. 43-79, March 1993.
- [Jen0] Jensen, Jens Ingemann: *A dynamic model of the carbon dioxide and oxygen stores of the body and their control*. Proceedings of 11th IMACS World Conference on Scientific Computation and Simulation, Oslo 1985.
- [Kel] Kelman, Richard G: *Digital computer subroutine for the conversion of oxygen tension into saturation*. Journal of applied physiology 21. 1375-?, 1966.
- [Ler] Lerou Jos G.C.; Dirksen, Ris; Kolmer, Herman H. Beneken & Booij, Leo H.D.J: *A System Model for closed-circuit inhalation anesthesia. I. Computer Study* Anesthesiology 75:345-355, 1991
- [Lon] Longobardo, Guy S; Cherniack, Neil S. & Fishman, Alfred P: *Cheyne-Stokes breathing produced by a model of the human respiratory system* Journal of applied physiology, 1966 vol. 21(6): 1839-1846

- [Map] Mapleson, W.W: *Circulation-time models of the uptake of inhaled anaesthetics and data for quantifying them* British Journal of Anaesthesia 45:319-334, 1973
- [Mil1] Milanese, M. & G. P. Molino: *Structural Identifiability of Compartmental Models and Pathophysiological Information from the Kinetics of Drugs*. Mathematical Biosciences 26, 175-190 (1975).
- [Mil2] Miller, David A. & Granger, Wesley M: *A block diagram, graphic and microcomputer analysis of the O₂ transport system* Physiologist 25(2): 111-?, 1982.
- [Mor] More, W. J.: *Physical chemistry*. 5. edition, Longmann, London, 1972.
- [Nun] Nunn, J. F.: *Applied Respiratory Physiology*. Butterworths, London, 1987.
- [Olo] Olofsen, Erik: *Modelling arterial blood desaturation during apnoea*. Preprint, University Hospital Leiden, Leiden, The Netherlands, August 1994.
- [Olu] Olufsen, Mette; Nielsen, Finn; Jensen, Per Føge & Pedersen, Stig Andur: *The models underlying the anaesthesia simulator Sophus* IMFUFA tekst 278, IMFUFA, Roskilde Universitetscenter, Danmark, 1994.
- [Pes] Peskin, Charles S.: *Lectures on Mathematical Aspects of Physiology*. Frank C. Hoppenstaedt (ed): *Matemtical Aspects of Physiology*.
- [Pii] Piiper, J. & Scheid, P: *Model for capillary-alveolar equilibrium with special reference to O₂ uptake in hypoxia* Respir. Physiol. 46, 193 (1981)
- [Poo] Poon, Chi-Sang & Wiberg, Donald M: *Dynamics of Gaseous Uptake in the lungs: The Concentrations and Second Gas Effects* IEEE Transactions on Biomedical Engineering, Vol 28, p. 823-831, 1981.
- [Pre] Press, William; Vetterling, William; Teukolsky, Saul A; Flannery, Brian P: *Numerical Recipes in C* Cambridge University Press, 1992.

-
- [Rey] Reynolds, W.J. & Milhorn H. T: *Transient Ventilatory Response to Hypoxia with and without Controlled Alveolar p_{CO_2}* Journal of Applied Physiology, Vol 35 p. 187-186, 1973.
- [Rid0] Rideout, Vincent C.: *Mathematical and Computer Modelling of Physiological Systems*. Prentice Hall, Englewood Cliffs, 1991.
- [Ril] Riley, R.L. & Cournand, A: "Ideal" alveolar air and the analysis of ventilation-perfusion relationships in the lungs J appl physiol 1, 825, 1949.
- [Rub] Rubinow, S. I.: *Introduction to mathematical biology, Kap 3: Tracers in Physiological Systems*. Wiley & Sons 1975.
- [Sau] Saunders, Kenneth B; Bali, Hari N. & Carson, Ewert R: *A breathing model of the respiratory system: the controlled system* J theor biol 84:135-161, 1980.
- [Sch0] Schwid, Howard A. & Daniel O'Donnell: *The Anesthesia Simulator-Recorder: A device to train and evaluate anesthesiologists' responses to critical incidents*. Anesthaesiology 72:191-197, 1990.
- [She] Sheiner, Lewis B; Stanski, Donald R; Vozeh, Samuel; Miller, Ronald D. & Ham, Jay: *Simultaneous modeling of pharmacokinetics and pharmacodynamics: Applications to d-tubocurarine* Clin. Pharmacol. Ther. vol. 25 no.3:358-371, 1979.
- [Sig0] Siggaard-Andersen, O; Wimberley P.D; Fogh-Andersen, N & Gothgen, I.H: *Measured and derived quantities with modern pH and blood gas equipment: calculation algorithms with 54 equations*. Scandinavian Journal of Clinical Laboratory Investigations 1988, 48, suppl. 189.
- [Sig1] Siggaard-Andersen, Ole og Ivar H. Gothgen: *The oxygen status of the arterial blood*. Radiometer, København, 1989.
- [Sig2] Siggaard-Andersen, Ole: *The acid-base status of the blood* 4 ed, Munksgaard, København, 1974
- [Sig3] Siggaard-Andersen, Ole; Wimberley, Peter D; Gøthgen, Ivar & Siggaard-Andersen, Mads: *A Mathematical Model of the Hemoglobin-Oxygen dissociation curve of the Human Blood and of Oxygen Partial Pressure as a Function of Temperature* Clin. Chem, Vol 30, p. 1646-1651, 1984.

- [Sig5] Siggaard-Andersen, M. & Siggaard-Andersen, O: *Oxygen status algorithm, version 3, with some applications* Acta Anaesthesiologica Scandinavica, Vol 39, p. 13-20, 1995.
- [Sig6] Siggaard-Andersen, O. & Gøthgen, I. H: *Oxygen and acid-base parameters of arterial and mixed venous blood, relevant versus redundant* Acta Anaesthesiologica Scandinavica, Vol 39, p. 21-27, 1995.
- [Sig7] Siggaard-Andersen, Ole; Fogh-Andersen, Niels & Gøthgen, Ivar H: *Oxygen status of arterial and mixed venous blood* Critical Care Medicine, Vol 23, p. 1284-1293, 1995.
- [Sin] Singer, Richard B & Hastings: *An improved clinical method for the estimation of disturbances of the acid-base balance of human blood* Medicine (Baltimore), vol 27, p. 223-242, 1948.
- [Son] Soni, N. Fawcett, W.F. & Halliday, F.C: *Beyond the lung: oxygen delivery and tissue oxygenation.* Anaesthesia, Vol. 48, p 704-711, 1993.
- [Swa] Swanson G. D: *Respiratory control. A modelling perspective* Plenum Press, New York, 1989.
- [Van] Vander Arthur J; Sherman, James H. & Luciano, Dorothy S: *Human physiology* Fifth ed, McGraw-Hill Publishing Company, New York. 1990.
- [Wes0] West, John B: *Blood flow to the lung and gas exchange* Anesthesiology 41(2), 124, 1974.
- [Wes1] West, John B: *Ventilation/Blood flow and gas exchange* Blackwell, Oxford, UK, 1965.
- [Wes2] West, John B.: *Respiratory Physiology* The Williams & Wilkins Company, Baltimore, USA, 1979.
- [Wid] Widdicombe, John & Davies, Andrew: *Respiratory physiology* Second ed, Physiological Principles of Medicine Series, Edward Arnold, London, 1991.

Liste over tidligere udkomne tekster
tilsendes gerne. Henvendelse herom kan
ske til IMFUFA's sekretariat
tlf. 46 75 77 11 lokal 2263

-
- | | |
|--|--|
| <p>217/92 "Two papers on APPLICATIONS AND MODELLING
IN THE MATHEMATICS CURRICULUM"
by: Mogens Niss</p> <p>218/92 "A Three-Square Theorem"
by: Lars Kadison</p> <p>219/92 "RUPNOK - stationær strømning i elastiske rør"
af: Anja Boisen, Karen Birkelund, Mette Olufsen
Vejleder: Jesper Larsen</p> <p>220/92 "Automatisk diagnosticering i digitale kredsløb"
af: Bjørn Christensen, Ole Møller Nielsen
Vejleder: Stig Andur Pedersen</p> <p>221/92 "A BUNDLE VALUED RADON TRANSFORM, WITH
APPLICATIONS TO INVARIANT WAVE EQUATIONS"
by: Thomas P. Branson, Gestur Olafsson and
Henrik Schlichtkrull</p> <p>222/92 On the Representations of some Infinite Dimensional
Groups and Algebras Related to Quantum Physics
by: Johnny T. Ottesen</p> <p>223/92 THE FUNCTIONAL DETERMINANT
by: Thomas P. Branson</p> <p>224/92 UNIVERSAL AC CONDUCTIVITY OF NON-METALLIC SOLIDS AT
LOW TEMPERATURES
by: Jeppe C. Dyrre</p> <p>225/92 "HATMODELLEN" Impedansspektroskopi i ultrarent
en-krystallinsk silicium
af: Anja Boisen, Anders Gorm Larsen, Jesper Varmer,
Johannes K. Nielsen, Kit R. Hansen, Peter Bøggild
og Thomas Hougaard
Vejleder: Petr Viscor</p> <p>226/92 "METHODS AND MODELS FOR ESTIMATING THE GLOBAL
CIRCULATION OF SELECTED EMISSIONS FROM ENERGY
CONVERSION"
by: Bent Sørensen</p> | <p>227/92 "Computersimulering og fysik"
af: Per M.Hansen, Steffen Holm,
Peter Maibom, Mads K. Dall Petersen,
Pernille Postgaard, Thomas B.Schrøder,
Ivar P. Zeck
Vejleder: Peder Voetmann Christiansen</p> <p>228/92 "Teknologi og historie"
Fire artikler af:
Mogens Niss, Jens Høyrup, Ib Thiersen,
Hans Heddal</p> <p>229/92 "Masser af information uden betydning"
En diskussion af informationsteorien
i Tor Nørretranders' "Mærk Verden" og
en skitse til et alternativ baseret
på andenordens kybernetik og semiotik.
af: Søren Brier</p> <p>230/92 "Vinklens tredeling - et klassisk
problem"
et matematisk projekt af
Karen Birkelund, Bjørn Christensen
Vejleder: Johnny Ottesen</p> <p>231A/92 "Elektrondiffusion i silicium - en
matematisk model"
af: Jesper Voetmann, Karen Birkelund,
Mette Olufsen, Ole Møller Nielsen
Vejledere: Johnny Ottesen, H.B.Hansen</p> <p>231B/92 "Elektrondiffusion i silicium - en
matematisk model" Kildetekster
af: Jesper Voetmann, Karen Birkelund,
Mette Olufsen, Ole Møller Nielsen
Vejledere: Johnny Ottesen, H.B.Hansen</p> <p>232/92 "Undersøgelse om den simultane opdagelse
af energiens bevarelse og isærøeles om
de af Mayer, Colding, Joule og Helmholtz
udførte arbejder"
af: L.Arleth, G.I.Dybkjær, M.T.Øsørgård
Vejleder: Dorthe Posselt</p> <p>233/92 "The effect of age-dependent host
mortality on the dynamics of an endemic
disease and
instability in an SIR-model with age-
dependent susceptibility
by: Viggo Andreassen</p> <p>234/92 "THE FUNCTIONAL DETERMINANT OF A FOUR-DIMENSIONAL
BOUNDARY VALUE PROBLEM"
by: Thomas P. Branson and Peter B. Gilkey</p> <p>235/92 OVERFLADESTRUKTUR OG POREUDVIKLING AF KOKS
- Modul 3 fysik projekt -
af: Thomas Jessen</p> |
|--|--|
-

- 236a/93 INTRODUKTION TIL KVANTE
HALL EFFEKTEN
af: Ania Boisen, Peter Bøggild
Vejleder: Peder Voetmann Christiansen
Erland Brun Hansen
- 236b/93 STRØMSSAMMENBRUD AF KVANTE
HALL EFFEKTEN
af: Anja Boisen, Peter Bøggild
Vejleder: Peder Voetmann Christiansen
Erland Brun Hansen
- 237/93 The Wedderburn principal theorem and
Shukla cohomology
af: Lars Kadison
- 238/93 SEMIOTIK OG SYSTEMEGENSKABER (2)
Vektorbånd og tensorer
af: Peder Voetmann Christiansen
- 239/93 Valgsystemer - Modelbygning og analyse
Matematik 2. modul
af: Charlotte Gjerrild, Jane Hansen,
Maria Hermannsson, Allan Jørgensen,
Ragna Clauson-Kaas, Poul Lützen
Vejleder: Mogens Niss
- 240/93 Patologiske eksempler.
Om sære matematiske fysiske betydning for
den matematiske udvikling
af: Claus Dræby, Jørn Skov Hansen, Runa
Ulsøe Johansen, Peter Meibom, Johannes
Kristoffer Nielsen
Vejleder: Mogens Niss
- 241/93 FOTOVOLTAISK STATUSNOTAT 1
af: Bent Sørensen
- 242/93 Brovedligeholdelse - bevar mig vel
Analyse af Vejdirektoratets model for
optimering af broreparationer
af: Linda Kyndlev, Kåre Fundal, Kamma
Tulinus, Ivar Zeck
Vejleder: Jesper Larsen
- 243/93 TANKEEKSPERIMENTER I FYSIKKEN
Et 1.modul fysikprojekt
af: Karen Birkelund, Stine Sofia Korremann
Vejleder: Dorthe Posselt
- 244/93 RADONTRANSFORMATIONEN og dens anvendelse
i CT-scanning
Projektrapport
af: Trine Andreassen, Tine Guldager Christiansen,
Nina Skov Hansen og Christine Iversen
Vejledere: Gestur Olafsson og Jesper Larsen
- 245a+b
/93 Time-Of-Flight målinger på krystallinske
halvledere
Specialerapport
af: Linda Szkotak Jensen og Lise Odgaard Gade
Vejledere: Petr Viscor og Niels Boye Olsen
- 246/93 HVERDAGSVIDEN OG MATEMATIK
- LÆREPROCESSER I SKOLEN
af: Lena Lindenskov, Statens Humanistiske
Forskningsråd, RUC, IMFUFA
- 247/93 UNIVERSAL LOW TEMPERATURE AC CON-
DUCTIVITY OF MACROSCOPICALLY
DISORDERED NON-METALS
by: Jeppe C. Dyre
- 248/93 DIRAC OPERATORS AND MANIFOLDS WITH
BOUNDARY
by: B. Booss-Bavnbek, K.P.Wojciechowski
- 249/93 Perspectives on Teichmüller and the
Jahresbericht Addendum to Schappacher,
Scholz, et al.
by: B. Booss-Bavnbek
With comments by W.Abikoff, L.Ahlfors,
J.Cerf, P.J.Davis, W.Fuchs, F.P.Gardiner,
J.Jost, J.-P.Kahane, R.Lohan, L.Lorch,
J.Radkau and T.Söderqvist
- 250/93 EULER OG BOLZANO - MATEMATISK ANALYSE SET I ET
VIDENSKABSTEORETISK PERSPEKTIV
Projektrapport af: Anja Juul, Lone Michelsen,
Tomas Højgård Jensen
Vejleder: Stig Andur Pedersen
- 251/93 Genotypic Proportions in Hybrid Zones
by: Freddy Bugge Christiansen, Viggo Andreassen
and Ebbe Thue Poulsen
- 252/93 MODELLERING AF TILFÆLDIGE FÆNOMENER
Projektrapport af: Birthe Friis, Lisbeth Helmgård,
Kristina Charlotte Jakobsen, Marina Mosbæk
Johannessen, Lotte Ludvigsen, Mette Hass Nielsen
- 253/93 Kuglepakning
Teori og model
af: Lise Arleth, Kåre Fundal, Nils Kruse
Vejleder: Mogens Niss
- 254/93 Regressionsanalyse
Materiale til et statistikkursus
af: Jørgen Larsen
- 255/93 TID & BETINGET UAFHÆNGIGHED
af: Peter Harremoës
- 256/93 Determination of the Frequency Dependent
Bulk Modulus of Liquids Using a Piezo-
electric Spherical Shell (Preprint)
by: T. Christensen and N.B.Olsen
- 257/93 Modellering af dispersion i piezoelektriske
keramikker
af: Pernille Postgaard, Jannik Rasmussen,
Christina Specht, Mikko Østergård
Vejleder: Tage Christensen
- 258/93 Supplerende kursusmateriale til
"Lineære strukturer fra algebra og analyse"
af: Mogens Brun Heefelt
- 259/93 STUDIES OF AC HOPPING CONDUCTION AT LOW
TEMPERATURES
by: Jeppe C. Dyre
- 260/93 PARTITIONED MANIFOLDS AND INVARIANTS IN
DIMENSIONS 2, 3, AND 4
by: B. Booss-Bavnbek, K.P.Wojciechowski

- 261/93 OPGAVESAMLING
Bredde-kursus i Fysik
Eksamensopgaver fra 1976-93
- 262/93 Separability and the Jones Polynomial
by: Lars Kadison
- 263/93 Supplerende kursusmateriale til "Lineære strukturer fra algebra og analyse" II
af: Mogens Brun Heefelt
- 264/93 FOTOVOLTAISK STATUSNOTAT 2
af: Bent Sørensen
-
- 265/94 SPHERICAL FUNCTIONS ON ORDERED SYMMETRIC SPACES
To Sigurdur Helgason on his sixtyfifth birthday
by: Jacques Faraut, Joachim Hilgert and Gestur Olafsson
- 266/94 Kommensurabilitets-oscillationer i laterale supergitre
Fysikspeciale af: Anja Boisen, Peter Bøggild, Karen Birkelund
Vejledere: Rafael Taboryski, Poul Erik Lindelof, Peder Voetmann Christiansen
- 267/94 Kom til kort med matematik på Eksperimentarium - Et forslag til en opstilling
af: Charlotte Gjerrild, Jane Hansen
Vejleder: Bernhelm Booss-Bavnbek
- 268/94 Life is like a sewer ...
Et projekt om modellering af aorta via en model for strømning i kloaker
af: Anders Marcussen, Anne C. Nilsson, Lone Michelsen, Per M. Hansen
Vejleder: Jesper Larsen
- 269/94 Dimensionsanalyse en introduktion metaprojekt, fysik
af: Tine Guldager Christiansen, Ken Andersen, Nikolaj Hermann, Jannik Rasmussen
Vejleder: Jens Højgaard Jensen
- 270/94 THE IMAGE OF THE ENVELOPING ALGEBRA AND IRREDUCIBILITY OF INDUCED REPRESENTATIONS OF EXPONENTIAL LIE GROUPS
by: Jacob Jacobsen
- 271/94 Matematikken i Fysikken. Opdaget eller opfundet NAT-BAS-projekt
vejleder: Jens Højgaard Jensen
- 272/94 Tradition og fornyelse
Det praktiske elevarbejde i gymnasiets fysikundervisning, 1907-1988
af: Kristian Hoppe og Jeppe Guldager
Vejledning: Karin Beyer og Nils Hybel
- 273/94 Model for kort- og mellemdistanceløb
Verifikation af model
af: Lise Fabricius Christensen, Helle Pilemann, Bettina Sørensen
Vejleder: Mette Olufsen
- 274/94 MODEL 10 - en matematisk model af intravenøse anæstetikas farmakokinetik
3. modul matematik, forår 1994
af: Trine Andreasen, Bjørn Christensen, Christine Green, Anja Skjoldborg Hansen, Lisbeth Helmgård
Vejledere: Viggo Andreasen & Jesper Larsen
- 275/94 Perspectives on Teichmüller and the Jahresbericht 2nd Edition
by: Bernhelm Booss-Bavnbek
- 276/94 Dispersionsmodellering
Projektrapport 1. modul
af: Gitte Andersen, Rehannah Borup, Lisbeth Friis, Per Gregersen, Kristina Vejro
Vejleder: Bernhelm Booss-Bavnbek
- 277/94 PROJEKTARBEJDSPEDAGOGIK - Om tre tolkninger af problemorienteret projektarbejde
af: Claus Flensted Behrens, Frederik Voetmann Christiansen, Jørn Skov Hansen, Thomas Thingstrup
Vejleder: Jens Højgaard Jensen
- 278/94 The Models Underlying the Anaesthesia Simulator Sophus
by: Mette Olufsen(Math-Tech), Finn Nielsen (RISØ National Laboratory), Per Føge Jensen (Herlev University Hospital), Stig Andur Pedersen (Roskilde University)
- 279/94 Description of a method of measuring the shear modulus of supercooled liquids and a comparison of their thermal and mechanical response functions.
af: Tage Christensen
- 280/94 A Course in Projective Geometry
by Lars Kadison and Matthias T. Kromann
- 281/94 Modellering af Det Cardiovaskulære System med Neural Puls kontrol
Projektrapport udarbejdet af:
Stefan Frello, Runa Ulsøe Johansen, Michael Poul Curt Hansen, Klaus Dahl Jensen
Vejleder: Viggo Andreasen
- 282/94 Parallelle algoritmer
af: Erwin Dan Nielsen, Jan Danielsen, Niels Bo Johansen

- 283/94 Grænser for tilfældighed
(en kaotisk talgenerator)
af: Erwin Dan Nielsen og Niels Bo Johansen
- 284/94 Det er ikke til at se det, hvis man ikke
lige ve' det!
Gymnasimatematikens begrundelsesproblem
En specialerapport af Peter Hauge Jensen
og Linda Kyndlev
Vejleder: Mogens Niss
- 285/94 Slow coevolution of a viral pathogen and
its diploid host
by: Viggo Andreassen and
Freddy B. Christiansen
- 286/94 The energy master equation: A low-temperature
approximation to Bässler's random walk model
by: Jeppe C. Dyre
- 287/94 A Statistical Mechanical Approximation for the
Calculation of Time Auto-Correlation Functions
by: Jeppe C. Dyre
- 288/95 PROGRESS IN WIND ENERGY UTILIZATION
by: Bent Sørensen
- 289/95 Universal Time-Dependence of the Mean-Square
Displacement in Extremely Rugged Energy
Landscapes with Equal Minima
by: Jeppe C. Dyre and Jacob Jacobsen
- 290/95 Modellering af uregelmæssige bølger
Et 3.modul matematik projekt
af: Anders Marcussen, Anne Charlotte Nilsson,
Lone Michelsen, Per Mørkegaard Hansen
Vejleder: Jesper Larsen
- 291/95 1st Annual Report from the project
LIFE-CYCLE ANALYSIS OF THE TOTAL DANISH
ENERGY SYSTEM
an example of using methods developed for the
OECD/IEA and the US/EU fuel cycle externality study
by: Bent Sørensen
- 292/95 Fotovoltaisk Statusnotat 3
af: Bent Sørensen
- 293/95 Geometridiskussionen - hvor blev den af?
af: Lotte Ludvigsen & Jens Frandsen
Vejleder: Anders Madsen
- 294/95 Universets udvidelse -
et metaprojekt
Af: Jesper Duelund og Birthe Friis
Vejleder: Ib Lundgaard Rasmussen
- 295/95 A Review of Mathematical Modeling of the
Controlled Cardiovascular System
By: Johnny T. Ottesen
- 296/95 RETIKULER den klassiske mekanik
af: Peder Voetmann Christiansen
- 297/95 A fluid-dynamical model of the aorta with
bifurcations
by: Mette Olufsen and Johnny Ottesen
- 298/95 Mordet på Schrödingers kat - et metaprojekt om
to fortolkninger af kvantemekanikken
af: Maria Hermannsson, Sebastian Horst,
Christina Specht
Vejledere: Jeppe Dyre og Peder Voetmann Christiansen
- 299/95 ADAM under figenbladet - et kig på en samfunds-
videnskabelig matematisk model
Et matematisk modelprojekt
af: Claus Dræby, Michael Hansen, Tomas Højgård Jensen
Vejleder: Jørgen Larsen
- 300/95 Scenarios for Greenhouse Warming Mitigation
by: Bent Sørensen
- 301/95 TOK Modellering af træers vækst under påvirkning
af ozon
af: Glenn Møller-Holst, Marina Johannessen, Birthe
Nielsen og Bettina Sørensen
Vejleder: Jesper Larsen
- 302/95 KOMPRESSORER - Analyse af en matematisk model for
aksialkompressor
Projektrapport af: Stine Bøggild, Jakob Hilmer,
Pernille Postgaard
Vejleder: Viggo Andreassen
- 303/95 Masterlignings-modeller af Glasovergangen
Termisk-Mekanisk Relaksation
Specialerapport udarbejdet af:
Johannes K. Nielsen, Klaus Dahl Jensen
Vejledere: Jeppe C. Dyre, Jørgen Larsen
- 304a/95 STATISTIKNOTER Simple binomialfordelingsmodeller
af: Jørgen Larsen
- 304b/95 STATISTIKNOTER Simple normalfordelingsmodeller
af: Jørgen Larsen
- 304c/95 STATISTIKNOTER Simple Poissonfordelingsmodeller
af: Jørgen Larsen
- 304d/95 STATISTIKNOTER Simple multinomialfordelingsmodeller
af: Jørgen Larsen
- 304e/95 STATISTIKNOTER Mindre matematisk-statistisk opslagsværk
indeholdende bl.a. ordforklaringer, resuméer og
tabeller
af: Jørgen Larsen

- 305/95 The Maslov Index:
A Functional Analytical Definition
And The Spectral Flow Formula

By: B. Booss-Bavnbek, K. Furutani
- 306/95 Goals of mathematics teaching

Preprint of a chapter for the forthcoming International Handbook of Mathematics Education (Alan J. Bishop, ed)

By: Mogens Niss
- 307/95 Habit Formation and the Thirdness of Signs

Presented at the semiotic symposium

The Emergence of Codes and Intensions as a Basis of Sign Processes

By: Peder Voetmann Christiansen
- 308/95 Metaforer i Fysikken

af: Marianne Wilcken Bjerregaard, Frederik Voetmann Christiansen, Jørn Skov Hansen, Klaus Dahl Jensen Ole Schmidt

Vejledere: Peder Voetmann Christiansen og Petr Viscor
- 309/95 Tiden og Tanken

En undersøgelse af begrebsverdenen Matematik udført ved hjælp af en analogi med tid

af: Anita Stark og Randi Petersen

Vejleder: Bernhelm Booss-Bavnbek
- 310/96 Kursusmateriale til "Lineære strukturer fra algebra og analyse" (E1)

af: Mogens Brun Heefelt
- 311/96 2nd Annual Report from the project
LIFE-CYCLE ANALYSIS OF THE TOTAL DANISH ENERGY SYSTEM

by: Hélène Connor-Lajambe, Bernd Kuemmel, Stefan Krüger Nielsen, Bent Sørensen
- 312/96 Grassmannian and Chiral Anomaly

by: B. Booss-Bavnbek, K.P. Wojciechowski
- 313/96 THE IRREDUCIBILITY OF CHANCE AND THE OPENNESS OF THE FUTURE

The Logical Function of Idealism in Peirce's Philosophy of Nature

By: Helmut Pape, University of Hannover
- 314/96 Feedback Regulation of Mammalian Cardiovascular System

By: Johnny T. Ottesen
- 315/96 "Rejsen til tidens indre" - Udarbejdelse af a + b et manuskript til en fjernsynsudsendelse + manuskript

af: Gunhild Hune og Karina Goyle

Vejledere: Peder Voetmann Christiansen og Bruno Ingemann
- 316/96 Plasmaoscillation i natriumklynger

Specialerapport af: Peter Meibom, Mikko Østergård

Vejledere: Jeppe Dyre & Jørn Borggreen
- 317/96 Poincaré og symplektiske algoritmer

af: Ulla Rasmussen

Vejleder: Anders Madsen
- 318/96 Modelling the Respiratory System

by: Tine Guldager Christiansen, Claus Dræby

Supervisors: Viggo Andreassen, Michael Daniclsen
- 319/96 Externality Estimation of Greenhouse Warming Impacts

by: Bent Sørensen
- 320/96 Grassmannian and Boundary Contribution to the -Determinant

by: K.P. Wojciechowski et al.
- 321/96 Modelkompetencer - udvikling og afprøvning af et begrebsapparat

Specialerapport af: Nina Skov Hansen, Christine Iversen, Kristin Troels-Smith

Vejleder: Morten Blomhøj
- 322/96 OPGAVESAMLING

Bredde-Kursus i Fysik 1976 - 1996
- 323/96 Structure and Dynamics of Symmetric Diblock Copolymers

PhD Thesis

by: Christine Maria Papadakis
- 324/96 Non-linearity of Baroreceptor Nerves

by: Johnny T. Ottesen
- 325/96 Retorik eller realitet ?

Anvendelser af matematik i det danske Gymnasiums matematikundervisning i perioden 1903 - 88

Specialerapport af Helle Pilemann

Vejleder: Mogens Niss
- 326/96 Devisteori

Eksemplificeret ved Gentzens bevis for konsistensen af teorien om de naturlige tal

af: Gitte Andersen, Lise Mariane Jeppesen, Klaus Frovin Jørgensen, Ivar Peter Zeck

Vejledere: Bernhelm Booss-Bavnbek og Stig Andur Pedersen
- 327/96 NON-LINEAR MODELLING OF INTEGRATED ENERGY SUPPLY AND DEMAND MATCHING SYSTEMS

by: Bent Sørensen
- 328/96 Calculating Fuel Transport Emissions

by: Bernd Kuemmel